

# Transport and Structure in Fuel Cell Proton Exchange Membranes

Michael Anthony Hickner

Dissertation submitted to the faculty of Virginia Polytechnic Institute and State  
University in partial fulfillment of the requirements for the degree of

DOCTOR OF PHILOSOPHY  
in  
Chemical Engineering

---

James E. McGrath, co-chairman

---

Garth L. Wilkes, co-chairman

---

Donald G. Baird

---

Richey M. Davis

---

Thomas A. Zawodzinski

August 27, 2003  
Blacksburg, Virginia

Keywords: fuel cell, proton exchange membrane, sulfonated polymer, membrane  
transport, direct methanol

Copyright 2003, Michael Anthony Hickner

# Transport and Structure in Fuel Cell Proton Exchange Membranes

by  
Michael Anthony Hickner

James E. McGrath, co-chairman  
Chemistry

Garth L. Wilkes, co-chairman  
Chemical Engineering

(ABSTRACT)

Transport properties of novel sulfonated wholly aromatic copolymers and the state-of-the-art poly(perfluorosulfonic acid) copolymer membrane for fuel cells, Nafion, were compared. Species transport (protons, methanol, water) in hydrated membranes was found to correspond with the water-self diffusion coefficient as measured by pulsed field gradient nuclear magnetic resonance (PFG NMR), which was used as a measure of the state of absorbed water in the membrane. Generally, transport properties decreased in the order Nafion > sulfonated poly(arylene ether sulfone) > sulfonated poly(imide). The water diffusion coefficients as measured by PFG NMR decreased in a similar fashion indicating that more tightly bound water existed in the sulfonated poly(arylene ether sulfone) (BPSH) and sulfonated poly(imide) (sPI) copolymers than in Nafion.

Electro-osmotic drag coefficient ( $E_D$  number of water molecules conducted through the membrane per proton) studies confirmed that the water in sulfonated wholly aromatic systems is more tightly bound within the copolymer morphology. Nafion, with a water uptake of 19 wt % ( $\lambda = 12$ , where  $\lambda = N \text{ H}_2\text{O}/\text{SO}_3\text{H}$ ) had an electro-osmotic drag coefficient of 3.6 at 60°C, while BPSH 35 had an electro-osmotic drag coefficient of 1.2 and a water uptake of 40 wt % ( $\lambda = 15$ ) under the same conditions.

Addition of phosphotungstic acid decreased the total amount of water uptake in BPSH/inorganic composite membranes, but increased the fraction of loosely bound water. Zirconium hydrogen phosphate/BPSH hybrids also showed decreased bulk water uptake, but contrary to the results with phosphotungstic acid, the fraction of loosely bound water was decreased. This dissimilar behavior is attributed to the interaction of phosphotungstic acid with the sulfonic acid groups of

the copolymer thereby creating loosely bound water. No such interaction exists in the zirconium hydrogen phosphate materials. The transport properties in these materials were found to correspond with the water-self diffusion coefficients.

Proton exchange membrane (PEM) transport properties were also found to be a function of the molecular weight of sulfonated poly(arylene thioether sulfone) (PATs). Low molecular weight (IV ~ 0.69) copolymers absorbed more water on the same ion exchange capacity basis than the high molecular weight copolymers (IV ~ 1.16). Surprisingly, protonic conductivity of the two series was similar. Moreover, the methanol permeability of the low molecular weight copolymers was increased, resulting in lower membrane selectivity and decreased mechanical properties.

The feasibility of converting the novel sulfonated wholly aromatic systems to membrane electrode assemblies (MEAs) for use in fuel cells was studied by comparing free-standing membrane properties to those of MEAs assembled with standard Nafion electrodes. Significantly higher interfacial resistance was measured for BPSH samples. Fluorine was introduced into the copolymer backbone by utilizing bisphenol-AF in the copolymer synthesis (6F copolymers). These 6F copolymers showed a markedly lower interfacial resistance with Nafion electrodes and correspondingly greater direct methanol fuel cell performance. It was proposed that the addition of the hexafluoro groups increased the compatibility of the PEM with the highly fluorinated Nafion electrode.

Key words: proton exchange membrane, direct methanol, fuel cell, transport properties, electro-osmotic drag, state of water

## AUTHOR'S ACKNOWLEDGEMENTS

The author would like to thank his principal advisor, James E. McGrath, for all of his support and guidance throughout my doctoral studies. How can a blade of grass thank the sun?

I would also like to thank Garth Wilkes and Tom Zawodzinski for their technical guidance. They have shown me what it takes to be a scientist. I am grateful to Richey Davis and Don Baird for helping me through the Ph.D. process and their critical review of this project and dissertation. My work is better for their input.

A special mention should be paid to the MST-11 team at Los Alamos National Laboratory. Bryan Pivovar has been a trusted mentor and great friend. Wayne, Piotr, Judith, Francisco, Tommy, Guido, Francois, Hayley, John, John, John, Christian, Fernando, Eric, Don, Peter, Jay, Mike, Andrew, Dave. My stay up on the hill was a fun and unique period in my life.

The materials used in this dissertation were the result of other's work namely Feng Wang, Yu Seung Kim, Bryan Einsla, Kent Wiles, and William Harrison. Thanks guys, there wouldn't have been much to write about without your polymers and composites.

Thank you to my colleagues and fellow graduate students for making the laboratory a much more interesting place to exist for a time.

John, Val, Laura, Zach, Anna, and Olivia. This process started long ago with you.

# TABLE OF CONTENTS

Abstract.....	ii
Author's Acknowledgements.....	iv
Table of Contents.....	v
List of Figures.....	ix
List of Tables .....	xiii
Chapter 1. Literature Review.....	1
1.1 Proton Exchange Membrane Fuel Cells – Applications and Systems.....	1
1.1.1 General Fuel Cell Concepts .....	1
1.1.2 Polymer Electrolyte Membrane Fuel Cells.....	4
1.1.3 Hydrogen and Reformate Fuel.....	8
1.1.4 Methanol Fuel .....	10
1.1.5 The Membrane Electrode Assembly.....	13
1.1.6 The Future of Fuel Cells .....	16
1.2 Commercial Proton Exchange Membranes for Fuel Cells .....	16
1.2.1 Nafion .....	17
1.2.1.1 Morphology.....	19
1.2.1.2 Solvent Swelling Properties and Water/Methanol Transport .....	27
1.2.1.3 Protonic Conductivity .....	30
1.2.1.4 Electro-osmosis.....	35
1.2.2 Other Commercial Proton Exchange Membranes .....	37
1.2.2.1 Ballard Power Systems .....	37
1.2.2.2 W.L. Gore & Associates .....	41
1.2.2.3 Dais Analytic .....	43
1.3 New Proton Exchange Membrane Research.....	44
1.3.1 Post-Sulfonated Polymers.....	45
1.3.2 Direct Copolymerization of Sulfonated Monomers.....	47
1.3.3 Polymer/Polymer Composite Membranes .....	54
1.3.4 Polymer/Inorganic Composite Membranes .....	59

1.3.5	Future Directions for Membrane Research.....	69
1.4	State of Water in Hydrophilic Polymers.....	70
Chapter 2. The Influence of Chemical Structure on the Transport Properties of Proton		
Exchange Membranes.....		
2.1	Abstract.....	77
2.2	Introduction.....	78
2.3	Experimental.....	82
2.3.1	Materials.....	82
2.3.2	Water Uptake.....	85
2.3.3	Protonic Conductivity.....	86
2.3.4	Electro-osmotic Drag.....	86
2.3.5	Methanol Permeability.....	87
2.3.6	Water Self-Diffusion Coefficient.....	87
2.4	Results and Discussion.....	89
2.5	Conclusions.....	102
Chapter 3. Electro-Osmotic Drag and Methanol Flux in Sulfonated Poly(arylene ether sulfone) Copolymers: Elucidating Morphology from Transport.....		
3.1	Abstract.....	105
3.2	Introduction.....	106
3.3	Theory.....	109
3.4	Experimental.....	115
3.4.1	Materials.....	115
3.4.2	Electro-osmotic Drag.....	117
3.5	Results and Discussion.....	118
3.5.1	The Effect of Ion Content on Electro-osmotic Drag.....	118
3.5.2	The Influence of Temperature on Electro-osmotic Drag.....	121
3.5.3	Limiting Crossover Current and Convective Velocity.....	124
3.5.4	Qualitative Membrane Morphology Model.....	130
3.6	Conclusions.....	133
3.7	List of Symbols.....	136

Chapter 4. The State of Water and Transport Properties in Organic/Inorganic Composite	
Proton Exchange Membranes .....	137
4.1 Abstract.....	137
4.2 Introduction.....	138
4.3 Experimental.....	141
4.3.1 Membrane Preparation.....	141
4.3.2 Water Uptake .....	143
4.3.3 Protonic Conductivity .....	143
4.3.4 Atomic Force Microscopy .....	144
4.3.5 Methanol Permeability.....	144
4.3.6 Water Self-Diffusion Coefficient.....	148
4.4 Results and Discussion .....	149
4.4.1 Morphology.....	150
4.4.2 Water Uptake .....	152
4.4.3 Protonic Conductivity .....	154
4.4.4 Methanol Permeability.....	156
4.5 Conclusions.....	162
Chapter 5. Transport and Mechanical Properties of Proton Exchange Membranes: Effect of	
Molecular Weight .....	164
5.1 Abstract.....	164
5.2 Introduction.....	165
5.3 Experimental.....	168
5.3.1 Materials .....	168
5.3.2 Molecular Weight Characterization.....	170
5.3.3 Dynamic Tensile Modulus.....	170
5.3.4 Water Uptake .....	171
5.3.5 Protonic Conductivity .....	172
5.3.6 Methanol Permeability.....	173
5.3.7 Relative Selectivity .....	173
5.4 Results and Discussion .....	174

5.5	Conclusions.....	184
Chapter 6.	Fabricating High Performance Membrane Electrode Assemblies From non-Nafion Proton Exchange Membranes .....	187
6.1	Abstract.....	187
6.2	Introduction.....	188
6.3	Experimental.....	194
6.3.1	Materials and Membrane Preparation.....	194
6.3.2	Free-Standing Membrane Conductivity.....	196
6.3.3	Free-Standing Membrane Methanol Permeability.....	197
6.3.4	Membrane Electrode Assembly Fabrication.....	198
6.3.5	Fuel Cell Protonic Conductivity as Determined by High Frequency Resistance	199
6.3.6	Limiting Current Method for Determining Fuel Cell Methanol Permeability ...	200
6.3.7	Electrochemical Selectivity .....	202
6.4	Results.....	203
6.4.1	Methanol Permeability.....	203
6.4.2	Protonic Conductivity.....	206
6.5	Conclusions.....	215
Chapter 7.	Recommendations for Future Research .....	218
7.1	Influence of Chemical Structure on the State of Water and Transport Properties of Proton Exchange Membranes .....	218
7.2	Elucidating Morphology From Transport.....	219
7.3	Effect of Inorganic Additives on the Transport Properties of Organic/Inorganic Nanocomposite Proton Exchange Membranes.....	220
7.4	The Importance of Molecular Weight in High Performance Direct Methanol Fuel Cell Proton Exchange Membranes .....	221
7.5	Fabrication of High Performance MEAs .....	222
Vita	.....	224

## LIST OF FIGURES

Figure 1-1: Basic Fuel Cell Components.....	4
Figure 1-2: Chemical Structure of Nafion .....	5
Figure 1-3: Fuel Cell Stack <sup>1</sup> .....	7
Figure 1-4: MEA Schematic .....	14
Figure 1-5: Chemical Structure of Nafion .....	18
Figure 1-6: X-Ray Scattering of Nafion Membranes and Different Levels of Hydration <sup>11</sup> .....	20
Figure 1-7: X-ray Reflections Comparing Recast Annealed Membranes <sup>11</sup> .....	21
Figure 1-8: Nafion AFM Micrographs Before and After Swelling in Liquid Water – Boxes are 300 x 300 nm Width <sup>15</sup> .....	25
Figure 1-9: Electro-osmotic Drag Coefficients of Perfluorosulfonic Acid Membranes <sup>37</sup> .....	36
Figure 1-10: Ballard BAM3G Synthesis <sup>39</sup> .....	40
Figure 1-11: Sulfonated Block Polyimide Copolymer Synthesis <sup>51</sup> .....	48
Figure 1-12: Neutron Scattering Profiles of Block and Random Sulfonated Polyimides <sup>51</sup> .....	49
Figure 1-13: Direct Copolymerization of Sulfonated Poly(arylene ether)s <sup>21</sup> .....	52
Figure 1-14: Direct Copolymerization of Sulfonated Monomers versus Post Sulfonation .....	53
Figure 1-15: Water Swelling of Sulfonated Poly(arylene ether sulfone)/HPA Composites <sup>65</sup> .....	67
Figure 1-16: Conductivity of HPA Composites <sup>65</sup> .....	68
Figure 1-17: Dynamic Scanning Calorimetry Thermogram Illustrating Two Water Freezing Peak in a Water-swollen PVA Hydrogel <sup>70</sup> .....	72
Figure 1-18: Differential Scanning Calorimetry Thermograms of Hydrated Membranes (a) non- crosslinked (b) crosslinked with 5 mol % BVPE (c) crosslinked with 5 mol % DVB <sup>73</sup> .....	74
Figure 1-19: DSC Thermograms of Nafion 1135 at Various Water Contents <sup>74</sup> .....	75
Figure 2-1: Chemical Structure of Nafion .....	79
Figure 2-2: Chemical Structure of BPSH .....	82
Figure 2-3: Chemical Structure of PATS.....	83
Figure 2-4: Chemical Structure of sPI .....	84

Figure 2-5: NMR Stimulated Echo Pulse Sequence .....	88
Figure 2-6: Protonic Conductivity of Nafion, PATS, BPSH, and Sulfonated Polyimide on an Ion Exchange Capacity Basis .....	90
Figure 2-7: Electro-osmotic Drag Coefficients at 60°C for Fully Hydrated Nafion, BPSH, and Sulfonated Polyimide Membranes .....	93
Figure 2-8: Methanol Permeability of Nafion, BPSH, PATS, and Sulfonated Polyimide Copolymers .....	95
Figure 2-9: Water Self-Diffusion Coefficients for Nafion, PATS, and Sulfonated Polyimide Membranes - Fully Hydrated Samples at 30°C .....	97
Figure 2-10: Chemical Structure of (a) Nafion and (b) BPSH .....	98
Figure 2-11: Proposed Model Relating Extent of Phase Separation to Membrane Transport Properties .....	101
Figure 3-1: Sources of Water at the DMFC Cathode .....	107
Figure 3-2: Methanol Crossover Measurements Using Limiting Current in a DMFC .....	110
Figure 3-3: A Model for the Opposing Movement of Species Through a Pore in the Limiting Crossover Current Experiment.....	113
Figure 3-4: Chemical Structure of Sulfonated Poly(arylene ether sulfone) Copolymers .....	116
Figure 3-5: Electro-osmotic Drag Coefficient versus Ion Exchange Capacity for BPSH and Nafion 117 Copolymers .....	118
Figure 3-6: Chemical Structure of Nafion .....	120
Figure 3-7: Electro-osmotic Coefficient versus Temperature .....	122
Figure 3-8: Flux versus Concentration for N117 at 80°C.....	124
Figure 3-9: Convective Velocities for Nafion 117 at 80°C .....	126
Figure 3-10: Convective Velocities for Limiting Current Experiments with 5 M Methanol ....	127
Figure 3-11: A Domain Model of Nafion and BPSH Copolymer Membranes .....	132
Figure 4-1: Chemical Structure of BPSH Copolymers Containing Hydrophobic and Hydrophilic Units .....	140
Figure 4-2: Membrane Separated Cell.....	145
Figure 4-3: NMR Stimulated Echo Pulse Sequence .....	148
Figure 4-4: Phase Mode Atomic Force Micrographse of BPSH 40, BPSH 40 with 30 wt %	

Phosphotungstic Acid (PTA), and BPSH 40 with 30 wt % Zirconium Hydrogen Phosphate (ZrP).....	150
Figure 4-5: Pure BPSH Copolymer, BPSH/Phosphotungstic Acid (PTA), and BPSH Zirconium Hydrogen Phosphate (ZHP) Composite Membranes: All Show Optical Clarity.....	152
Figure 4-6: Water Absorption of BPSH 40, BPSH 40 with 30 wt % Phosphotungstic Acid (PTA), and BPSH 40 with 30 wt % Zirconium Hydrogen Phosphate (ZrP).....	153
Figure 4-7: Protonic Conductivity of BPSH 40, BPSH 40 with 30 wt % Phosphotungstic Acid (PTA), and BPSH 40 with 30 wt % Zirconium Hydrogen Phosphate (ZrP).....	155
Figure 4-8: Methanol Permeability of BPSH 35, BPSH 35 with 30 wt % Phosphotungstic Acid (PTA), and BPSH 35 with 30 wt % Zirconium Hydrogen Phosphate (ZrP) Between 30°C and 80°C.....	157
Figure 4-9: Water Self-Diffusion Coefficient of BPSH 35, BPSH 35 with 30 wt % Phosphotungstic Acid (PTA), and BPSH 35 with 30 wt % Zirconium Hydrogen Phosphate (ZrP).....	159
Figure 5-1: Chemical Structure of the PATS Copolymer.....	169
Figure 5-2: Protonic Conductivity of High MW and Low MW PATS Copolymers.....	176
Figure 5-3: Water Uptake of High MW and Low MW PATS Copolymers.....	177
Figure 5-4: Methanol Permeability of High MW and Low MW PATS Copolymer Membranes - Fully Hydrated Membranes at 30°C.....	180
Figure 5-5: Selectivity of High MW and Low MW PATS Copolymers.....	181
Figure 5-6: Dynamic Tensile Modulus of High MW and Low MW PATS Copolymer Membranes.....	183
Figure 6-1: Membrane Electrode Assembly and Gas Diffusion Layer Resistances of Components and Interfaces.....	191
Figure 6-2: Chemical Structure of Nafion.....	194
Figure 6-3: Chemical Structure of BPSH.....	195
Figure 6-4: Chemical Structure of Bisphenol AF-Based Poly(Arylene Ether Sulfone) Copolymer (6F).....	196
Figure 6-5: Comparison of Methanol Permeability For Free-standing Membranes and Membrane Electrode Assemblies.....	204

Figure 6-6: Comparison of Methanol Permeability, Protonic Conductivity, and Relative Selectivity for BPSH and 6F Copolymers – 80°C in Liquid Water .....	208
Figure 6-7: DMFC Polarization Curves for Nafion 117, BPSH, and 6F MEAs – 80°C 0.5M CH <sub>3</sub> OH .....	210

## LIST OF TABLES

Table 1-1: An Overview of Fuel Cells <sup>1</sup> .....	3
Table 1-2: Dielectric Constant of Nafion 1100 as a Function of Membrane Water Content <sup>19</sup> ...	28
Table 2-1: Water Uptake and Lambda Values for the Copolymers.....	94
Table 3-1: A Comparison of Selected BPSH Properties with Nafion 117 .....	119
Table 3-2: Electro-osmotic Drag Coefficients ( $E_{Dcalc}$ ) Calculated Convective Velocity from Convective, Comparison to Experimentally Determined Electro-osmotic Drag Coefficient ( $E_{Dexp}$ ).....	128
Table 4-1: Comparison of Nafion and BPSH 35 Water Uptake and Transport Properties – 30°C Fully Hydrated Membranes .....	161
Table 5-1: Intrinsic Viscosity and Molecular Weight for Low MW and High MW PATS Copolymers .....	175
Table 5-2: Lambda Values for .....	179
Table 6-1: Membrane and MEA Conductivities for BPSH and Nafion Copolymers.....	206
Table 6-2: Membrane and MEA Conductivities for 6F Copolymers .....	209
Table 6-3: Comparison of Membrane Conductivities and Hydrogen/Air High Frequency Resistance for BPSH Copolymers and Nafion .....	211

# CHAPTER 1. LITERATURE REVIEW

## 1.1 Proton Exchange Membrane Fuel Cells – Applications and Systems

This dissertation will focus on elucidating the transport properties and structure of a new class of proton exchange membranes (PEM), which may have application in both hydrogen and direct methanol fuel cells. Specifically, the goals of this dissertation are to correlate the chemical structure of the membrane, the binding of water in the membrane's morphology, and the transport of protons, methanol, and water through the membrane. Ultimately, these transport properties will determine the membrane's performance in a fuel cell environment. This study is motivated by the need to determine which features of copolymer chemical structure may be more advantageous for use in fuel cells.

To begin, general fuel cell concepts will be outlined followed by a review of the current membrane literature and discussion of equipment and systems. Once sufficient understanding of the physical systems has been developed, characteristics of the membranes will be discussed in detail.

### 1.1.1 General Fuel Cell Concepts

Fuel cells offer the promise of a low-polluting, highly efficient energy source, which can be designed to utilize an almost limitless abundance of fuel. In their most basic form, fuel cells use hydrogen and oxygen from the air to create water and electricity. With the goal of achieving

more environmentally friendly energy sources that do not rely so heavily on fossil fuels, fuel cells have become the leading candidate to replace internal combustion engines and other lower energy density power storage devices such as batteries.

The basic principle of fuel cells was discovered in 1839 by Sir William Grove.<sup>1</sup> However, fuel cells found their first major application when NASA utilized hydrogen-powered fuel cells to produce electricity and water for the Gemini space missions.<sup>2</sup> The high cost and short lifetimes of these systems has prevented the use of fuel cells in mass markets. Although the comparison between fuel cells and batteries is obvious because they serve many of the same applications, fuel cells differ from batteries in two distinct characteristics. First, fuel cells are considered to be energy conversion devices whereas batteries are both energy storage and energy devices. Fuel cells do not need to be recharged with an external source of power such as batteries, they simply need to be replenished or refilled with an appropriate fuel. This brings up the second major difference between batteries and fuel cells; the fuel in a battery is stored internally, whereas a fuel cell stores its fuel externally to its core components.

Since 1984, the U.S. Department of Energy (DOE) has funded research in fuel cell technology. This has led to an explosion in the growth of fuel cell research efforts and the commercialization of fuel cell technology. DOE has recently announced that it will reduce funding for hybrid electric vehicles and concentrate efforts on the widespread commercialization of fuel cells. This

---

1. Zalbowitz, M., S. Thomas, *Fuel Cells: Green Power*, Department of Energy 1999.

2. Appelby, A., *Scientific American* **1999**, 74-79.

refocusing of governmental resources is complimented by the private efforts being undertaken by the automotive and other major companies.

The major types of fuel cells, classified by the type of electrolyte, are outlined in Table 1-1.

**Table 1-1: An Overview of Fuel Cells<sup>1</sup>**

Fuel Cell	Electrolyte	Operating Temperature (°C)	Electrochemical Reactions
Polymer Electrolyte Membrane (PEMFC)	Solid organic polymer	30-80	Anode: $\text{H}_2 \rightarrow 2\text{H}^+ + 2\text{e}^-$ Cathode: $\frac{1}{2}\text{O}_2 + 2\text{H}^+ + 2\text{e}^- \rightarrow \text{H}_2\text{O}$ <hr/> Cell: $\text{H}_2 + \frac{1}{2}\text{O}_2 \rightarrow \text{H}_2\text{O}$
Alkaline (AFC)	Aqueous solution of potassium hydroxide soaked in a matrix	90-100	Anode: $\text{H}_2 + 2(\text{OH}^-) \rightarrow 2\text{H}_2\text{O} + 2\text{e}^-$ Cathode: $\frac{1}{2}\text{O}_2 + \text{H}_2\text{O} + 2\text{e}^- \rightarrow 2(\text{OH}^-)$ <hr/> Cell: $\text{H}_2 + \frac{1}{2}\text{O}_2 \rightarrow \text{H}_2\text{O}$
Phosphoric Acid (PAFC)	Phosphoric acid soaked in a matrix	175-200	Anode: $\text{H}_2 \rightarrow 2\text{H}^+ + 2\text{e}^-$ Cathode: $\frac{1}{2}\text{O}_2 + 2\text{H}^+ + 2\text{e}^- \rightarrow \text{H}_2\text{O}$ <hr/> Cell: $\text{H}_2 + \frac{1}{2}\text{O}_2 \rightarrow \text{H}_2\text{O}$
Molten Carbonate (MCFC)	Solution of lithium, sodium, and/or potassium carbonates soaked in a matrix	600-1000	Anode: $\text{H}_2 + \text{CO}_3^{2-} \rightarrow \text{H}_2\text{O} + \text{CO}_2 + 2\text{e}^-$ Cathode: $\frac{1}{2}\text{O}_2 + \text{CO}_2 + 2\text{e}^- \rightarrow \text{CO}_3^{2-}$ <hr/> Cell: $\text{H}_2 + \frac{1}{2}\text{O}_2 + \text{CO}_2 \rightarrow \text{H}_2\text{O} + \text{CO}_2$  (CO <sub>2</sub> is consumed at anode and produced at cathode, thus it is included in each side of the equation)
Solid Oxide (SOFC)	Solid zirconium oxide with a small amount of yttria	600-1000	Anode: $\text{H}_2 + \text{O}^{2-} \rightarrow \text{H}_2\text{O} + 2\text{e}^-$ Cathode: $\frac{1}{2}\text{O}_2 + 2\text{e}^- \rightarrow \text{O}^{2-}$ <hr/> Cell: $\text{H}_2 + \frac{1}{2}\text{O}_2 \rightarrow \text{H}_2\text{O}$

This thesis research will focus on polymer electrolyte membrane fuel cells (PEMFC). This class of fuel cells currently operates at moderate temperatures (30°C to 80°C) and uses a hydrated polymer-based electrolyte membrane (PEM) to separate the fuel and oxidizer compartments and to conduct protons from the anode to the cathode. The basic geometry of a fuel cell is shown in Figure 1-1.

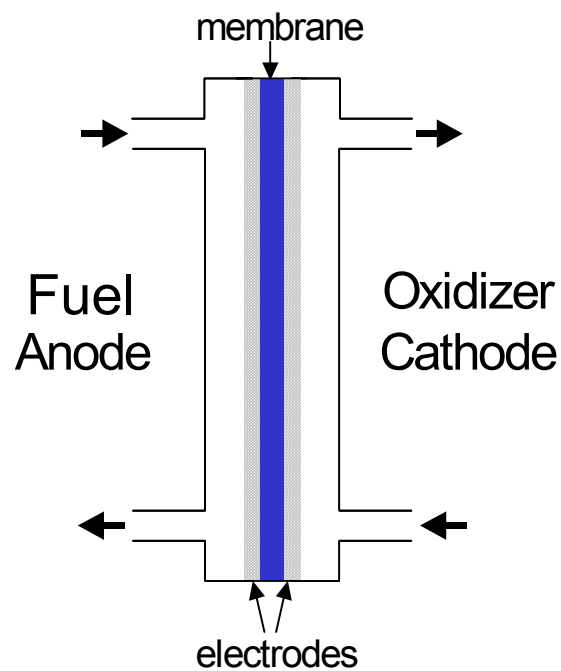


**Figure 1-1: Basic Fuel Cell Components**

### 1.1.2 Polymer Electrolyte Membrane Fuel Cells

Polymer electrolyte fuel cells were the first type of fuel cell demonstrated in the space flight program. Originally, the proton exchange membrane (or alternatively polymer electrolyte membrane) was a sulfonated poly(styrene divinylbenzene) copolymer. These membranes

showed very poor lifetimes due to oxidative degradation of the polymer backbone. In 1968 DuPont commercialized a proton exchange membrane based on poly(perfluorosulfonic acid) under the trade name Nafion.<sup>3</sup> The highly fluorinated structure shown in Figure 1-2 displays a much greater resistance to degradation in a fuel cell environment and thus increasingly longer fuel cell lifetimes.

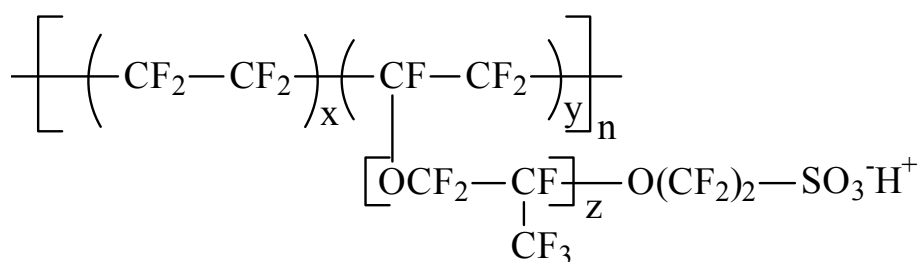


**Figure 1-2: Chemical Structure of Nafion**

Since then, other companies, such as Asahi in Japan and briefly Dow in the U.S., have investigated membranes based on poly(perfluorosulfonic acid) structures, but Dow has exited the business and Asahi remains a small player. Nafion has remained the industry standard proton exchange membrane and almost all current PEM fuel cell research from a device standpoint focuses on this type of electrolyte. Major applications for Nafion also include chlorine synthesis via electrolysis (chlor-alkali processes).<sup>4</sup>

---

3. Grot, W., To E.I. du Pont de Nemours and Company, U.S. 3,718,627, 1968.

4. Berzins, T., *J. Electrochem. Soc.* **1977**, 124(8), C318.

Moderate operating temperatures for PEM fuel cells are required because of the need for aqueous proton transport and the polymers used have relatively low glass transition temperatures ( $T_g$ ), especially when hydrated. Polymeric electrolytes based on sulfonic acid ion conducting sites require humidified reactant streams to hydrate the membrane and increase its conductivity. In current poly(perfluorosulfonic acid) copolymer membranes, hydration must be quite high to produce sufficient conductivity, restricting the operating temperatures of PEM fuel cells to about 80°C to prevent membrane or catalyst layer dry out. One current thrust of fuel cell research is to increase the operating temperature of PEM fuel cells to 120°C or above. This may be possible by producing membranes that retain water and conductivity and are more thermally and mechanically robust at high temperatures.

A single PEM fuel cell illustrated in Figure 1-1, but there are few devices that can operate on just a single membrane because its power output is typically less than 0.5 Watts. An increase in power output of a fuel cell is achieved by integrating single cells in series by constructing a fuel cell stack where the voltage of each single cell is additive. A fuel cell stack of three membranes is shown in Figure 1-3.

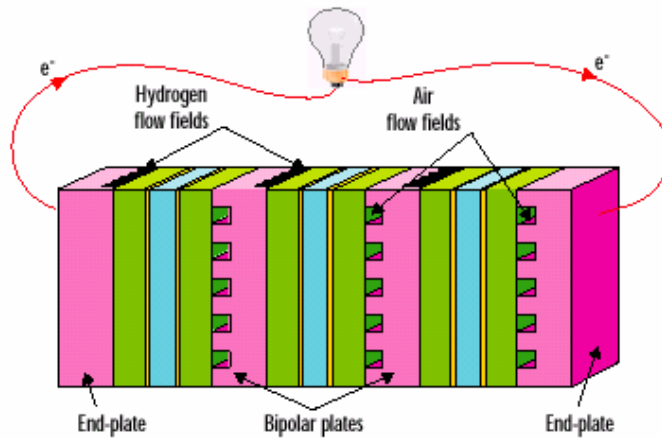


**Figure 1-3: Fuel Cell Stack<sup>1</sup>**

Thus far, PEM fuel cells have shown the most promise in automotive and portable power microelectronics applications. Renewed interest in the commercial development of fuel cells has fostered much research into new proton exchange membranes. Requirements for the next generation proton exchange membranes include; high protonic conductivity over a range of water contents, dimensional stability in hydrated, high temperature environments, low reactant permeation, and low electrical conductivity.

The desired balance of properties of the proton exchange membrane change depending on the choice of fuel. The following sections will outline the specific details of both hydrogen/air and methanol/air fuel cells and the types of proton exchange membranes used in each.

### 1.1.3 Hydrogen and Reformate Fuel

At this time, hydrogen is the fuel of choice for high performance, high power fuel cell applications. Hydrogen powered fuel cells are also the “greenest” fuel cells since their only product is water. However, hydrogen has no current distribution infrastructure and is difficult to store under normal conditions. Containment and distribution problems remain to be solved before hydrogen fuel can function on a large scale.

One advantage of hydrogen is that it undergoes easily catalyzed reactions under mild conditions. At the anode, hydrogen is oxidized to liberate two electrons and two protons:



The protons are conducted from the catalyst layer through the proton exchange membrane and the electrons travel through the electronic circuit. At the cathode, oxygen is reduced



to give the overall cell reaction:



Both reactions can be catalyzed by nanocrystalline platinum (often dispersed on carbon black), but other modified catalysts are often used to minimize carbon monoxide poisoning at the anode. As an example, most state-of-the-art anode catalysts are alloys of platinum and ruthenium supported on carbon black. The ruthenium helps to maintain fuel cell performance even when hundreds of parts per million of carbon monoxide in the anode feed stream, while the carbon black support increases the surface area of the heterogeneous catalyst to increase utilization.

Nafion is the most prevalent copolymer membrane used in hydrogen fuel cells. Specifically, Nafion 1135 (1100 equivalent weight, 3.5 mils thick) and Nafion 112 (1100 equivalent weight, 2 mils thick) are the products most often used. Thinner membranes can be used because the decrease in cell resistance more than offsets any performance losses associated with the permeability of hydrogen and oxygen through the membrane. Even though poly(perfluorosulfonic acid) copolymer membranes are expensive, they are the standard by which other membrane candidates are judged.

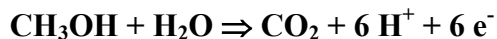
The principles outlined for pure hydrogen fuel cells also apply to reformat fuel cell systems. Reformate catalytically derived from hydrocarbons is typically 40 % nitrogen 20 % carbon dioxide and 40 % hydrogen, with trace impurities of carbon monoxide. The challenge of reformat systems is to overcome the dilution of hydrogen by the non-reactive gases and reduce the effect of carbon monoxide poisoning on platinum-based catalysts. Reformate systems are attractive for on-board reforming of traditional hydrocarbon fuels such as diesel fuel, gasoline, or even methanol. This addresses some of the distribution and storage problems that are yet to be overcome with hydrogen.

Perhaps the largest current challenge (together with high cost and reliability) for the widespread use of fuel cells in automobiles is their low operating temperature. Current membrane technology dictates that the maximum temperature for hydrogen fuel cells remains at about 80°C. The small difference between ambient and operating temperature makes it hard to remove excess heat from the system generated by the electrochemical reactions. Increasing the operating temperature would create more high quality waste heat to be used in the system e.g. to heat a home or radiated to the environment. Raising the operating temperature of hydrogen fuel cells simultaneously solves many problems with current systems. Membrane development programs for hydrogen fuel cells focus almost exclusively on raising the operating temperature of the cell while remaining mechanically stable and low-cost. One may conclude that high temperature operation (e.g. 120-150°C) is one area where the Nafion systems have limitations as a PEM.

#### 1.1.4 Methanol Fuel

Methanol is the most attractive of the hydrocarbon fuels because the relative ease of oxidation at the anode to liberate protons and electrons. In particular, methanol fuel cell research has focused on the direct oxidation of liquid methanol from a methanol/water solution fed to the anode. In the direct methanol fuel cell anode reaction, methanol and water are oxidized to liberate electrons and protons as follows:

**Equation 1-4**



The cathode reaction is similar to a hydrogen fuel cell:



To give an overall cell reaction of:



Note that even though water is cancelled out of the reactants side in the overall cell reaction, it is necessary at the anode for the oxidation of methanol.

The oxidation of methanol can also be achieved with nanocrystalline platinum, but alloys of platinum and ruthenium are currently the catalysts of choice. For the most part, direct methanol fuel cells rely on unsupported catalysts because the precious metal loadings need to be much greater than what carbon supported catalysts can provide. Very fine metal or alloy nanoparticles with diameters on the order of 3-10 nm are used to increase activity.

Even though the reaction stoichiometry dictates that only one molecule of water is necessary to catalyze methanol oxidation at the anode (23 M solution), direct methanol fuel cells are usually fueled with a much lower methanol feed concentration, usually between 0.3 M to 2 M methanol in water. The primary reason for operating direct methanol fuel cells with a low methanol feed

concentration is related to the methanol permeation through the proton exchange membrane. If the methanol concentration is lowered at the anode, there is less of a driving force for the unoxidized methanol to diffuse across the membrane. Methanol that is not oxidized at the anode can diffuse through the proton exchange membrane and react at the cathode. This problem is most often called “methanol crossover.” Methanol that diffuses across the membrane reacts at the cathode, removing available catalytic sites from the oxygen reduction reaction, thus causing a mixed potential at the cathode. Diffusion of methanol through the membrane acts essentially as “chemical short circuits” in the fuel cell and lowers the open circuit voltage, the voltage efficiency of the cell, and the overall fuel efficiency of the system.

Diluting the methanol feed stream with excess water to combat methanol crossover presents a problem of water management within the cell. The electrodes need to maintain a good three-phase interface between the reactant gases, electrical conductivity (catalyst), and ionic conductivity (ion conducting polymer). If the electrodes are too wet, the reactant gas pathways to the catalyst are blocked and the reactions cease. As the current density of the device increases, the chance for flooding (excess water buildup) at the cathode increases. In addition, diluting the methanol with water greatly decreases the fuel density of the stored methanol. This discussion of water management relates to a phenomenon called electro-osmotic drag, wherein water molecules are transported across the proton exchange membrane in direct proportion to the current density. Electro-osmosis will be discussed in detail later.

Direct methanol fuel cells have not developed as rapidly as hydrogen fuel cells largely because Nafion membranes are very poor methanol barriers. Typically, a relatively thick Nafion 117

(1100 equivalent weight, 7 mils thick) is used for direct methanol fuel cells. Any performance penalties associated with the increased resistance of a thicker membrane are more than offset by the complimentary decrease in methanol crossover. There has been much fuel cell engineering to combat methanol crossover in Nafion-based direct methanol fuel cells, but the results are still not sufficient to promote direct methanol fuel cells for wide-ranging commercialization. Consequently, methanol crossover is a central issue of much of the new membrane development in direct methanol fuel cell research.

#### 1.1.5 The Membrane Electrode Assembly

Catalysts and membranes are parts of the basic unit of the fuel cell, the membrane electrode assembly (MEA). The membrane electrode assembly consists of two electrically and ionically conductive electrodes containing the platinum catalyst bonded to the proton exchange membrane. A schematic of the MEA with accompanying electrochemical reactions is shown in Figure 1-4.

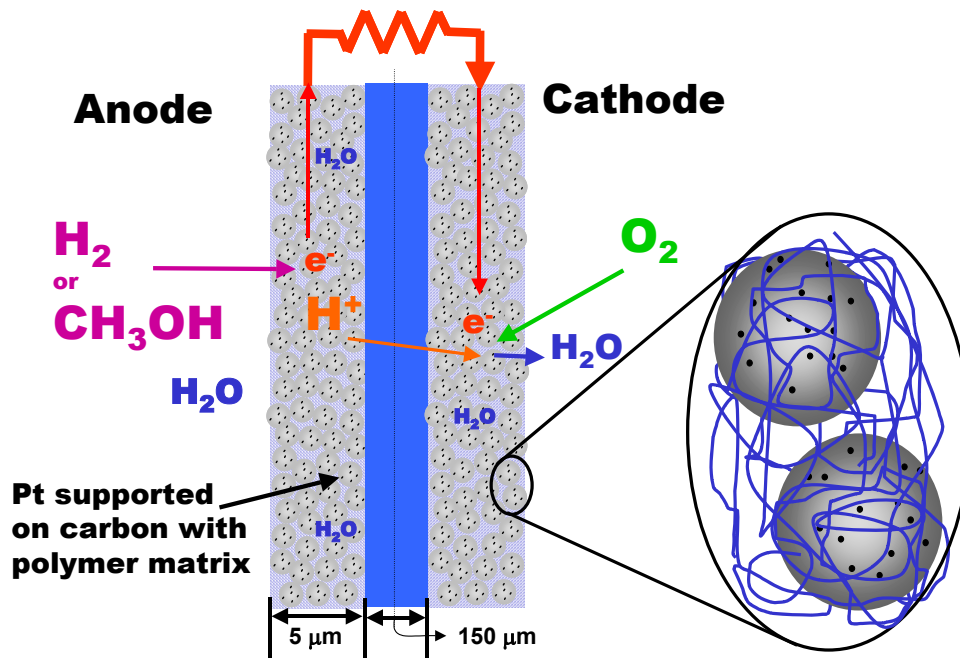


Figure 1-4: MEA Schematic

The electrodes can contain either unsupported (methanol fuel cells) or supported (hydrogen fuel cells) catalysts and are usually composed of the same copolymer as the proton exchange membrane. The precious metal loading is determined by the amount of catalyst per active area and the ionomer content of the electrode can vary between 5-20 weight %, depending on the application requirements.

Two basic methods for bonding the electrodes to the proton exchange membrane have been developed. Both methods involve making a catalyst “ink” composed of the ion conducting copolymer dispersed in a diluent (usually 5% polymer by weight), the catalyst particles, and any other additives to ease processing. In the first method, this ink is painted directly onto the

membrane and dried to form the condensed catalyst layer or electrode. This method requires that the ink solution does not dissolve the membrane during painting, or otherwise compromise its integrity during the painting process. After painting, the MEA is ready to be placed into the fuel cell or processed further before fuel cell testing.<sup>5</sup>

In the second, two-step method, the catalyst ink is first painted and dried onto a decal or “blank” the size of the desired active area. The painted and dried decal is then hot-pressed against the membrane at temperatures of typically 150-200°C and pressures of 3000 psi, to bond the composite in the electrode to the membrane. If the correct conditions and decal are chosen, the electrode can become well adhered to the membrane and the decal can simply be peeled off.<sup>6</sup> Each method has its advantages and disadvantages, which will be noted later as appropriate.

Since the MEA is the heart of a fuel cell, considerable ongoing research is attempting to elucidate its exact structure and component interactions. The phenomena of “break in” and aging of the MEA structure is of major concern. Break in relates to the slow increase in performance observed over the first 24 hours once a fresh MEA is placed in a fuel cell and aging is, of course, the slow degradation of performance during long-term fuel cell operation. Researchers are investigating the electrode and membrane structure, and interaction between the membrane and electrode for possible physical changes that may be occurring over time, in order to correlate these physical property changes with fuel cell performance.

---

5. Ren, X., S. Gottesfeld, To The Regents of the University of California, U.S. 6,296,964, 1999.

6. Wilson, M., To The Regents of the University of California, U.S. 5,211,984, 1993.

### 1.1.6 The Future of Fuel Cells

In February 2002, Secretary of Energy Spencer Abraham announced the replacement of the Partnership for a New Generation Vehicle (PNGV) with a program named Freedom Cooperative Automotive Research or Freedom CAR.<sup>7</sup> PNGV was started in 1993 and focused on increasing the fuel efficiency of vehicles to 80 miles per gallon by 2004. Even though fuel cell research was funded under the PNGV umbrella, Freedom CAR represents a shift of focus from improving traditional internal combustion engine technology to a concentrated effort to make fuel cell powered cars available to consumers by 2010. About this time, Daimler Chrysler unveiled its fuel cell concept car, AUTOmomy, powered by Ballard fuel cell stacks.<sup>8</sup> What was unique about Daimler Chrysler's concept besides being fuel cell powered was that its body shapes could be interchanged from a sedan, to a mini-van, to even a pickup truck all using the same chassis. Not only are fuel cells going to usher in a new age of vehicle power, but they may also open new design concepts in transportation.

## 1.2 Commercial Proton Exchange Membranes for Fuel Cells

There are several commercially available proton exchange membranes and MEAs. By far, the majority of the commercially available systems are based on Nafion. Nafion also has the largest body of literature devoted to its study because of its industrial importance. Not only are Nafion membranes important, but Nafion composite systems have become important in the industrial

---

7. Brown, A., *Chemical Engineering Progress* **2002**, 98(2), 12-14.

8. [www.money.cnn.com/2002/01/08/autos/auto\\_tech/](http://www.money.cnn.com/2002/01/08/autos/auto_tech/) January 8, **2002**.

and academic research realm. In composite structures, Nafion can be impregnated into an inert matrix (i.e. Gore membranes<sup>9</sup>), or additives can be added to a supporting Nafion matrix for improved physical or electrochemical properties.

There are currently very few commercial alternatives to Nafion membranes for fuel cell applications. In addition to the Gore membranes, the only other alternatives are Ballard Advanced Materials (BAM), and Dais membranes. Ballard and Dais membranes are apparently used primarily in-house and are not widely available. This section will highlight a small, but critical fraction of the research that has been conducted on Nafion. Topics discussed will include Nafion's microphase separated morphology, its conductivity and solvent uptake, and research involving electro-osmosis. This section will then briefly outline the general features and properties of Ballard, Gore, and Dais materials, using limited published information. Critical factors for proton exchange membranes are protonic conductivity, reactant impermeability (low methanol, hydrogen, and oxygen permeability), low water transport through electro-osmotic drag, mechanical integrity, and cost.

### 1.2.1 Nafion

Nafion is by far the leading membrane in all types of PEM fuel cells. It was first conceived during the space program in the 1960's.<sup>3</sup> The chemical structure of Nafion is shown in Figure 1-5.

---

9. Bahar, B., C. Cavalca, S. Cleghorn, J. Kolde, D. Lane, M. Murthy, G. Rusch, *J. of New Matl. for Electrochem. Syst.* **1999**, 2(3), 179-182.

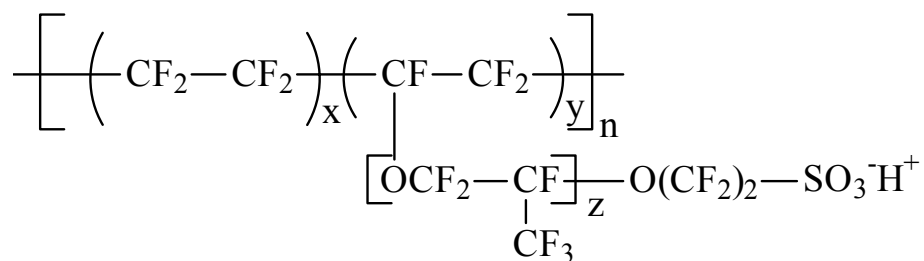


**Figure 1-5: Chemical Structure of Nafion**

It is prepared by the free radical copolymerization of tetrafluoroethylene and the sulfonated comonomer. About 13 mole % of the vinyl ether containing a pendant sulfonyl fluoride is employed to afford the proper equivalent weight (milli-equivalents of sulfonic acid/gram polymer) for fuel cell applications (usually 1100 meq/g). The sulfonyl fluoride is subsequently hydrolyzed to the sulfonic acid once the polymer has been converted to membrane form.

Nafion has stood the test of time as a commercial product, and thus been studied for decades. However, with all of the research centered on Nafion and its physical properties, questions remain. Current research on Nafion's microstructure, conductivity, transport properties, and electro-osmosis will be reviewed in light of the research performed in the experimental section of this thesis.

### 1.2.1.1 Morphology

#### *Morphology by Indirect NMR Relaxation Studies*

Magic angle spinning NMR experiments have used the different backbone ( $\text{CF}_2$ ) and pendant chain ( $\text{OCF}_2$  and  $\text{CF}_3$ ) resonance signals to learn information about the proposed reverse micellar domain structure of both dry Nafion membranes and membranes swollen with water and ethanol.<sup>10</sup> Spin diffusion experiments showed that in dry Nafion the thickness of the pendant group domain was found to be 3.8 nm, with a periodicity of about 10nm. This analysis assumed that the domain structure was composed entirely of pendant group domains and backbone  $\text{CF}_2$  domains. Xenon-129 NMR diffusion data was used to support the two-domain model of separate pendant chain domains and backbone domains. Upon addition of 20 wt % water, the domains swelled to 6.8 nm, without a change in overall periodicity. However, with 20 wt % ethanol addition, the domains were measured to be 11nm with a periodicity of 19nm. The authors attributed the increased swelling of Nafion in ethanol to a morphological rearrangement. A morphological rearrangement is possible, but the swelling medium's dielectric constant may play a larger role in the observed domain size.

---

10. Meresi, G., Y. Wang, A. Bandis, P.T. Inglefield, A.A. Jones, W-Y. Wen, *Polymer* **2001**, 42, 6153-6160.

## Morphology by X-ray Scattering

X-ray scattering was employed to elucidate the morphological differences between commercial Nafion membranes and similar membranes recast from aqueous/alcohol dispersions.<sup>11</sup> With the commercial membranes, a crystalline reflection (attributed to crystallites in the PTFE-like backbone) superimposed on an amorphous halo was observed in the dry membrane. Upon hydration, the crystalline reflection steadily decreased and the amorphous halo disappeared as shown in Figure 1-6.

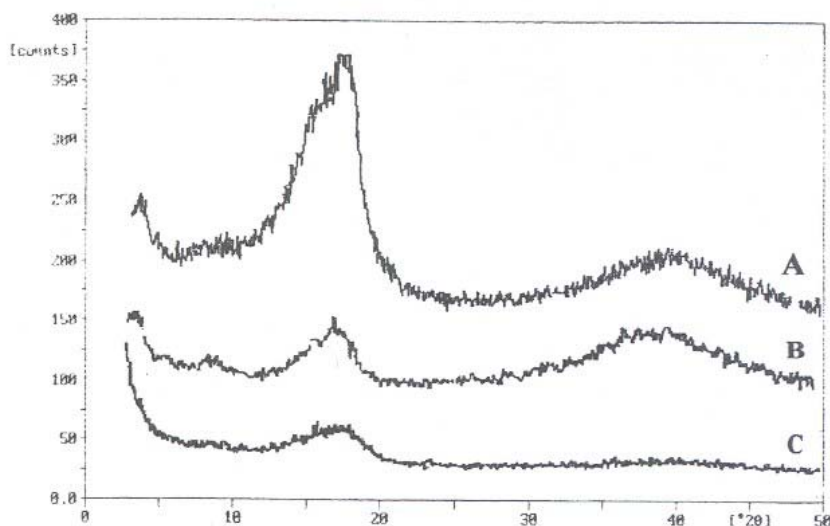


Fig. 9. A: dried Nafion-117 membrane; B: medium hydrated Nafion-117 membrane; C: fully hydrated Nafion-117 membrane.

## Figure 1-6: X-Ray Scattering of Nafion Membranes and Different Levels of Hydration<sup>11</sup>

---

11. Laporta, M., M. Pegoraro, L. Zanderighi, *Macromolecular Materials and Engineering* **2000**, 282, 22-29.

This behavior suggests that any order in the polymer is destroyed upon hydration or the features in the hydrated membranes are of such a size as to be undetectable by this method. The diffractograms of the recast Nafion membrane showed similar features to that of commercial Nafion once the recast membranes were annealed at 473K for 1 hour as shown in Figure 1-7.

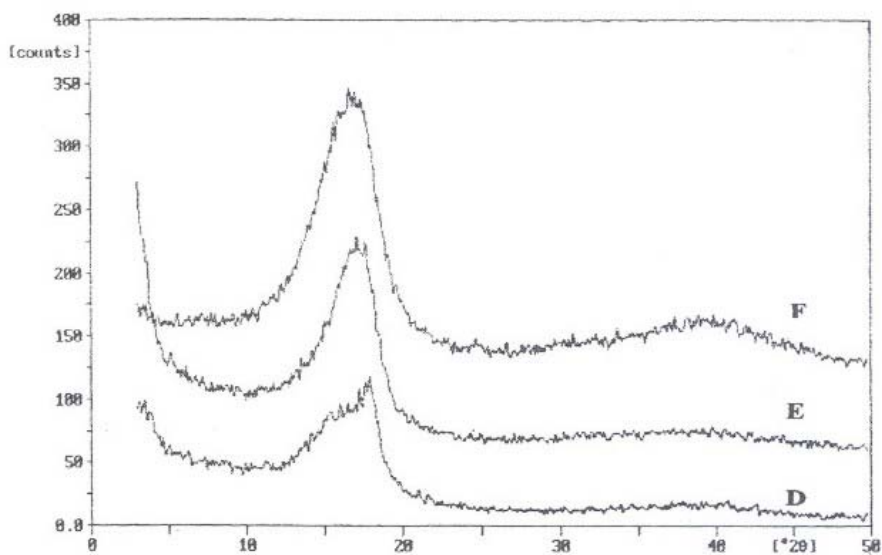


Fig. 10. D: NCD membrane *with* annealing; E: NCD membrane *without* annealing; F: *aI* membrane *without* annealing.

### Figure 1-7: X-ray Reflections Comparing Recast Annealed Membranes<sup>11</sup>

Thus, simply casting and vacuum drying the Nafion from aqueous/alcohol solutions at low temperatures is not sufficient to produce a membrane that is similar to the commercial product. The difference between commercial Nafion membranes and recast membranes is especially

evident in water uptake and conductivity experiments as will be discussed later. It is not well appreciated that the commercial film is apparently extruded in the sulfonyl fluoride ( $-\text{SO}_2\text{F}$ ) form and then subsequently hydrolyzed to the sulfonic acid ( $-\text{SO}_3\text{H}$ ). This has caused discrepancies in the literature when researchers have reported data on Nafion without being meticulous about its source and process history.

Gebel investigated the structural evolution of perfluorosulfonated ionomer membranes upon increasing hydration.<sup>12</sup> The scattering maximum or “ionomer peak” was observable up to very large water contents of 65 wt %. When the scattering results are taken in the context of swelling and conductivity experiments, a phase inversion of the membrane was observed at a water content of 50 wt %. Perfluorosulfonated ionomer membranes with high water contents were formed by placing the membranes in autoclaves with water at 120°C for a few hours. A model was proposed where the sulfonic acid domains remain as cylindrical pores with the sulfonic acid groups on the edges of the pores surrounded by an unsulfonated matrix until the water content reaches 50 wt %. At this point a phase inversion occurs where unsulfonated matrix is no longer continuous and the sulfonic acid groups reside on the outside of rod-like micellar structures. This model can give some insight as to the reverse casting process from aqueous/alcohol solutions. Cast membranes must be annealed to consolidate the reverse micellar geometry and regain the original membrane’s swelling and conductivity properties. The residual crystallinity of the PTFE-based backbone is another complicating feature.

---

12. Gebel, G., *Polymer* **2000**, 41, 5829-5838.

Elliot et al.<sup>13</sup> attempted to provide a model for Nafion membranes during swelling through SAXS. They cite the seeming discrepancy between the bulk membrane swelling, the microscopic or domain swelling, and existing SAXS data. The authors assigned the broad reflection in the SAXS patterns to individual ionic clusters. The upturn at low scattering angles referred to as “cluster peak” or “ionomer peak” is assigned to the interference between the individual spherical ionic clusters or some other larger cluster formation. The authors performed SAXS measurements on oriented membranes. The diffraction patterns from the drawn membranes evolved in such a way that the authors were able to assign the “cluster peak” to agglomerates of the smaller clusters observed in the Bragg reflection. Interparticle scattering models are not able to rectify the difference between microscopic domain swelling and macroscopic bulk swelling of the membrane because they assume an affine expansion.<sup>14</sup> Careful inspection of the SAXS patterns by the authors using a maximum entropy model showed that the number of scattering centers was indeed decreasing as the membrane becomes more hydrated. This reorganization of the ionic structure of the material is due to the constraints of the fluoropolymer matrix that surrounds the ionic domains of the material.

### *Morphology by AFM*

Until quite recently it was difficult to directly observe the microphase separated domain structure of Nafion. Many of the traditional techniques such as TEM, x-ray scattering, and SEM were not able to provide direct evidence of domain structure in sulfonic acid proton conductors. High-

---

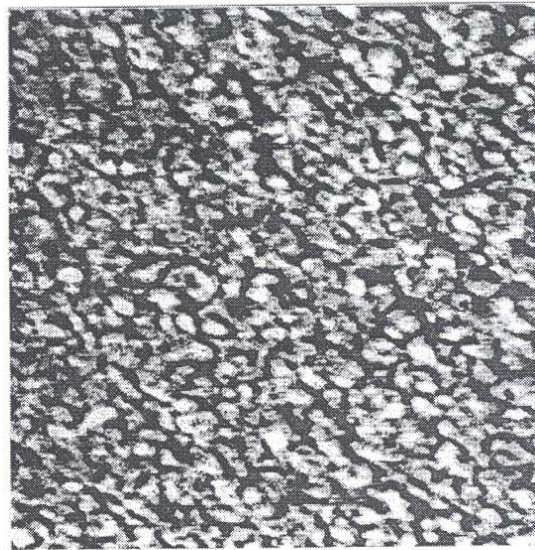
13. Elliot, J.A., S. Hanna, A.M.S. Elliot, G. E. Cooley, *Macromolecules* **2000**, 33, 4161-4171.

14. MacKnight, W.J., W.P. Taggart, R.S. Stein, *J. Polym. Sci., Polym. Symp.* **1974**, 45, 118.

resolution imaging of both the ionic and crystal domains in Nafion was achieved using novel AFM techniques.<sup>15</sup> The researchers used the AFM to confirm the reverse micellar model of Nafion with the sulfonic acid side chains forming domains in an unsulfonated matrix of backbone material. In the unswollen membrane under ambient humidity conditions, domains in the size range of 4-10nm were observed. When the Nafion 117 membranes were soaked in deionized water, domains of 7-15 nm were observed and the domains developed a more continuous character, forming large channels of an ion rich phase (Figure 1-8).

---

15. McLean, R.S., M. Doyle, B.B. Sauer, *Macromolecules* **2000**, 33, 6541-6550.



A



B

**Figure 8.** Low-energy phase images of Nafion 117 (K<sup>+</sup>) ionomer membrane after exposure to room temperature humidity (A) versus deionized water exposure (B). Only phase data are shown, and scan boxes are 300 × 300 nm with a scale of 0–80°.

**Figure 1-8: Nafion AFM Micrographs Before and After Swelling in Liquid Water – Boxes are 300 x 300 nm Width<sup>15</sup>**

The experiments in liquid water shown in the AFM micrograph correspond to a bulk swelling of 50%.

#### *Structure of Reconstituted Membranes by ESR and ENDOR*

Schlick et al.<sup>16</sup> used electron spin resonance and electro nuclear double resonance (ENDOR) to study the structure of reconstituted membrane both with and without annealing. They found that membranes recast from an ethanol-water mixture and annealed at 350K for about an hour gave similar spectra as the original membrane. In experiments involving membranes swollen with different solvents, the authors found that the distance of the counter cation and the fluorine group changed for different solvent mixtures. The ENDOR results show that the counter cations are closer to the polymer for membranes swollen with methanol than for membranes swollen with water or methanol/water mixtures. This supports the conclusion that for membranes swollen with water, the system separates into ionic and non-ionic domains with the ionic domains incorporating a large number of cations.

#### *Pore Structure of Nafion by Porosimetry Methods*

The pore structure of Nafion was explored by Divisek et al. using a new thermodynamic method of standard porosimetry.<sup>17</sup> The advantage of this method is that the porosity of the membrane

---

16. Schlick, S., G. Gebel, M. Pineri, G. Rius, F. Volino, *Colloids and Surfaces A: Physio. And Eng. Abs.* **1993**, 78, 181-188.

17. Divisek, J., M. Eikerling, V. Mazin, H. Schmitz, U. Stimming, Yu.M. Volkovich, *J. Electrochem. Soc.* **1998**, 145(8), 2677-2683.

can be studied using different solvents, in this case mostly water. The study of PEMs for fuel cells under their operating conditions is critical in understanding the behavior of these materials because the membrane properties are strongly influenced by their environment. Their measurements showed that there is a wide range of pore sizes in Nafion with an average value on the order of 2 nm, which is reasonably close to that observed by other methods.

#### *Confirmation of Spherical Morphology by Modeling*

An interesting means was taken by Li and Nemat-Nasser to model the microphase separated domain morphology of Nafion.<sup>18</sup> They used a minimization of free energy approach in the model to describe Nafion's spherical morphology. Their model was able to accurately predict the domain sizes for dry Nafion in a variety of cationic forms ( $H^+$ ,  $Li^+$ ,  $Na^+$ ,  $K^+$ ,  $Rb^+$ , and  $Cs^+$ ), Nafion with various water contents, and Nafion with different equivalent weights. Perhaps most interestingly, the model also predicts the transition from insulator to conductor upon hydration.

#### 1.2.1.2 Solvent Swelling Properties and Water/Methanol Transport

##### *Dielectric Study of Nafion - Conductivity and State of Water*

Paddison et al.<sup>19</sup> used dielectric spectroscopy to quantify the state of water in Nafion membranes and support conductivity measurements performed in a different geometrical cell (in-plane

---

18. Li, J.Y., S. Nemat-Nasser, *Mechanics of Materials* **2000**, 32, 303-314.

19. Paddison, S.J., D.W. Reagor, T.A. Zawodzinski, *J. Electroanal. Chem.* **1998**, 459, 91-97.

versus through-plane). This body of research demonstrated that the dielectric constant of Nafion varied strongly with water content. Their results show that the dielectric constant of Nafion membrane increases with increasing hydration and, like water, decreases with increasing frequency. The dielectric constant of dry Nafion was found to be 4 which compares to a literature value of 2 for pure Teflon. Dielectric constants were measured on membranes equilibrated with water vapor. Table 1-2 shows the results of these studies as a function of membrane water content.

**Table 1-2: Dielectric Constant of Nafion 1100 as a Function of Membrane Water Content<sup>19</sup>**

Water Vapor Activity	Water Content ( $\lambda$ )	Dielectric Constant ( $\epsilon'$ )
0.964	13	20
0.748	6	13
0.414	3	8
0.139	2	5
0	1	4

The increase in dielectric constant with water absorption of the membrane seems to indicate that past a certain point of critical water content the water in the membrane becomes loosely bound or loosely associated with the sulfonic acid groups. This information can be coupled with both the macroscopic membrane swelling, conductivity, and first principle modeling studies to support the idea that the first few water molecules absorbed by the membrane are tightly bound by the sulfonic acid group and not available to assist in proton conduction. Membranes that rely on sulfonic acid to conduct protons must be well hydrated to achieve a desirable level of conductivity in fuel cells. This fact does not bode well for higher temperature operation where water concentration is low and the membrane may become dehydrated.

Paddison et al.<sup>20</sup> also studied the dielectric spectra of post sulfonated poly(ether ether ketone) (PEEK) membranes. These systems have some chemical similarity to some of the copolymers produced in the McGrath group.<sup>21</sup> At similar water contents (on a sulfonic acid basis) the PEEK membranes displayed a much lower dielectric constant than the Nafion membranes. The authors asserted that this seemed to indicate that the water molecules are more tightly bound in the PEEK membranes. This hypothesis has been partially supported by quantum mechanical calculations for the first hydration sphere of sulfonic acid.<sup>22</sup> Another possible explanation is that the pores where the water resides does not have the same character in PEEK as in Nafion. Decreasing the size of the watery domains could have an effect on the dielectric constant of the swollen membranes and this hypothesis is still under investigation.

#### *Methanol Transport Through Nafion Membranes*

Methanol flux through MEAs composed of Nafion membranes was studied by an electrochemical method using DMFC hardware.<sup>23</sup> The major advantage of this method is that the methanol permeation through the entire MEA and gas diffusion backings is measured, instead of just the membrane permeation. This measurement is technologically important, because it can be performed on the exact geometry and materials of a working DMFC and the contributions of the gas diffusion backings and electrodes can be accounted for. Results from

---

20. Paddison, S.J., G. Bender, K.D. Kreuer, N. Nicoloso, T.A. Zawodzinski, *J. New Matl. for Electrochem. Sys.* **2000**, 3(4), 291-300.

21. Wang, F., M. Hickner, Y.S. Kim, T.A. Zawodzinski, J.E. McGrath, *J. of Membr. Sci.* **2002**, 197, 231-242.

22. Paddison, S.J., L.R. Pratt, T. Zawodzinski, D.W. Reagor, *Fluid Phase Equilibria* **1998**, 151, 235-243.

23. Ren, X., T.E. Springer, T.A. Zawodzinski, S. Gottesfeld, *J. Electrochem. Soc.* **2000**, 147(2), 466-474.

this experiment agree closely with those measurements made on stand-alone membranes, demonstrating that the membrane has the greatest resistance to methanol permeation. The activation energy of proton conduction for fully hydrated Nafion 117 membranes between 30°C and 130°C was found to be 2.3 kcal/mole while the activation energy of methanol diffusion was found to be 4.8 kcal/mole under the same conditions. Interestingly, this paper illustrates the importance of temperature and processing history on the properties of Nafion. Lower methanol permeation and proton conductivity was observed for a presumably more ordered membrane annealed at 100°C for about 12 hours. Membranes treated in 2M methanol at 130°C for over 6 hours showed the highest stable methanol permeation. The temperature and processing history of Nafion presumably changes the morphological arrangement of its domain structure. Annealing the dry membrane at high temperatures may eliminate some of the hydrophilic proton conductive domains decreasing conductivity and methanol permeation, while autoclaving the membrane in liquid methanol solutions may swell the hydrophilic domains and promote increased conductivity and methanol permeation.

#### 1.2.1.3 Protonic Conductivity

##### *Nafion Conductivity by Reflectance Technique*

A common theme in PEM research is to investigate membrane performance as a function of the level of membrane hydration. Anantaraman and Gardner<sup>24</sup> made conductivity measurements on

---

24. Anantaraman, A.V., C.L. Gardner, *J. Electroanal. Chem.* **1996**, 414, 115-120.

Nafion under various relative humidities using a coaxial probe reflectance technique. Because the gap of the probe is large compared to the membrane thickness, the authors assumed that the measured conductance represents an average membrane resistance. They found a sharp upturn in conductivity near 100% relative humidity indicating that those last molecules of loosely bound water play an important role in determining Nafion's high conductivity at high water contents.

Another set of experiments was performed where the membranes were exposed to a humidity gradient. In every case, the conductivity observed for these experiment was intermediate to that measured for the pure humidity case i.e. the conductivity of a sample with a gradient of 45/100 was intermediate to samples equilibrated at 45 or at 100. Measurements of local conductivity were also attempted using a small coaxial probe. With the small-probe geometry a more local conductivity measurement was made. The authors validated this technique by measuring the conductivity of a membrane with the probe contacting the 45% RH in a 45/100% RH cell ( $\sigma = 1.47 \cdot 10^{-3}$  S/cm) and then reversing the measurement with the probe contacting the 100 % side of the membrane ( $\sigma = 9.26 \cdot 10^{-3}$  S/cm). This technique could provide a possible method for measuring local conductivities in a fuel cell in-situ in response to various anode and cathode conditions.

## *Conductance of Nafion as a Function of Water Content and Temperature*

Temperature also has an important role in determining Nafion's conductivity. Cappadonia et al.<sup>25</sup> explored the effect of both water content and temperature on the conductivity of Nafion membranes. They found that the conductivity displayed two regions of Arrhenius behavior: a low temperature region with a high activation energy of conduction and a high temperature region with a low activation energy. The transition from the low to high temperature regime occurred at about  $-130^{\circ}\text{C}$  was hypothesized that this discontinuity in conductivity was due to the freezing of water (phase change) in the membrane at this temperature. The freezing point depression behavior observed corresponds to differential scanning calorimetry experiments performed by Chen et al.<sup>26</sup> and Rennie and Clifford<sup>27</sup> who defined a relationship between the freezing point depression of water confined in pores and the pore radius. These experiments corroborate the pore model of Nafion with loosely bound water in the pores providing the major impetus for conductivity.

Zawodzinski et al.<sup>28</sup> compared three chemically similar membranes' (Nafion 117, Membrane C, and Dow) water uptake and transport properties to describe the transport of mobile species in a fuel cell. The three transport properties they focused on were protonic conductivity, diffusion coefficient of water, and electro-osmotic drag coefficient. Even though all of the membranes

---

25. Cappadonia, M., J.W. Erning, S.M.S. Niaki, U. Stimming, *Solid State Ionics* **1995**, 65-69.

26. Chen, R.S., J.P. Jayakody, S.G. Greenbaum, Y.S. Pak, G. Xu, M.G. McLin, J.J. Fontanella, *J. Electrochem. Soc.* **1993**, 140, 889-895.

27. Rennie, G.K., J.J. Clifford, *J. Chem. Soc. Faraday Trans.* **1977**, 73, 680-689.

28. Zawodzinski, T.A., T.E. Springer, J. Davey, R. Jestel, C. Lopez, J. Valerio, S. Gottesfeld, *J. Electrochem. Soc.* **1993**, 140(7), 1981-1985.

studied were based on poly(perfluorosulfonic acid) conducting sites, the Dow membrane had a 50% greater conductivity in liquid water over a wide temperature range. The water content of the immersed membrane on a per sulfonate basis for the Dow membrane was about 15% higher than that of the other two. That, coupled with the lower equivalent weight (greater number of sulfonic acid groups) accounts for the increased conductivity even though the character of the perfluorosulfonic acid groups is identical. This would seem to imply that increasing the water content of a membrane would increase its conductivity. Producing a more swellable membrane through morphological or molecular weight mechanisms may be a method for increasing the conductivity of the membrane without adding additional acid functionality, although mechanical behavior might be affected.

#### *Nafion Conductivity in Water and Methanol solutions*

Edmondson et al.<sup>29</sup> studied Nafion 117 membranes swollen in various concentrations of methanol solutions. They found that as the methanol content of the membrane increased, its bulk ionic conductivity decreased. For instance, a membrane containing 40 wt % of a 1.4:1 molar methanol:water solution (whose water weight percent is 11.7) had the same conductivity of a membrane containing just 11.7 wt % water. The authors' assertion is that at high liquid contents, the conductivity of the membrane is dominated by the liquid phase and reflects the particular composition of the liquid phase. However, at low solution uptakes, once the conductivity of pure methanol is accounted for, a residual conductivity remains in a membrane completely saturated with methanol. The authors ascribe this residual conductivity to increased segmental motion of

---

29. Edmondson, C.A., P.E. Stallworth, M.C. Wintersgill, J.J. Fontanella, Y. Dai, S. Greenbaum, *Electrochemi. Acta* **1998**, 43(10-11), 1295-1299.

the polymer chains, specifically the sulfonic acid bearing side chains and support their conclusions with NMR measurements. This plasticization effect of both the side chains and the fluorine-based backbone could also account for Nafion's unusually high methanol permeability as noted earlier. The argument that segmental mobility plays a role in conductivity especially at low water contents could be an avenue for exploration in the area of high temperature membranes where the water concentration is low. By designing polymers with attached but "mobile" proton conductors, membranes could retain sufficient conductivity to operate well in fuel cells. Unfortunately, increased segmental motion usually accompanies a decline in polymer physical properties, such as modulus and strength.

In similar experiments from the same laboratory, the conductivity of various equivalent weights of Nafion was measured over a range of water contents.<sup>30, 31, 32</sup> The results were presented as conductivity versus lambda, or the molar ratio of water molecules to sulfonic acid sites. As anticipated, their plot clearly shows that membranes with a higher equivalent weight display greater conductivities for the same water content because there is more water per unit volume in higher equivalent weight membranes at a given lambda. They also noted that it has been shown that different equivalent weight Nafion membrane display similar conductivities, if they contain a given weight % water.

---

30. Wintersgill, M.C., J.J. Fontanella, *Electrochim. Acta* **1998**, 43(10-11), 1533-1538.

31. Fontanella, J.J., M.C. Wintersgill, R.S. Chen, Y. Wu, S.G. Greenbaum, *Electrochimica Acta* **1995**, 40(13), 2321-2326.

32. Chen, R.S., P.E. Stallworth, S.G. Greenbaum, J.J. Fontanella, M.C. Wintersgill, *Electrochimica Acta* **1995**, 40(3), 309-313.

#### 1.2.1.4 Electro-osmosis

Electro-osmosis measurements have been performed on poly(perfluorosulfonic acid) membranes (mostly Nafion) equilibrated with water in the vapor state.<sup>33,34</sup> Zawodzinski et al. introduced several unique ideas. They observed that the electro-osmotic drag coefficient for various poly(perfluorosulfonic acid) membranes (Nafion, Dow, and Membrane C) remained very close to 1.0 over a wide range of water vapor activities (membrane water contents of  $\lambda = 5-14$ ). Also, the electro-osmotic drag coefficient increased to 2.5 for membranes immersed in liquid water. They rationalized their results in light of two seemingly competing factors: increased water content facilitates proton conduction by a hopping mechanism and increased water content leads to greater electro-osmotic drag coefficients. As the membrane water content increases, the water contained in the membrane becomes more bulk-like, thus aiding proton conduction by hopping: this fact is not disputed by Zawodzinski<sup>35</sup> and others.<sup>36</sup> A larger contribution by hopping would seem to indicate a lower electro-osmotic drag coefficient, but that is not the case. Increasing bulk-like water in swollen membranes aids proton hopping, but the bulk-like water is more easily transported or dragged across the membrane by the movement of protons. These results highlight the electro-osmosis problem with direct methanol fuel cells. Because most DMFCs have a liquid feed on the anode, the operating conditions are more akin to fully hydrated

---

33. Zawodzinski, T.A., J. Davey, J. Valerio, S. Gottesfeld, *Electrochimica Acta* **1995**, 40(3), 297-302.

34. Fuller, T., J. Newman, *J. Electrochem. Soc.* **1992**, 139, 1332-1337.

35. Zawodzinski, T.A., M. Neeman, L.D. Sillerud, S. Gottesfeld, *J. Phys. Chem.* **1991**, 95, 6040-6044.

36. Kreuer, K.D., T. Dippel, W. Meyer, J. Maier, *Mat. Res. Soc. Symp. Proc.* **1993**, 293, 273.

membranes with high electro-osmotic drag. Hydrogen and reformat fuel cells with vapor feeds on anode and cathode may not suffer these high electro-osmosis problems.

Work by Ren and Gottesfeld<sup>37</sup> suggested that the electro-osmotic drag of various types of poly(perfluorosulfonic acid) membranes with varying chemical structures is quite similar as shown in Figure 1-9.

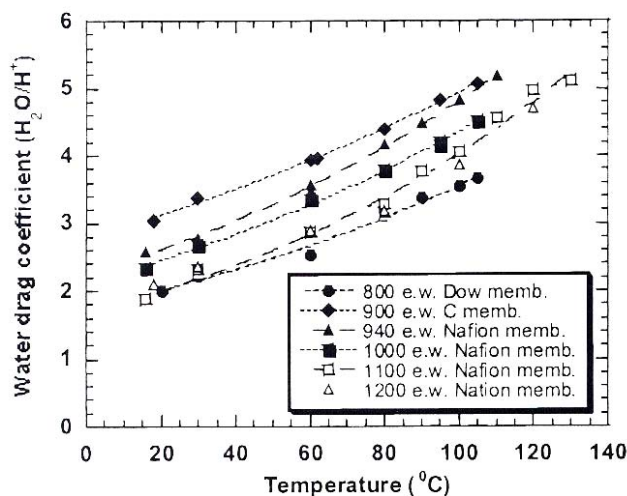


Figure 6. Temperature effect on the water drag coefficients of several PFSA membranes equilibrated with liquid water on both sides in DMFCs.

### Figure 1-9: Electro-osmotic Drag Coefficients of Perfluorosulfonic Acid Membranes<sup>37</sup>

The electro-osmotic drag coefficient only varies by about 1  $H_2O/H^+$  over a wide range of equivalent weights. It would be interesting to compare the variation in electro-osmotic drag coefficients to the morphological features of each membrane. Given that all membranes are of

37. Ren, X., S. Gottesfeld, *J. Electrochem. Soc.* **2001**, 148(1), A87-A93.

the same chemical type, larger electro-osmotic drag coefficients would be an indication of larger hydrophilic domains. In this thesis and future studies, the important morphological effects produced by different types of chemical structures will be considered.

### 1.2.2 Other Commercial Proton Exchange Membranes

Membrane alternatives to Nafion exist, however they are not as widely used and thus, have a much smaller body of open literature devoted to their study. Ballard Power Systems and W.L. Gore & Associates represent two different ends of the fuel cell membrane industry spectrum. Ballard apparently primarily develops their materials for in-house manufacturing of fuel cell stacks. They do not sell their membranes on the commercial market. Gore, on the other hand, is a membrane supplier that not made fuel cells or fuel cell stacks. Their membranes are readily available, and some fuel cell stack companies utilize Gore membranes exclusively. Dais Analytic also produces novel sulfonated block copolymer membranes for in-house use but on a much smaller scale and at an earlier stage of development than the other corporations. This section will briefly discuss the membrane technology of each source, as it has been reported in the literature.

#### 1.2.2.1 Ballard Power Systems

Perhaps the most studied membranes aside from Nafion (and other closely related poly(perfluorosulfonic acid) copolymers), are the Ballard Advanced Material (BAM) family of

membranes produced by Ballard Power Systems. This area of membrane development reportedly began in 1988 and is primarily focused on the post sulfonation of thermally stable, engineering-grade polymers including poly(styrene), poly(trifluorostyrene), poly(phenylene oxide), and other polyaromatics.<sup>38</sup> The main objective of this program was to identify classes of polymers that were less expensive and had a somewhat similar hydrophilic/hydrophobic domain structure as Nafion.

The first synthetic efforts by Ballard included non-fluorinated polymers such as poly(quinoxalines) and poly(phenylene oxides), in addition to other low-cost commodity polymers which were sulfonated in post-polymerization reaction steps. The poly(phenylquinoxaline) phase of this work investigated the influence of monomer structure to alter the flexibility of the chain, morphology, ect. with the goal of forming tough, ductile films. The poly(phenylquinoxaline) polymers were sulfonated with chlorosulfonic acid and solvent cast to form membranes. Steck<sup>39</sup> reported that because of the rigidity of the polymer backbone, ionic cluster formation was seemingly very unlikely. In view of recent AFM results with similarly stiff polymers such as poly(imides),<sup>40</sup> that conclusion was likely made without experimental data. The short-term performance of these membranes was reportedly comparable to that of standard Nafion membranes, however their lifetimes were short, on the order of 500 hours. Very

---

38. Steck, A.E., *New Materials for Fuel Cell Systems I*, pp. 74-92, Editions de l'Ecole Polytechnique de Montreal, Montreal, 1995.

39. Steck, A.E., C. Stone, *Membrane materials in fuel cells*, 2nd Int. Symp. on New Materials for Fuel Cells and Modern Battery Systems, Montreal, Canada, July 1997, pp. 792-807.

40. (a) Gunduz, N., J. McGrath, *Abstr. Pap. ACS* **2000**, 219(2), 122; (b) Einsla, B., Y.T. Hong, Y.S. Kim, F. Wang, N. Gunduz, J.E. McGrath, *J. Poly. Sci. A* **2003**, submitted.

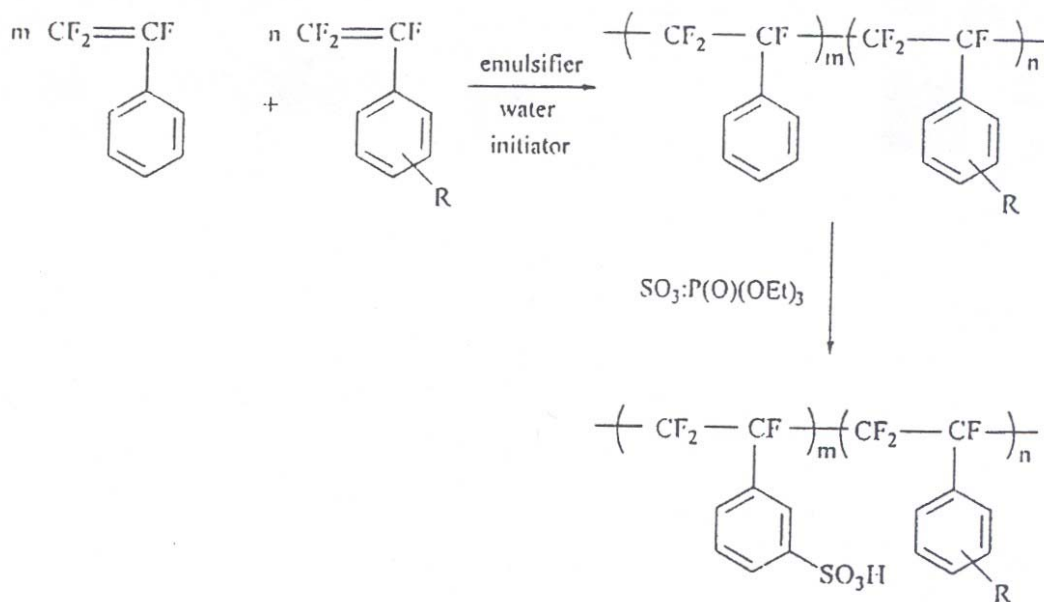
little discussion of the failure mode has been made available; e.g. membrane failure, changing membrane properties, electrode attachment issues, etc.

The next generation of Ballard membrane development (BAM2G) focused on the poly(phenylene oxide) family of polymers.<sup>39</sup> It's unclear why these workers thought that these materials would display more stability than the poly(phenylquinoxaline) membranes. However, the synthesis of this class of polymers was reported to be facile, reproducible, and scalable to large quantities, not surprisingly in light of General Electric's NORYL<sup>®</sup> family. Again, the proton exchange sites were added by various post sulfonation chlorosulfonic acid routes. Interestingly, Steck reports the structure of a poly(arylether sulfone) derived from bisphenol-AF and 4,4-dichlorodiphenyl sulfone. This polymer could be considered analogous to those produced by McGrath, et al.<sup>41</sup> The major difference, of course, being that the Ballard polymer was post-sulfonated as many others have done. Even though various electron withdrawing strategies were attempted to combat degradation of the backbone chain, all polyaromatic-based membrane synthesized by Ballard did not show sufficient lifetimes in a fuel cell environment. All of the membranes seemed to suffer from pinholes (loss of effective reactant gas separation) assumed to be caused by embrittlement of the post sulfonated polymer although no clear evidence was given for mode of pinhole failure. In addition, many critical details of the polymers such as molecular weight, degree of sulfonation, initial mechanical behavior, and morphology were not discussed.

---

41. (a) Harrison, W., F. Wang, J. Mecham, T. Glass, M. Hickner, J. McGrath, *Abstr. Pap. ACS* **2001**, 221(2), U415; (b) Harrison, W.L., F. Wang, J.B. Mecham, V.A. Bhanu, M. Hill, Y.S. Kim, J.E. McGrath, *J. Poly. Sci. A* **2003**, 41(14), 2264-2276.

To combat the assumed chemical instability of the polyaromatic backbone, development at Ballard switched to sulfonating rather expensive and likely brittle poly(trifluorostyrene). This produced the family known as BAM3G membranes, which are reportedly in use today in Ballard fuel cells.<sup>39</sup> The membrane backbones are copolymers of trifluorostyrene and another trifluorostyrene-based comonomer with a pendant R group on the styrenic ring. As before and as in most synthesis work, these membranes were post-sulfonated, this time using a sulfur trioxide-triethylphosphate complex of the type reported by Johnson et al.<sup>42</sup> A synthetic scheme for BAM3G membranes is shown in Figure 1-10.



Scheme 10. Preparation of BAM3G

Figure 1-10: Ballard BAM3G Synthesis<sup>39</sup>

42. Johnson, B.C., I. Yilgor, C. Tran, M. Iqbal, J.P. Wightman, D.R. Lloyd, J.E. McGrath, *J. Poly. Sci. A* **1984**, 22(3), 721-737.

BAM3G membranes preserved the high-performance aspects of BAM2G, but displayed the elusive property of longevity. Both single cells and fuel cell stacks containing BAM3G have been demonstrated in excess of 15,000 hours with acceptable performance degradation. At the time of the review published by Steck and Stone,<sup>39</sup> Ballard maintained a 100,000 ft<sup>2</sup> per year capacity to produce these BAM3G membranes. They foresaw meeting increased demand with a cost-competitive membrane for the automotive market. The predictions of major automotive companies make this likely.

#### 1.2.2.2 W.L. Gore & Associates

Gore membranes and MEAs were introduced by W.L. Gore & Associates around 1995 with the introduction of their PRIMEA<sup>®</sup> product.<sup>9</sup> All of Gore's current products (GORE-SELECT<sup>®</sup> membranes and PRIMEA MEAs) are based on a porous GORE-TEX<sup>®</sup> support impregnated with Nafion. This combination of materials works particularly well because both GORE-TEX and Nafion are fluorinated copolymers making compatibility between the two components more advantageous. This type of composite was first reported in 1985 by Penner and Martin.<sup>43</sup> The motivation for their research was attempting to replace a thick Nafion membrane with a Gore-Tex composite to lower the amount (and thus the cost) of the membrane. However, the cost of additional processing to form the composite was not taken into account. Perhaps, what the authors should have considered as their primary motivation were the advantages gained by

---

43. Penner, R., C. Martin, *J. Electrochem. Soc.* **1985**, 132, 514-515.

having a hydrophobic, rigid, porous support. The Gore-Tex/Nafion composites have much greater strength and less swelling than a pure Nafion membrane. These properties are highly desirable for fuel cell applications.

The major disadvantages of the Gore composite system are the differential swelling between the Nafion and the Gore-Tex, which could cause delamination, and the high ionic resistance of the composite. The process that Gore uses for forming the composites has not been revealed, however it is most likely a combination of surface treatment on the Gore-Tex followed by impregnation of the Nafion from an aqueous/alcohol solution.<sup>44</sup>

The low intrinsic conductivities of the membranes dictate that the composite must be as thin as 5 to 20  $\mu\text{m}$  to approach the areal resistance of the pure ionomer membrane. As the thickness of the membrane is decreased to combat resistive losses, the gas crossover rates increase. Gas crossover, while not much of an issue with thicker membranes, becomes important with the very thin composites. Open circuit voltages suffer, as well as the mechanical integrity of the membrane during MEA fabrication and fuel cell operation.

Gore membranes have found a niche in fuel cell applications, and have been demonstrated in a number of systems. However, the Gore composites still use Nafion, which has its typical shortcomings of low hydrated glass transition temperature and low conductivity at low water contents and will not perform well under high temperature and low relative humidity conditions. The proton exchange membrane composite is intriguing because this technique allows

---

44. Bahar, B., A. Hobson, J. Kolde, D. Zuckerbrod, to W.L. Gore and Associates, Inc., U.S. 5,547,551, 1996.

fabrication of thin, mechanically stable membranes. As will be discussed later, other types of polymer/polymer composites have been attempted, and this area of research will probably remain active with new types of polymer supports and ion conducting phases being explored.

### 1.2.2.3 Dais Analytic

Dais Analytic's membranes have been primarily based on sulfonated styrene/ethylene-butylene/styrene (S-SEBS) copolymers for ambient temperature low current density systems.<sup>45</sup> These polymer differ from Nafion in backbone composition, hydrocarbon versus fluorocarbon, and the nature of the sulfonate group, aryl sulfonic acid versus perfluorosulfonic acid. In general, the Dais materials have shown higher water uptakes than Nafion, but lower conductivities at a given weight percent water. However, the Dais polymers have a higher ion exchange capacity than Nafion 1100 EW. The membranes show similar conductivity values at a constant waters/sulfonate ratio.

In related work, sulfonated Kraton<sup>®</sup> materials were shown to give a protonic conductivity of 0.08 S/cm when fully hydrated.<sup>46</sup> These membranes were shown to have phase separated domains of 20-30 nm using electron microscopy. Most notably, these membranes have shown poor lifetimes in fuel cell life tests. Even though the literature reports are spotty, their aliphatic hydrocarbon backbone is a suspected reason for their poor long-term performance. Also, the rigors of the

---

45. Edmonson, C.A., J.J. Fontanella, S.H. Chung, S.G. Greenbaum, G.E. Wnek, *Electrochemical Acta* **2001**, 46, 1623-1628.

46. Wnek, G.E., J.M. Serpico, S.G. Ehrenberg, E. Zador, *Abst. of the ACS* **1999**, 217(2), 340-PMSE.

post-sulfonation reactions cannot have positive effects on the backbone chain lengths and may cleave backbone chains during sulfonation leading to lower molecular weight copolymers.

In principle, the Dais systems may have applications that require very inexpensive membranes and do not have to last a long time under rigorous conditions. Research seems to be progressing using this type of membrane.<sup>47</sup>

### 1.3 New Proton Exchange Membrane Research

The recent governmental emphasis and industrial interest in fuel cells has fostered a host of new proton exchange membrane research. The objectives of new membrane research include: lower cost, higher temperature operation, improved conductivity at lower water contents, and decreased fuel crossover (especially methanol). New membrane technology can be subdivided into the following three areas: post-reactions on polymers to form ion conducting membranes, direct copolymerization of ion containing monomers to form ion conducting polymers, and composite structures based on polymer/polymer composites or polymer/inorganic composites. Each area has certain advantages and the new membranes have much more specific operating targets than a “one size fits all” approach. Specific material targets include lower methanol crossover for DMFC operation (low reactant permeability), higher conductivity at low water contents for high temperature (e.g. 120-150°C) membranes, thin membranes with sufficiently high strength for high-performance systems, or physically and chemically robust and inexpensive membranes for non-specialized applications.

---

47. Serpico, J.M., S.G. Ehrenberg, J.J. Fontanella, X. Jiao, D. Perahia, K.A. McGrady, E.H. Sanders, G.E. Kellogg, G.E. Wnek, *Macromolecules* **2002**, 35(15), 5916-5921.

### 1.3.1 Post-Sulfonated Polymers

#### *Post Sulfonated Poly(arylene ether ketone) Membranes*

Kreuer<sup>48</sup> has identified many of the tradeoffs between a poly(perfluorosulfonic acid) PEM and a sulfonated poly(arylene ether) PEM for fuel cell use. Specifically, the difference between the two membranes as a result of the character of their sulfonic acid moiety and the polymer microstructure is discussed. Interestingly, this work was in progress as the McGrath group at Virginia Tech was coming to many of the same conclusions about sulfonated poly(arylene ether sulfones).<sup>49</sup> Poly(perfluorosulfonic acid membranes such as Nafion have a  $pK_a$  of about  $-6$  as compared to an aromatic sulfonic acid moiety in sulfonated PEEK of  $-1$ . The implication of the difference in  $pK_a$  values is that there can be a lower ion conductor concentration in the Nafion membrane as compared to the PEEK membrane to produce the same conductivity under equal conditions. The microstructural differences between the two polymer systems are a little subtler. Kreuer asserts that the PEEK membranes have smaller hydrophilic domains due to the stiff polymer backbone and the decreased polarity difference between the sulfonic acid and the polymer backbone. Kreuer's major evidence for this hypothesis is the increased scattering angle of the ionomer peak in PEEK membranes as compared to Nafion. Also, the decreased intensity of the ionomer peak points to a broader interface between hydrophilic and hydrophobic domains.

---

48. Kreuer, K.D., *J. Membr. Sci.* **2001**, 185, 29-39.

49. Hickner, M., F. Wang, Y. Kim, B. Pivovar, T. Zawodzinski, J. McGrath, *Abstr. Pap. ACS* **2001**, 222(1), U467.

### *Crosslinked Sulfonated Poly(ether sulfone) Membranes*

Koter, Kerres<sup>50</sup> et al. investigated proton exchange membranes in addition to those based on poly(perfluorosulfonic acid). Specifically, they were interested in sulfonated bisphenol-A based partially aliphatic poly(ether sulfone) membranes, but they cite developments in similar membranes such as sulfonated PEEK, or other crosslinked types of poly(arylene ethers). In the introduction to their work, they stress the importance of studying the morphology of the new membranes, but they did not attempt to get direct evidence of morphology through microscopy, for example. Instead, they investigated the water uptake, ion exchange capacity, and transport properties for a variety of sulfonated poly(ether sulfones) crosslinked with 1,4-dibromobutane, 1,6-dibromohexane, 1,8-dibromooctane, and 1,12-dibromododecane. One of the comparisons they made between their new membranes and standard Nafion was the concentration of sulfonic acid sites on a volume basis. Even though the ion exchange capacity of the membranes varied from 0.83 to 1.29 mol/kg (meq/g), the concentration of acid sites on a volume basis when swollen with water was surprisingly similar (0.88 to 1.16 mol/dm<sup>3</sup> across seven membrane samples including Nafion 117). The membranes with different ion exchange capacities swelled differently (both in terms of weight % uptake and volume change), the volume concentration of acid sites becomes more similar across many different membranes (e.g. membranes with high IECs swell more, therefore the ions become dispersed in the swollen membrane). However, they did not report conductivity values for the membranes immersed in water. This group also found

---

50. Koter, S., P. Piotrowski, J. Kerres, *J. Membr. Sci.* **1999**, 153, 83-90.

that the poly(ether sulfone) membranes that they had synthesized were much less permeable to electrolytes than the Nafion 117 membrane. From these experiments, they concluded that their new membranes “are characterized by more narrow conducting paths than the Nafion membrane” which is in agreement with Kreuer’s work.<sup>48</sup> One weak point of this argument as stressed above, is that the hypothesis of smaller ion conducting paths is not supported by direct microscopic evidence such as AFM, TEM, or SEM.

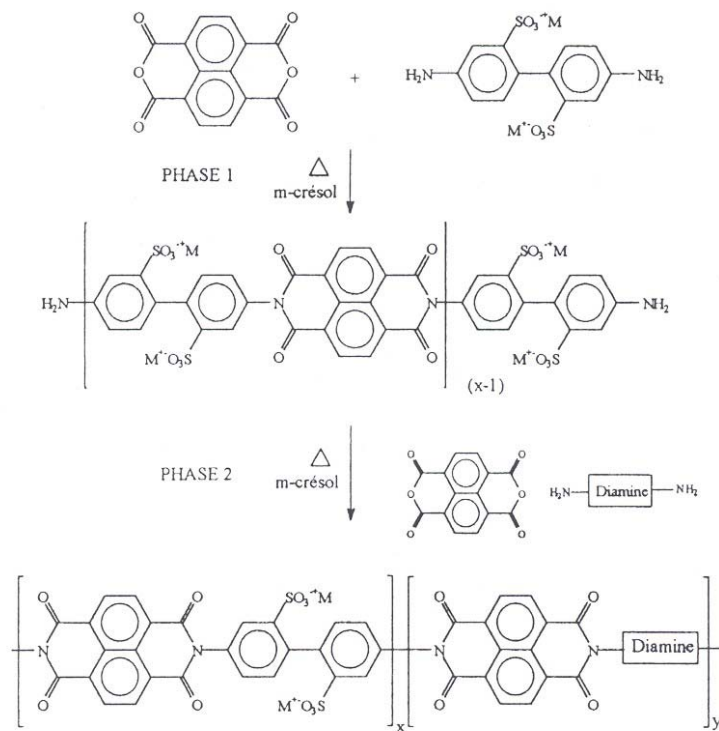
### 1.3.2 Direct Copolymerization of Sulfonated Monomers

Genies, et al.<sup>51</sup> were perhaps the first researchers to conceive of making aromatic proton exchange membranes for fuel cells by direct copolymerization of sulfonated monomers. Their research has been primarily focused on producing sulfonated poly(imides) from naphthalenic dianhydrides and sulfonated diamines. Once the chemistry was demonstrated, these copolymers showed promising results in DMFC systems, however their solubilities were very poor in common organic solvents and required m-cresol for membrane casting. These initial results led to a search for more soluble materials that could be polymerized to high molecular weight and cast from common solvents.

Most of the sulfonated polyimides discussed in the work are block copolymers of sulfonated and unsulfonated blocks using a two-step synthetic approach. A generic synthesis is shown in Figure 1-11.

---

51. Genies, C., R. Mercier, B. Sillion, N. Cornet, G. Gebel, M. Pineri, *Polymer* **2001**, 42, 359-373.



Scheme 3.

### Figure 1-11: Sulfonated Block Polyimide Copolymer Synthesis<sup>51</sup>

These block copolymers were prepared with ion exchange capacities varying from 0.5 to 1.9 meq/g. The authors assert that the number of waters associated with each sulfonate group ( $\lambda$ ) remained relatively steady over a range of ion exchange capacities for a given polymer structure. This is somewhat different from Nafion membranes where the  $\lambda$ -value increases significantly as the ion exchange capacity is increased. Given these results, it seems as though the unsulfonated polyimide block is constraining the swelling of the membrane. Given the high water uptake of the membranes (20-40 weight %), one would expect the membranes to have a high protonic conductivity, but that is not the case. Most of their materials showed protonic conductivities on the order of  $2 \cdot 10^{-3}$  S/cm to  $7 \cdot 10^{-3}$  S/cm.

Scattering experiments were performed on random and block sulfonated polyimides. The block polymers exhibited a large, well-defined ionomer peak, while a random sulfonate copolymer had a very broad reflection at larger angles (Figure 1-12).

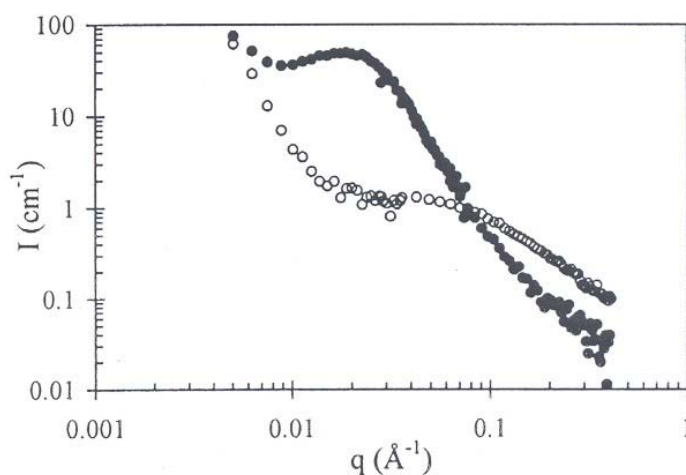


Fig. 7. SANS spectra obtained for swollen statistical (○) and  $x = 5$ ,  $X/Y = 40/60$  sequenced (●) SPI copolymers (BDSA/NTDA/mAPFI).

### Figure 1-12: Neutron Scattering Profiles of Block and Random Sulfonated Polyimides<sup>51</sup>

This result would seem to indicate that the ionic domains are not as tightly organized in the random copolymer, while the block polymer gives a highly ordered, phase-separated structure with a characteristic length that is somewhat larger than the random copolymer domains.

Hydrolytic stability of sulfonated polyimides remains an issue. Less strained naphthalic-based polyimide membranes showed the best hydrolytic stability of the group and remained viable for

1000 hours in water at 80°C. After this time they became very brittle, but it is unknown how this test specifically relates to long-term fuel cell performance.

Allcock et al.<sup>52</sup> have explored the properties of phosphazine copolymers with both sulfonic acid and sulfonimide proton conducting groups. They have controlled the swelling of these types of membranes by incorporating 4-methylphenoxide groups and subsequent crosslinking via  $\gamma$  radiation. Overall, these copolymers showed lower protonic conductivity than Nafion for a given equivalent weight possibly due to their increased water swelling or less acidic groups in the case of the sulfonic acid containing systems.

Wang et al.<sup>53,21</sup> used sulfonated activated aryl halide monomers to copolymerize sulfonated poly(arylene ether)s. The copolymers reported by Wang et al. could be considered somewhat similar to the post-sulfonated PEEK materials discussed earlier, however the direct copolymerization route affords some advantages over previously studied materials.<sup>48</sup> In an earlier work, Ueda et al.<sup>54</sup> reported a similar synthesis of bisphenol-A based aromatic poly(ether sulfone)s containing pendant sodium sulfonate groups, however details were somewhat limited and no mention of potential applications was stated. Also, the copolymer composition was limited to less than 30 mole percent sulfonation. Robeson and Matzner<sup>55</sup> used a similar synthesis

---

52. (a) Allcock, H.R., R.J. Fitzpatrick, L. Salvati, *Chem. Mater.* **1991**, 3, 1120-1132; (b) Hoffmann, M.A., C.M. Ambler, A.E. Maher, E. Chalkova, X.Y. Zhou, S.N. Lvov, H.R. Allcock, *Macromolecules* **2002**, 35, 6490-6493.

53. Wang, F., PhD Dissertation, Chinese Academy of Sciences, 1998.

54. Ueda, M., H. Toyota, T. Ouchi, J. Sugiyama, K. Yonetake, T. Masuko, T. Teramoto, *J. Polym. Sci. A – Polym. Chem.* **1993**, 31(4), 853-858.

55. Robeson, L., Matzner, M., To Union Carbide, U.S. 4,380,598; 1983.

of presulfonated monomers, although their application used the alkali or alkaline earth metal salt of the sulfonate to impart fire resistance to the polymer.

Direct copolymer synthesis using sulfonated monomers by a step growth mechanism enables the exact determination of the polymer microstructure. Since most of the copolymers are random copolymers, the exact sequence of sulfonated units is statistical, but the connectivity of the monomers and the position of the sulfonic acid groups can only occur in one fashion. This makes varying the chemical structure and the sulfonic acid content of the polymers rather easy and facilitates detailed studies of structure-property relationships. In addition, the molecular weights of the directly polymerized sulfonated copolymers can be designed to be much higher than post-sulfonated commercial thermoplastics allow.

The family of copolymers produced by Wang et al. at Virginia Tech are based on the chemistry shown in Figure 1-13.

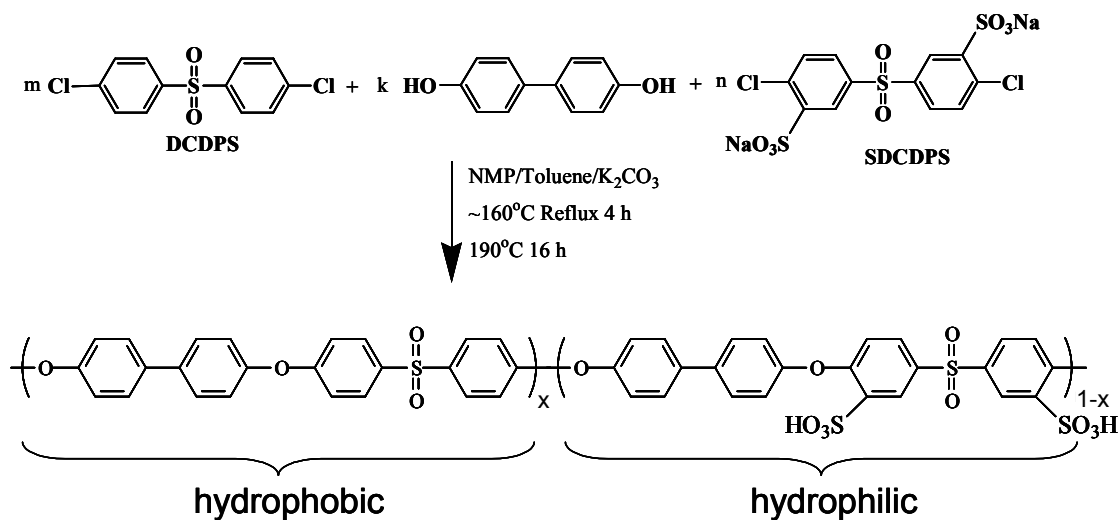
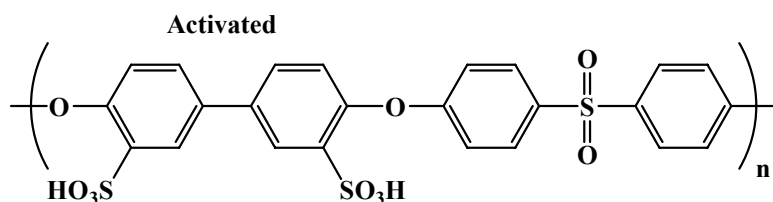
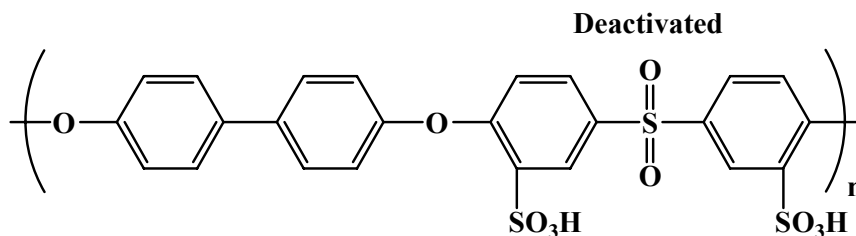


**Figure 1-13: Direct Copolymerization of Sulfonated Poly(arylene ether)s<sup>21</sup>**

Theory predicts that there may be some stability advantages afforded by the direct copolymerization of sulfonated monomers. Since the sulfonate resides meta to the electron withdrawing sulfone moiety, some additional stability is afforded over the post sulfonated analog where the sulfonate group lies ortho to the electron donating ether linkage. Computer models predict that the acidity is also higher. The differences between the two synthetic strategies for forming sulfonated arylene ether polymers are highlighted in Figure 1-14.



Post sulfonation occurs on the most reactive, but least stable, position  
High electron density leads to relatively easy desulfonation



Monomer sulfonation on the deactivated position  
Enhanced stability due to low electron density

**Figure 1-14: Direct Copolymerization of Sulfonated Monomers versus Post Sulfonation**

With post-sulfonated polymers, while the reactions are reasonable well-controlled, there is often debate as to where the sulfonation actually occurs and it is not unusual to observe “gel” fractions in the product. With direct copolymerization, the sulfonation sites are very well-defined.

There are three basic differences between the sulfonated poly(arylene ether)s and Nafion. First, the backbones are much different. The PTFE-like backbone (about 87 mole percent) of Nafion is much more flexible than the stiff, aromatic sulfone or ether-linked backbone of the poly(arylene ether)s. Second, the high fluorine content of Nafion may promote phase separation from the polar ionic groups more strongly than the non-fluorinated poly(arylene ether)s. Finally, the sulfonic acid groups are attached directly to the backbone in the case of the sulfonated poly(arylene ether)s, forming an aryl sulfonic acid moiety as opposed to the perfluoro sulfonic acid attached to a long ether-linked side chain. These important differences impact the ability of the hydrophilic (sulfonic acid) and hydrophobic (backbone) to phase separate into a

microdomain structure. Also, the acidity difference between the aryl sulfonic acid and the perfluoro sulfonic acid may contribute to the copolymers phase separation characteristics.

### 1.3.3 Polymer/Polymer Composite Membranes

A few investigators have focused on making robust proton exchange membranes for fuel cells by blending polymers or forming polymer/polymer composites. Generally, in this arrangement, one polymer serves as a structural support and the other serves as the proton conducting component of the composite. The disadvantage of this type of arrangement is that the composite usually has a lower bulk conductivity than a pure proton conducting homopolymer membrane because of the non-proton conducting component. Suppliers combat this shortfall by making thinner composites, however thinner membranes tend to be more fragile and prone to failure during operation. Perhaps the most well-known polymer/polymer composites are the Gore PRIMEA and Gore-Select membranes. Both products have been reported as being composites of Gore-tex (specially processed, porous Teflon) and Nafion.<sup>9</sup>

### *Other Types of Nafion-based Composites*

Nouel and Fedkiw<sup>56</sup> explored the possibility of supporting Nafion on both Celgard<sup>®</sup> (Celanese) (microporous poly(ethylene) and poly(propylene)) and developmental microporous PTFE supports. These two different supports provide a contrast between the Celgard support that is not compatible with Nafion and the PTFE support, which is more like the fluorinated structure of Nafion. The supports were impregnated by a simple soaking and drying technique in 18% Nafion in ethanol to give about 70 wt % Nafion in the PTFE support and 50 wt % Nafion in the Celgard support. However, one flaw of this research may be that the membranes were only dried at 50 - 60°C after Nafion impregnation. This temperature may not be high enough to reform the original microphase structure of Nafion. The nitrogen and oxygen permeability of the composite Nafion/microporous support membranes showed a wide scatter, most likely as a result of the difficulty in reproducing the amount of Nafion contained in the composite. Also, the permeabilities of the composites were much higher than the permeability of Nafion 112 membranes, even when thickness was taken into consideration. This could pose a reactant gas crossover problem in an operating fuel cell. The authors account for the high gas permeability of the membranes by hypothesizing that the imbibed Nafion does not completely fill the porous support material, highlighting one disadvantage of this type of composite. A supported Nafion composite may be advantageous because the membrane can be made very thin, thus decreasing its areal resistance and resulting ohmic losses in a fuel cell. The researchers found that the

---

56. Nouel, K.M., P.S. Fedkiw, *Electrochimica Acta* **1998**, 43, 2381-2387.

conductivity both through and along the plane of the membranes were equal indicating that there was even distribution of the Nafion through the porous structure of the supports.

### *Polymer/Polymer Composites*

High ion exchange capacity polymers show good conductivity, but often suffer from poor mechanical properties due to high water swelling in hydrated environments. A method to combat this result of a high concentration of ionic groups is to reinforce the membrane with a non-swelling polymer that is still compatible with the ion-conducting polymer. This is similar to the strategy of Gore's membranes. However, research is being conducted to optimize the distribution of components and bonding between sulfonated and unsulfonated polymers. Bowne and coworkers<sup>57</sup> blended post-sulfonated PEEK with a polysulfone matrix. They were able to demonstrate the effect that blending solvents and additives during casting had on final membrane permeability and microphase structure. This research showed that even a small weight percent of sulfonated polymer had a large effect on overall membrane properties. Even though this specific body of research was not focused on producing proton exchange membranes for fuel cells, this type of structure could be used to produce reinforced PEMs with high ion exchange capacity polymers.

---

57. Bowen, W.R., T.A. Doneva, H.B. Yin, *J. Mem. Sci.* **2001**, 181, 253-263.

### *Nafion and Poly(styrene) Microbead Composites*

Chen and Leddy<sup>58</sup> studied composite membrane formation and properties of Nafion impregnated with poly(styrene) microbeads. The composites were formed by casting the solvent dispersed microbeads and a commercial Nafion solution from Solution Technology, Inc. to form 50:50 polymer:microbead membranes by volume. The membranes and composites were cast at room temperature and dried under vacuum. As we know from past studies, this casting protocol from water/aqueous solutions may yield membranes that do not have the same properties as thermally processed forms of recast Nafion and Nafion membranes from DuPont. However the effect of the microbeads can still be observed when compared with pure recast Nafion control samples. Their major result is that the microbead composites showed a higher titrated ion exchange capacity (13% higher) than the pure recast polymers. Their hypothesis for the increase in conductivity is that the microbeads in the composite as a second phase allow access to sulfonic acid sites that may be buried or are inaccessible in the thermally treated membranes. However, it is unfortunate that no indication of physical properties, water swelling, or conductivity was given. No heat treatment of the membrane and a 50% volume filled composite may have a large impact on the membrane's physical properties or applicability to operation in a fuel cell. Filling the membrane with 50 volume % of an impenetrable phase may also have ramifications for species transport across the membrane.

---

58. Chen, T-Y., J. Leddy, *Langmuir* **2000**, 16, 2866-2871.

### *Non-aqueous Proton Conduction with Polymer/polymer Blends*

Miyatake et al.<sup>59</sup> explored the capabilities of a system based on blending poly(thiophenylsulfonic acid) and poly(oxyethylene) with very low water contents. They found that a mixture of the polymers in a 1:2 (poly(thiophenylsulfonic acid):poly(oxyethylene)) ratio gave a conductivity of  $1 \times 10^{-3}$  S/cm at 150°C. The conductivity of pure poly(thiophenylsulfonic acid) was about three orders of magnitude lower than that of the blend. While not directly applicable to fuel cells because of the low conductivity, the results indicate that blending the hydrophilic, low  $T_g$  polymer with a sulfonic acid based proton conductor greatly increases the conductivity, perhaps without the presence of water. This seems to support the conclusion that segmental motion of proton conductors plays a role in bulk conductivity. From a technological aspect, this polymer/polymer system would be unstable and is probably not directly applicable to use in fuel cells. However, motifs such as the one reported in this work may prove to open new areas of research in high-temperature PEM development.

Kerres et al.<sup>60</sup> expanded on the previous idea of blending complementary polymers by exploring the possibility of blending a sulfonic acid containing polymer with a polymer with a basic nitrogen functionality. Specifically, they blended post-sulfonated poly(etheretherketone) or poly(ethersulfone) as the acidic component with poly(4-vinylpyridine), poly(benzimidazole), or poly(ethyleneimine) as the basic component. The polymers could be solution blended in NMP and cast onto glass substrates without observable macrophase separation. The most thermally

---

59. Miyatake, K., K. Fukushima, S. Takeoka, E. Tsuchida *Chem. of Matls.* **1999**, 11(5), 1171-1173.

60. Kerres, J., A. Ullrich, F. Meier, T. Häring, *Solid State Ionics* **1999**, 125, 243-249.

stable blend was a 90:10 sulfonated PEEK:PBI blend but the protonic conductivity in 0.5N HCl, was about an order of magnitude too low for all equivalent weights (IEC = 1.3,  $\sigma^{-1} = 30 \Omega\cdot\text{cm}$ ). The blend with the largest protonic conductivity was a sulfonated poly(sulfone)/diaminated poly(sulfone) (PSU(NH<sub>2</sub>)<sub>2</sub>) blend at 25°C in 0.5N HCl. Preliminary fuel cell experiments showed that the membrane performance was comparable to that of Nafion 112 in H<sub>2</sub>/O<sub>2</sub> fuel cells and showed lower methanol permeation in DMFCs. The authors assign the success of the membranes to specific interactions between the sulfonic acid and amine moieties thus increasing the acid strength and conductivity of the blend.

#### 1.3.4 Polymer/Inorganic Composite Membranes

Researchers have tried to overcome some of the performance issues of pure polymeric membranes or polymer/polymer composites by forming polymer inorganic composites. This type of composite can be configured in a number of ways:

- both polymer and inorganic components can be ionically conductive
- ionic polymer with inorganic filler for mechanical support
- ionic polymer with water-retaining inorganic filler
- ionically conductive inorganic additive with supporting polymer

This partial list only covers a few of the possible combinations. Polymer inorganic composite membranes are interesting because many of the inorganic additives used are able to operate at much higher temperatures than the pure polymers. Some of the possible advantages of

incorporating inorganic compounds into composite membranes include, enhanced proton conductivity, water retention at high temperatures, and mechanical support.

### *Comparative Study of Nafion with Different Additives*

Arimura et al.<sup>61</sup> incorporated a host of inorganic additives as well as other polymers into recast Nafion. They divided their additives into the following basic categories: inorganic moisture absorbing particles, alkyl or aromatic sulfonated compounds, ionic copolymers, and copolymers with a function of polymer chain alignment. The author's intentions of this work were to test how the following factors affect the ionic conductivity of proton exchange membranes: 1) a high concentration of sulfonic acid groups to increase the cationic site density in the hydrophilic domains 2) a high water content to enlarge hydrophilic domains in the membrane 3) alignment of channel structures to ease ion and water transport. All of the recast Nafion membranes with various additives were annealed at 150°C for two hours to attempt to regain the original characteristics of thermally processed Nafion membrane. The effect of moisture absorbing composite components on the conductivity of the dry membrane was quite noticeable. Porous silica gel containing composites were compared with composites formed with non-porous silica gel. The porous silica with 21 nm average size micropores showed an increase in conductivity of 1.6 times that of the plain recast Nafion, where the non-porous material had little effect. In all cases, water absorbing materials such as P<sub>2</sub>O<sub>5</sub> and molecular sieves induced a noticeable increase in conductivity over pure Nafion. It would be interesting to see the conductivity results of (even partially) humidified membranes, but that data was not reported.

---

61. Arimura, T., D. Ostrovskii, T. Okada, G. Xie, *Solid State Ionics* **1999**, 118, 1-10.

The sulfonated compounds explored in this research can be classified in two distinct groups when they are incorporated into the Nafion at 10 weight %. The aliphatic-based sulfonic acid containing compounds increased the conductivity of the hydrated composite over that of the membrane, but the naphthalene sulfonates showed no effect on conductivity or actually decreased the conductivity of the composite slightly. This effect can be understood using two different rationales. The authors speculate that the naphthalene sulfonates are too stiff to conform to the morphological structure of Nafion and thus the compatibility of the components was most likely poor. The stiff chains cannot orient in such a fashion to align the sulfonic acid groups within the hydrophilic domains. The flexible alkyl chains of the other additives can easily conform to the morphological structure of Nafion and contribute its additional sulfonic acid groups to the conductivity of the composite. Additionally, the flexibility of the alkyl groups may play a role in increasing the segmental motion of the polymer (as a plasticizer), thus increasing its conductivity. The effect of stiff polymeric additives versus flexible additives was observed with the addition of ionic copolymers into the Nafion composite. The researchers in this study observed a distinct trend where the polymeric additives on long side chains increased the conductivity of the composite whereas those with the sulfonate group on short side chains had a detrimental effect on the composite's conductivity. The flexible nature of the side chain and backbone itself also had a noticeable effect.

Interestingly, the final work in this detailed study shows the effect of polymeric composite additives that serve to align the structure of Nafion. The researchers used copolymers with long alkyl laurate or stearate components to attempt to align the hydrophilic structure in Nafion.

Their data shows a marked increase in conductivity for hydrated composites, which they assign to the structural alignment of Nafion. They do not report the weight percent of added ionic copolymer, but it would be surprising that a small amount of such a polymer could align Nafion's structure in a composite. Again, the argument is made that some of these flexible compounds increase the segmental motion in Nafion and their additional ionic groups add to the overall conductivity of the composite. The authors of this study feel they addressed their objectives sufficiently, but more would need to be done to study the chemical and mechanical stability of the composites. In addition, these strategies may not help with higher temperature operation of fuel cells; the notable exception being the water absorbing additives, which is currently a popular focus of high temperature membrane research.

#### *Zeolites in PTFE*

Poltarzewski et al.<sup>62</sup> tried to produce a proton exchange membrane for direct methanol fuel cells by dispersing zeolites (Zeolon 100 H – prepared in-house) in a poly(tetrafluoroethylene) matrix. The composite membranes displayed a linear increase in conductivity with zeolite mass loading up to 90 weight % zeolite loadings where the conductivity of the membrane was about  $10^{-2} \text{ S cm}^{-1}$ , which may be slightly low for fuel cell applications. The water absorption of the membranes also increased with zeolite loading up to 70 weight % uptake for the 90 weight % zeolite loaded sample. However, the high zeolite loading needed for sufficient conductivity greatly affects the mechanical properties of the membrane causing the tensile strength to plummet. However fragile the membrane was, the authors were still able to test the 90 weight %

---

62. Poltarzewski, Z., W. Wieczorek, J. Przyhuski, V. Antonucci, *Solid State Ionics* **1999**, 119, 301-304.

loaded sample in a direct methanol fuel cell. Current-voltage plots were obtained, but the results were not encouraging. The open circuit voltage of the cell was very low at 550 mV (methanol concentration not specified) and the cell was able to generate only  $30 \text{ mA cm}^{-2}$  at 100 mV. The authors noted that the poor fuel cell performance could have been caused by poor contact by fuel cell components. However, it is more likely that the low open circuit voltage is caused by methanol crossover in the cell. If the authors had reported the methanol concentration used in the tests, a more firm determination could be made.

#### *Phosphotungstic Acid and Poly(benzimidazole) Composite*

Using a similar approach, Staiti, Minutoli, and Hocevar<sup>63</sup> attempted to form a proton conducting composite by blending phosphotungstic acid supported on silica with poly(benzimidazole) (PBI). In this arrangement, the PBI is simply the supporting matrix for the proton conducting phosphotungstic acid. They report membranes cast from DMAc with good tensile strength and thermal stability up to 400°C. At 150°C and 100% relative humidity, a membrane with 60 weight % loading of the phosphotungstic acid had a conductivity of  $1.42 \cdot 10^{-3} \text{ S cm}^{-1}$ , which is a bit low for fuel cell proton exchange membranes. An ion-conducting polymer (even with low ion exchange capacity) used as the matrix material would surely enhance the conductivity of the composite, perhaps without degrading the mechanical properties of the base polymer too much.

The previous research shows that it is difficult to form a proton conducting composite using zeolitic materials or other proton conducting inorganics in conjunction with an inert polymer

---

63. Staiti, P., M. Minutoli, S. Hocevar, *J. Power Sources* **2000**, 90, 231-235.

matrix. The conductivities obtained by such composite structures are low for fuel cell use. Composites employing an ion conducting polymer and an inorganic water-retention compound or ionic compound tend to be much more successful in producing membranes that can be used in fuel cells. A discussion of several composites incorporating proton conducting polymers as well as a proton conducting inorganic filler follows.

#### *Post-sulfonated Polysulfone and Phosphatoantimonic Acid*

Genova-Dimitrova and coworkers<sup>64</sup> investigated the membrane and proton conducting properties of a composite structure formed by solution blending sulfonated bisphenol-A based poly(sulfone) and phosphatoantimonic acid. The authors found that sulfonating the poly(sulfone) to a level which gave sufficient proton conductivity for fuel cell applications imparted high water absorption and poor membrane mechanical properties. To boost the conductivity of the membrane and maintain mechanical integrity, the authors proposed using a sulfonated poly(sulfone) with a lower concentration of ionic groups and an inorganic ionically conductive filler (phosphatoantimonic acid). In conductivity investigations, they report a synergistic effect of the sulfonated poly(sulfone)/phosphatoantimonic acid composite. With 8% phosphatoantimonic acid, the conductivity of the pure polymer was increased 2-5 times for various equivalent weights of sulfonated poly(sulfone). The researchers also observed that the membrane containing the inorganic filler had higher moduli than the pure polymers. This is most likely due to some sort of coupling effect between the ionic groups on the polymer and the

---

64. Genova-Dimitrova, P., B. Baradie. D. Foscallo, C. Poinsignon, J.Y. Sanchez, *J. Membr. Sci.* **2001**, 185, 59-71.

inorganic filler such as hydrogen bonding noted by Kim et al.<sup>65</sup> In addition, the pure sulfonated polymer moduli increased with decreasing sulfonation level. This effect of ion concentration on mechanical properties is understandable in terms of water absorption. Because the membranes in the study were tested for mechanical properties after a hot water treatment, the membranes with more ionic groups contained more water and therefore showed more solvent plasticization.

### *Sulfonated PEEK and Heteropolyacid Composites*

Zaidi et al.<sup>66</sup> prepared a series of proton conducting composites based on a matrix of sulfonated PEEK containing 60 weight % heteropoly acids formed by solution blending in DMAc. SEM morphology studies show that the HPA was uniformly distributed throughout the membrane with particle sizes ranging from 0.05-0.15  $\mu\text{m}$ , however the authors do not comment on the bulk clarity of the composites, which would be helpful in characterizing how well the HPA was dispersed in the matrix polymer. It is noted that the best mechanical properties were formed with sulfonated PEEK having an IEC of 1.7 meq/g. This sulfonated matrix provided sufficient base conductivity without excessive swelling. The conductivity measurements employed in this study were not at equilibrium with respect to the water contained in the composite. The composites were soaked in water prior to measuring their conductivity and then placed in an open-atmosphere cell with stainless steel blocking electrodes. The authors recognized that the membranes were losing water and that the water loss affected the conductivity of the

---

65. a) Kim, Y., F. Wang, M Hickner, T. Zawodzinski, J.E. McGrath, *Abstr. of Papers of the ACS* **2001**, 222(2), U388; b) Kim, Y., F. Wang, M. Hickner, T. Zawodzinski, J.E. McGrath, *J. Membr. Sci.* **2003**, 212, 263-282.

66. Zaidi, S.M.J., S.D. Mikhailenko, G.P. Robertson, M.D. Guiver, S. Kaliaguine, *J. Membr. Sci.* **2000**, 173, 17-34.

membranes, however they assumed valid comparisons could still be drawn from such an experimental setup. It was observed throughout the study that the addition of the HPA compounds increased both the water uptake and the conductivity of the sulfonated PEEK polymers over a range of equivalent weights. In thermal studies, dynamic scanning calorimetry showed that the HPA containing composites had a higher glass transition temperature than the base polymer. This observation points to specific interactions between the sulfonated polymer chains and the HPA. The activation energies of conduction were found to be  $15 \text{ kJ mol}^{-1}$ , which is relatively high for membranes that absorb as much water as these composites. The authors also note that the composites were stable with respect to ionic conductivity when stored for 9 months in liquid water. The HPA did not seem to be easily removed from the composite, where it would have caused a drop in conductivity.

Kim et al.<sup>65</sup> have blended directly copolymerized sulfonated poly(arylene ether sulfone) with phosphotungstic acid. They have observed that the morphology of the sulfonated matrix polymer is preserved upon blending with the HPA. In this respect the sulfonated matrix acts as a template for distribution of the HPA to form a nanocomposite. What is interesting about these composites is that the HPA actually decreases the swelling of the composite while maintaining or even slightly increasing its conductivity. These two phenomena are shown in Figure 1-15 and Figure 1-16.

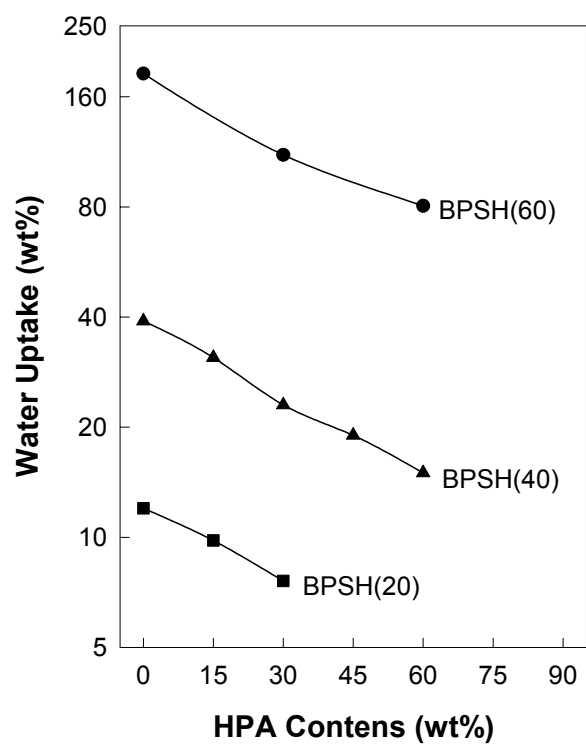
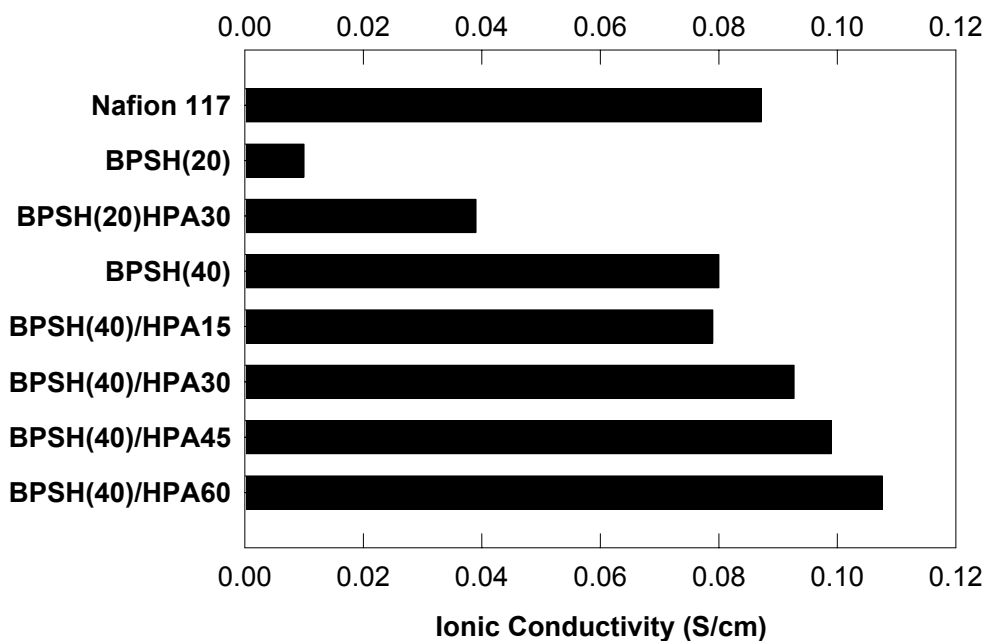


Figure 1-15: Water Swelling of Sulfonated Poly(arylene ether sulfone)/HPA Composites<sup>65</sup>



**Figure 1-16: Conductivity of HPA Composites<sup>65</sup>**

They have also observed a marked increase in the modulus of the composite materials in both the dry and hydrated state. This type of system where there are specific interactions between the HPA and the sulfonated copolymer could lead to a route for more robust proton exchange membranes for operation at 120 - 150°C in hydrogen fuel cells.

*Sulfonated Ion Conducting Polymers and Layered Zirconium Phosphonates*

Alberti<sup>67</sup> has pioneered research into proton conducting composites based on inorganic layered zirconium hydrogen phosphate compounds and proton conducting polymers such as sulfonated

---

67. Alberti, G., M. Casciola, R. Palombari, *J. Membr. Sci.* **2000**, 172, 233-239.

PEEK. The class of compounds known as zirconium sulfoarylphosphonates is itself a proton conductor like the previously mentioned HPAs. However, there is one major difference; the HPAs are water soluble and the zirconium systems are not. This may afford some additional stability advantage for the latter composites because the leaching of the inorganic from the copolymer may not be as severe as with some HPA composites. Alberti et al. has extended this research to incorporating titanium phosphate sulfophenylphosphonate into Nafion 100 membranes.<sup>68</sup> Titanium phosphate sulfophenylphosphonate was investigated because it has shown the greatest conductivity of the layered metal sulfonates. Composite membranes showed good conductivity up to 20 weight % filler, where the membranes started to become heterogeneous and brittle. This indicates poor coordination between the inorganic and organic phases. Nafion is very difficult to blend with fillers because it is so sensitive to processing. Other types of proton conducting polymers such as sulfonated poly(arylene ethers) could prove to be more advantageous in this type of composite.

### 1.3.5 Future Directions for Membrane Research

The next step-change in membrane development will be to maintain protonic conductivity while decreasing the membrane's water content. New composite membranes such as the inorganic/sulfonated polymers are interesting, but more research is needed. The one problem with current approaches is the inability to replace the sulfonic acid proton conducting moiety. Even sulfonimide functional groups do not allow the membrane to maintain sufficient

---

68. Alberti, G., U. Constantino, M. Casciola, S. Ferroni, L. Massinelli, P. Staiti, *Solid State Ionics* **2001**, 145, 249-255.

conductivity without water.<sup>69</sup> Until a new proton conducting mechanism is discovered and incorporated into proton exchange membranes, there can only be evolutionary (but still important) improvements in PEM fuel cell technology.

The next-generation DMFC membranes need to have lower methanol crossover. Unoxidized methanol diffusing through the membrane decreases the voltage efficiency of the cell and does not allow lowering the precious metal loading on the cathode. If direct methanol fuel cells are to become a wide-spread technology, crossover is well-recognized to be one of the first issues (along with catalyst durability) that needs to be addressed.

#### **1.4 State of Water in Hydrophilic Polymers**

It has been observed that the proton exchange membrane must remain well hydrated during fuel cell operation. Too little water in the membrane (most likely a consequence of low relative humidity gas feed streams) causes the protonic conductivity of the PEM, and thus the fuel cell performance, to drop dramatically. Water serves a critical importance in proton exchange membranes, but its fundamental role remains poorly understood. In future applications of fuel cells at high temperatures and low relative humidity (e.g. 100°C and 50% relative humidity), the concentration of water in the membrane is low and currently available membranes perform poorly under these conditions. Fundamental understanding of the role of water in the proton exchange membranes is critical to designing systems that are able to perform well without high concentrations of absorbed water.

---

69. Appleby, A., O. Velev, J. Leheloco, et al., *J. Electrochem. Soc.* **1993**, 140(1), 109-111.

It has been recognized that the water absorbed in hydrophilic polymer systems does not display the same calorimetric, diffusive, or nuclear magnetic resonance (NMR) relaxation characteristics as bulk water. The investigation of water-swollen hydrogels has lead researchers to define three states of water<sup>70</sup> as follows: (1) non-freezable, bound water – water that is strongly bound to the copolymer and shows no thermal transitions by DSC – this water is principally responsible for glass transition temperature ( $T_g$ ) depression of the copolymer; (2) freezable, bound water – water that is weakly bound to the copolymer, but still displays thermal transitions in DSC measurements; (3) free water – water that has the same thermal transitions as bulk water.

Slow scanning DSC was employed to resolve two peaks near 0°C for poly(vinyl alcohol) (PVA) water-swollen hydrogels. By scanning at 0.3°C per minute, these researchers were able to resolve a peak at -2°C which they assigned to the freezable, bound water, and a peak at 0°C corresponding to the free water (Figure 1-17).

---

70. Nakamura, K., T. Hatakeyama, H. Hatakeyama, *Polymer* **1983**, 24, 871.

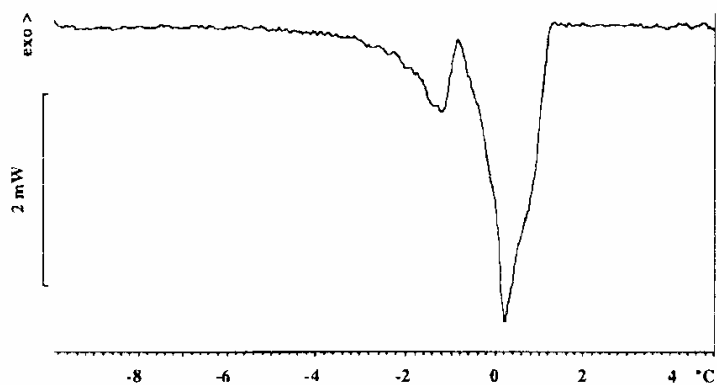


**Figure 1.** Thermogram recorded  $-10$ – $5$  °C at  $0.3$  °C/min for PVA-EDTA25 previously cooled for 15 min at  $-40$  °C.

**Figure 1-17: Dynamic Scanning Calorimetry Thermogram Illustrating Two Water Freezing Peak in a Water-swollen PVA Hydrogel<sup>70</sup>**

The characteristics of water absorbed in hydrogels has been investigated by McConville and Pope<sup>71</sup> using  $^1\text{H}$  NMR  $T_2$  relaxation measurements. They found that their results consistently showed two pools of protons, one with long correlation times labeled the “slow” water species and one with short correlation times labeled the “fast” water species. These two pools of protons are analogous to the concept of free (fast) and bound (slow) water. In addition, increasing relaxation times were correlated with increasing water content of the hydrogels. Barbieri et al.<sup>72</sup> have characterized the water contained in hydrogels using pulsed field gradient (PFG) NMR. They found that the water-swollen hydrogels displayed much lower water self-diffusion coefficients than bulk water – on the order of 1-2 orders of magnitude lower. The authors

---

71. McConville, P., J.M. Pope, *Polymer* **2001**, 42, 3559-3568.

72. Barbieri, R., M. Quaglia, M. Delfini, E. Brosio, *Polymer* **1998**, 39(5), 1059-1066.

pointed out that the diffusion coefficients measured were the average of all types of water in their samples weighted by the fraction of each type of water.

The behavior of absorbed water in proton exchange membranes has also been investigated by dynamic scanning calorimetry (DSC) and PFG NMR measurements. The three states of water model was adopted by Elomaa et al.<sup>73</sup> to facilitate interpretation of DSC investigations of styrene grafted, sulfonated poly(vinylidene fluoride). The authors of this study observed two overlapping peaks corresponding to different states of water absorbed in the proton exchange membranes. A broad peak from approximately  $-15^{\circ}\text{C}$  to  $-2^{\circ}\text{C}$  was assigned to the water that was strongly bound to the sulfonic acid groups with the sharp peak corresponding to the free water in the sample. The authors observed that as the degree of crosslinking increased or the degree of grafting decreased, the fraction of free water declined (in relation to the overall water content) and was in fact undetectable in the most heavily cross-linked system. The decline in free water with crosslinking can be observed in Figure 1-18 where the sharp peak of the uncrosslinked sample is decreased in the crosslinked specimens – especially in the case of 5% divinylbenzene (DVB) which is a more active crosslinker than bis(vinylphenyl)ethane (BVPE).

---

73. Elomaa, M., S. Heitala, M. Paronen et al., *J. Mater. Chem.* **2000**, 10, 2678-2684.

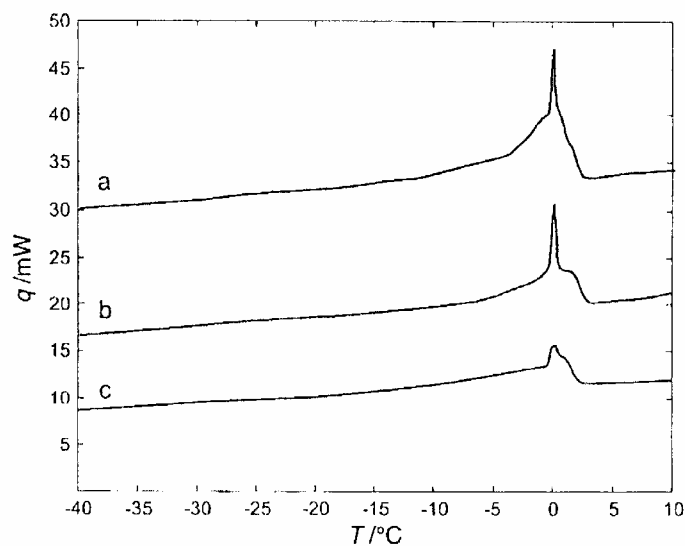


**Fig. 2** Thermograms of PVDF-g-PSSA membranes with a degree of grafting of around 70%. a) non-crosslinked membrane, b) membrane crosslinked with 5 mol% of BVPE, and c) membrane crosslinked with 5 mol% of DVB.

**Figure 1-18: Differential Scanning Calorimetry Thermograms of Hydrated Membranes (a) non-crosslinked (b) crosslinked with 5 mol % BVPE (c) crosslinked with 5 mol % DVB<sup>73</sup>**

The strongly bound water in these systems were not detectable by DSC and its presence was inferred from integration of the melting endotherms and water content of the samples.

Kim et al.<sup>74</sup> extended the previous DSC studies by investigating water's plasticization of the proton exchange membrane. Transitions around 0°C were observed corresponding to free and freezable bound water, but the thermograms were extended to high temperatures to observe the

---

74. Kim Y.S., L. Dong, M. Hickner, T.E. Glass, J.E. McGrath, *Macromolecules* **2003**, 36(17), 2003.

$T_g$  depression of the copolymer by the absorbed water (Figure 1-19). This  $T_g$  depression was due to the strongly bound, non-freezable water.

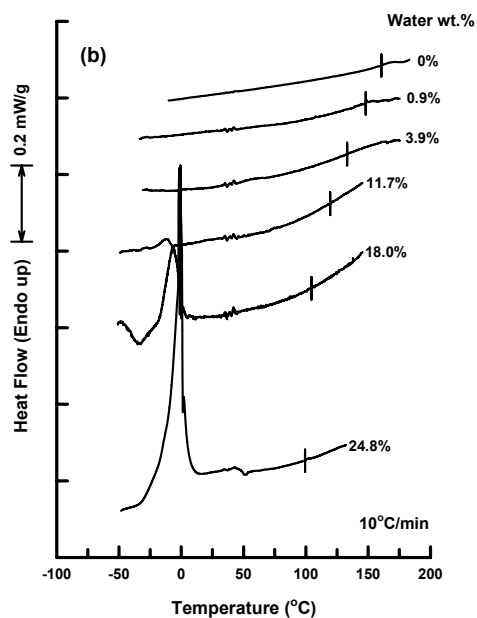


**Figure 1-19: DSC Thermograms of Nafion 1135 at Various Water Contents<sup>74</sup>**

In Figure 1-19 features of each of the three states of water are clearly visible. The  $T_g$  depression caused by the tightly bound, non-freezable water is denoted by the vertical lines intersecting each scan between 160°C for dry Nafion 1135 and 100°C for the fully hydrated sample. The presence of bound, freezable water becomes apparent at about 11.7% water where a broad melting peak is observed around 0°C. Free water with a sharp melting peak at 0°C is evident at full hydration.

PFG NMR was utilized by Zawodzinski et al.<sup>75</sup> to measure the water self-diffusion in Nafion and other poly(perfluorosulfonic acid) membranes. As the water activity decreased (and thus the water uptake and lambda value of the membrane), the water self-diffusion coefficient decreased in a similar fashion. Even at full hydration the self-diffusion coefficients were substantially lower than that of pure water – less than half for Nafion 117 and Membrane C and slightly greater than half for the Dow membrane (which absorbed more water than the other two membranes). The goal of these measurements was to provide data for fuel cell modeling efforts focusing on the transport of water through the membrane due to activity gradients and electro-osmosis and better understand protonic conductivity mechanisms at low water contents. There was no discussion of how the self-diffusion coefficients in this study related to the state of water in the copolymer membranes.

---

75. Zawodzinski, T.A. Jr., T.E. Springer, J. Davey, R. Jestel, C. Lopez, J. Valerio, S. Gottesfeld, *J. Electrochem. Soc.* **1993**, 140(7), 1981-1985.

# CHAPTER 2. THE INFLUENCE OF CHEMICAL STRUCTURE ON THE TRANSPORT PROPERTIES OF PROTON EXCHANGE MEMBRANES

## 2.1 Abstract

Sulfonated wholly aromatic copolymers have shown promising performance in direct methanol fuel cells primarily because of their low methanol permeability. Methanol permeability has previously been correlated with other transport properties such as electro-osmotic drag and proton conductivity to some extent. This work compares the transport properties of three types of sulfonated wholly aromatic copolymers, sulfonated poly(arylene ether sulfone), sulfonated poly(arylene thioether sulfone), and sulfonated poly(imide) with the standard proton exchange membrane, Nafion. The species transport in all the wholly aromatic systems was suppressed when compared to Nafion on an ion exchange capacity basis. This decrease in proton, methanol, and water transport can be rationalized by considering the state of water absorbed in the membrane as measured by  $^1\text{H}$  pulsed-field gradient NMR. Water absorbed in Nafion membranes is much more loosely bound than the water absorbed in sulfonated wholly aromatic copolymer membranes. This loosely bound water gives rise to enhanced transport. The state of the water in an ion containing membrane is determined by the ionic domain morphology as dictated by the ion clustering behavior. Nafion has a very distinct phase separated morphology with a high degree of phase separation between the hydrophilic and hydrophobic domains because of its fluorinated, flexible backbone and strong fluorosulfonic acid ionic groups located on long,

flexible side chains. Highly phase separated domains promote free and loosely bound water in the ionic regions. Wholly aromatic systems with somewhat stiffer backbone chains and ionic groups tethered directly to the backbone have a less distinct phase-separated morphology, which induces water that is absorbed into the copolymer to become more tightly bound water within the domain structure. This report elucidates the interplay between copolymer chemical structure, transport properties, and the state of absorbed water in molecularly designed proton exchange membranes for use in fuel cell applications.

Key words: poly(arylene ether), proton exchange membrane, ion containing polymer, water, transport properties

## **2.2 Introduction**

Developing new proton exchange membranes for both direct methanol and hydrogen fuel cells has been established as an important research area in the fuel cell community. As the push towards widespread commercialization of fuel cells has strengthened, the fuel cell industry has recognized that one of the keys to large improvements in performance is creating a membrane with enhanced physical properties relative to the current state of the art membrane for both hydrogen/air and direct methanol fuel cells, Nafion<sup>®</sup>. Nafion's structure (Figure 2-1) promotes excellent chemical stability due to its perfluorinated structure and good conductivity at low temperatures. However, Nafion is expensive, has high methanol permeability, and is prone to

viscoelastic relaxation at high temperatures (low hydrated  $T_g$ )<sup>76</sup> which decreases both its mechanical properties and its protonic conductivity no doubt related to the alteration of its ordered ionic morphology.

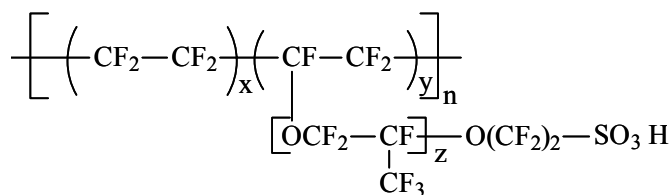


**Figure 2-1: Chemical Structure of Nafion**

Many new families of proton exchange membranes have been synthesized including sulfonated polyketones,<sup>77</sup> polyimides,<sup>78,79</sup> polybenzimidazole, and polysulfones<sup>80,81</sup>. Most of the previous work in this area has utilized post sulfonation reactions on already formed polymers – generally polymer modification schemes. However, there have been more recent reports in the literature focusing on direct copolymerization of sulfonated monomers.<sup>78,79,82</sup> These directly polymerized systems have advantages over the polymer modification reactions because precise control of the

---

76. Kim, Y.S., L. Dong, M. A. Hickner, B. S. Pivovar, and J. E. McGrath, *Polymer* **2003**, 44(19), 5729-5736.

77. Alberti, G., M. Casciola, L. Massinelli, B. Bauer, *J. Membr. Sci.* **2001**, 185, 73.

78. Genies, C., R. Mercier, B. Sillion, N. Cornet, G. Gebel, M. Pineri, *Polymer* **2001**, 42, 359.

79. Gunduz, N., T.Y. Inan, E. Yildiz, J.E. McGrath, *Polymeric Materials Science and Engineering* **2001**, 84, 911.

80. Nolte, R., K. Ledjeff, M. Bauer, R. Mulhaupt, *J. Membr. Sci.* **1993**, 83, 211.

81. Koter, S., P. Piotrowski, J. Kerres, *J. Membr. Sci.* **1999**, 153, 83-90.

82. Wang, F., M. Hickner, Y.S. Kim, T.A. Zawodzinski, J.E. McGrath, *J. Membr. Sci.* **2002**, 197, 231-242.

chemical structure of the copolymer can be achieved and high molecular weight copolymers can be synthesized to give good membrane forming characteristics and mechanical properties. Wholly aromatic sulfonated copolymers such as polyimides<sup>78</sup> and poly(arylene ether sulfone)s<sup>82</sup> have shown promising results for direct methanol fuel cells because of their low methanol permeability. The performance of liquid fed direct methanol fuel cells (DMFC) suffers because of methanol crossover where unreacted methanol at the anode diffuses through the membrane to the cathode catalyst layer. Methanol crossover impacts the performance of the fuel cell by lowering the cell's voltage efficiency (mixed potential at the cathode), decreasing its fuel efficiency (loss of methanol from the feed stream), and causing a higher heat load in the system. Decreasing the methanol crossover of DMFC proton exchange membranes is a key issue that must be addressed to produce high performance systems.

Decreasing the feed concentration of methanol to the cell has combated methanol crossover in Nafion systems. This operational approach lowers the methanol concentration gradient from anode to cathode and thus the driving force for methanol diffusion across the membrane. Unfortunately, this strategy causes a drastic decrease in the fuel energy density (diluting the methanol with water) or requires a complex water collection, fuel mixing, and recirculation scheme. Increasing the thickness of the membrane increases the mass transfer resistance to methanol diffusion and therefore decreases methanol crossover (methanol flux from anode to cathode). The current standard DMFC membrane is Nafion 117 (1100 equivalent weight, 7 mils (178  $\mu\text{m}$ ) thick) compared to the standard hydrogen/air Nafion membranes, which are usually 1135 or 112 (1100 equivalent weight, and 3.5 or 2 mils thick, respectively). The thicker

membrane is needed to decrease the methanol flux to the cathode, despite undesirable higher cell resistances that result due to the increased membrane thickness.

A major goal of new proton exchange membrane research for direct methanol fuel cells has been to decrease the methanol permeability of the proton exchange membrane without sacrificing protonic conductivity. The tradeoff between protonic conductivity and methanol permeability can be expressed as selectivity, or the ratio of conductivity to methanol permeability.<sup>83</sup> Relative selectivity is then the selectivity of the membrane of interest divided by the selectivity of control Nafion systems. A membrane with relative selectivity greater than unity is potentially more desirable than Nafion for application in direct methanol fuel cells. There have been reports of membranes with relative selectivity of greater than 3,<sup>84</sup> but questions remain about the fundamental origin of improved selectivity in wholly aromatic systems versus Nafion and the correlation of proton conductivity, methanol permeability, and electro-osmotic drag in water absorbing, sulfonated copolymers.

It is proposed in this paper that the transport properties (conductivity, methanol permeability, and electro-osmotic drag) of the membranes in this study are dependent on the state of water contained within the membrane. This idea was outlined in a recent communication<sup>85</sup> to *Macromolecules* and will be expanded upon herein.

---

83. Pivovar, B.S., Y. Wang, E.L. Cussler, *J. Membr. Sci.* **1999**, 154, 155-162.

84. (a) Gulati, K.M., C.A. Cavalca, and C.W. Martin, The 203rd Meeting of The Electrochemical Society, Inc., Paris, France, April 27-May 2, 2003; (b) Hickner, M., F. Wang, Y. Kim, J.E. and McGrath, The 200th Meeting of The Electrochemical Society, Inc., San Francisco, CA, September 2-7, 2001.

85. Kim Y.S., L. Dong, M. Hickner, T.E. Glass, J.E. McGrath, *Macromolecules* **2003**, 36(17), 2003.

## 2.3 Experimental

### 2.3.1 Materials

Nafion 117 (1100 equivalent weight, 0.007 mils thick) membranes were obtained from Los Alamos National Laboratory. Its chemical structure was shown in Figure 2-1. The membranes were prepared for measurement by standard preparation methods described elsewhere.<sup>86</sup>

Poly(arylene ether sulfone) copolymers (BPSH) were synthesized by direct polymerization of sulfonated monomers as described in detail in Ref. 82, and their chemical structure is shown in Figure 2-2.

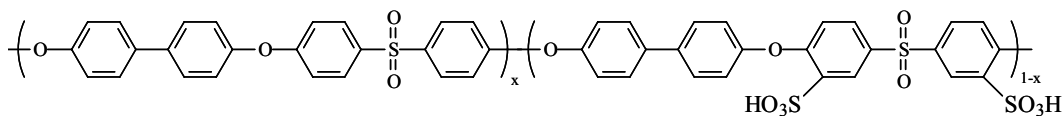


**Figure 2-2: Chemical Structure of BPSH**

Tough, ductile membranes were solution cast from the potassium cation form polymer on aluminum molds in a heated vacuum oven. Once filtered through a 0.45  $\mu\text{m}$  PTFE syringe filter, cast polymer solutions of 5 % (weight/volume) in N,N-dimethylacetamide (DMAc) were held

---

86. Zawodzinski, T.A., C. Derooin, S. Radzinski, J. Sherman, V.T. Smith, T.E. Springer, and S. Gottesfeld, *J. Electrochem. Soc.* **1993**, 140,1041.

under full vacuum at 40°C for 24 hours, then 100°C for 24 hours, and finally 150°C for 12 hours, then removed from the oven. The membranes were converted to the acid (proton) form by boiling in 0.5 M sulfuric acid (H<sub>2</sub>SO<sub>4</sub>) for 2 hours. The membranes were rinsed well then boiled in deionized (DI) water for 2 hours to remove any residual sulfuric acid.<sup>87</sup> The membranes underwent a final rinse in DI water and were then stored in DI water for at least one week before testing.

Sulfonated poly(arylene thioether sulfone) copolymers (PATS) were synthesized using a similar methodology to the BPSH copolymers as described elsewhere.<sup>88</sup> A bithioether was substituted for the biphenol of BPSH in the step growth polymerization scheme to achieve the PATS structure shown in Figure 2-3.

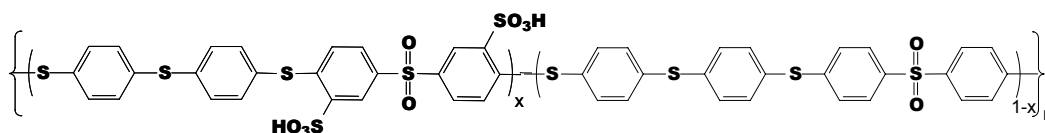


**Figure 2-3: Chemical Structure of PATS**

These membranes were solution cast from DMAc and converted to the acid form in an analogous manner to the BPSH membranes.

---

87. Kim, Y.S., F. Wang, M. Hickner, S. McCartney, Y.T. Hong, T.A. Zawodzinski, J.E. McGrath, *J. Poly. Sci., B: Poly. Phys.* **2003**, 41(22).

88. K.B. Wilkes, V.A. Bhanu, F. Wang, J.E. McGrath, *Polymer Preprints* **2002**, 43(2), 993-994.

Sulfonated polyimides (sPI) were synthesized by the copolymerization of pre-sulfonated monomers. The synthesis and characterization of these copolymers is detailed in Ref. 89 and their chemical structure is shown in Figure 2-4.

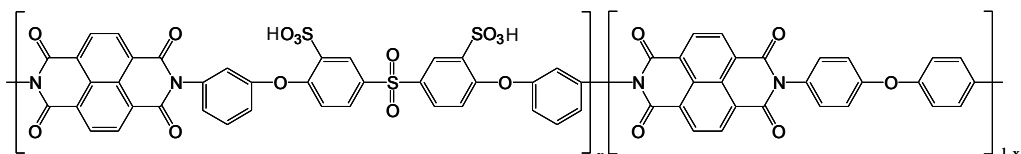


**Figure 2-4: Chemical Structure of sPI**

Sulfonated polyimide copolymers were cast in their triethylammonium salt form from 5% (weight/volume) polymer solutions in NMP on clean glass substrates. After filtering through a 0.45  $\mu\text{m}$  PTFE syringe filter, the cast polymer solutions were slowly dried under infrared heat in a nitrogen atmosphere. Once dry to the touch, the membranes were removed from the plates by submersion in water then dried completely at 160°C for at least 24 hours under full vacuum. These copolymers were converted to the acid form by immersion in boiling 0.5M  $\text{H}_2\text{SO}_4$  for 2 hours and then 1.5 M  $\text{H}_2\text{SO}_4$  for three days. This relatively long time was found to be necessary for complete conversion of the ionic groups to the acid form. The excess acid was removed by thorough rinsing, boiling in DI water for 2 hours followed by a final rinse. The membranes were stored in DI water for at least one week before testing.

---

89. (a) Y.T. Hong, B. Einsla, Y.S. Kim, J.E. McGrath, *Polymer Preprints* **2002**, 43(1), 666-667; (b) Einsla, B., Y.T. Hong, Y.S. Kim, F. Wang, N. Gunduz, J.E. McGrath, *J. Poly. Sci. A* **2003**, submitted.

### 2.3.2 Water Uptake

The water uptake of all membranes was determined by first soaking the membranes in 30°C water for at least one week after acidification. The water uptake of the membranes was determined by a simple weight-difference approach. Wet membranes were removed from the liquid water, blotted dry to remove surface droplets, and quickly weighed. After 3 - 5 measurements to ensure repeatability of the blotting process, the membranes were dried at 80-100°C under full vacuum for at least 24 hours and weighed again. The water uptake of the membranes was calculated according to Equation 2-1 where  $mass_{dry}$  and  $mass_{wet}$  refer to the mass of the wet membrane and the mass of the dry membrane, respectively.

**Equation 2-1** 
$$water\ uptake\ \% = \frac{mass_{wet} - mass_{dry}}{mass_{dry}} \times 100$$

The lambda value ( $\lambda$ ), number of water molecules absorbed per sulfonic acid, can be determined from the mass water uptake and the ion content of the dry copolymer as shown in Equation 2-2.

**Equation 2-2** 
$$\lambda = \frac{mass_{wet} - mass_{dry} / MW_{H_2O}}{IEC \cdot mass_{dry}}$$

Where  $MW_{H_2O}$  is the molecular weight of water (18.01 g/mol), and IEC is the ion exchange capacity of the dry copolymer in equivalents per gram.

### 2.3.3 Protonic Conductivity

Protonic conductivity at 30°C under full hydration (in liquid water) was determined using a Solartron 1260 Impedance/Gain-Phase Analyzer over the frequency range of 10 Hz - 1 MHz. The cell geometry was chosen to ensure that the membrane resistance dominated the response of the system.<sup>90</sup> The resistance of the film was taken at the frequency which produced the minimum imaginary response. The conductivity of the membrane can be calculated from the measured resistance and the geometry of the cell according to Equation 2-3.

**Equation 2-3**

$$\sigma = \frac{l}{Z' A}$$

Where  $\sigma$  is the protonic conductivity,  $l$  is the path length between the electrodes,  $A$  is the cross sectional area available for proton transport, and  $Z'$  is the real part of the impedance response corresponding to the membrane resistance.

### 2.3.4 Electro-osmotic Drag

The method developed by Ren et al.<sup>91</sup> has been adopted to measure the electro-osmotic drag coefficient ( $E_D$ ) of proton exchange membranes in a liquid fed DMFC. This method is desirable

---

90. Zawodzinski, T.A., M. Neeman, L. O. Sillerud and S. Gottesfeld. *J. Phys. Chem.* **1991**, 95, 6040-6044.

91. X.M. Ren, W. Henderson, and S. Gottesfeld, *J. Electrochem. Soc.* **1997**, 144 (9), L267.

because it mirrors the actual operation of a DMFC and does not require specialized instrumentation above the usual fuel cell testing equipment and an inexpensive carbon dioxide sensor. Membrane electrode assemblies for all membranes were prepared with standard Nafion-based electrodes using a direct painting method developed at Los Alamos National Laboratory.<sup>92</sup> Catalyst loadings were about 6 mg/cm<sup>2</sup> of platinum black on the cathode, and 9 mg/cm<sup>2</sup> of ruthenium/platinum black on the anode.

### 2.3.5 Methanol Permeability

The methanol permeability of each acid form membrane was determined in a standard membrane separated diffusion cell. This method has been reported previously by this group<sup>93</sup> and the numerical analysis of this experiment has been outlined by Cussler.<sup>94</sup>

### 2.3.6 Water Self-Diffusion Coefficient

Water self-diffusion coefficients ( $D_{H_2O}$ ) were measured using a Varian Inova 400 MHz (for protons) nuclear magnetic resonance (NMR) spectrometer with a 60 G/cm gradient diffusion probe. The diffusion coefficients for water absorbed in the membranes were determined using a

---

92. S.C. Thomas, X. Ren, S. Gottesfeld and P. Zelenay, *Electrochim. Acta* **2002**, 47, 3741-3748.

93. (a) Hickner, M., F. Wang, Y.S. Kim, T.A. Zawodzinski, J.E. McGrath, *AICHE Topical Conference Proceedings*, Spring National Meeting, New Orleans, LA, March 10-14, 2002; (b) Y. S. Kim, M. A. Hickner, L. Dong, B. S. Pivovar, and J. E. McGrath, *J. Membr. Sci.* **2003**, 212(1-2), 263-282.

94. E.L. Cussler, *Diffusion Mass Transfer in Fluid Systems*, 2nd Ed. Cambridge University Press, New York, 1997.

stimulated echo pulse sequence<sup>95</sup> as shown in Figure 2-5. A total of 16 points were collected at decreasing gradient strength and the signal-to-noise ratio was enhanced by coadding 4 scans.

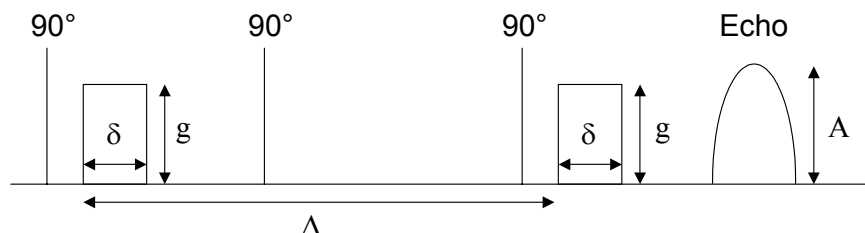


**Figure 2-5: NMR Stimulated Echo Pulse Sequence**

The measurement is conducted by observing the NMR signal intensity ( $A$ ) as a function of the gradient strength ( $g$ ). The diffusion coefficient is determined by fitting the data to Equation 2-4<sup>96</sup>

**Equation 2-4** 
$$A(g) = A(0) \exp[-\gamma^2 D g^2 \delta^2 (\Delta - \delta/3)]$$

where  $\gamma$  is the gyromagnetic ratio ( $26752 \text{ radG}^{-1}\text{s}^{-1}$  for protons),  $D$  is the diffusion coefficient,  $g$  is the gradient strength,  $\delta$  is the length of the gradient pulse, and  $\Delta$  is the time between gradient pulses.

---

95. Tanner, J.E., *J. Chem. Phys.* **1970**, 52, 2523.

96. Stejskal, E.O., J.E. Tanner, *J. Chem. Phys.* **1965**, 42, 288.

Membrane samples of approximately 5 mm by 15 mm by 150  $\mu\text{m}$  were equilibrated in liquid water for at least 24 hours. The samples were removed from the liquid water, blotted to remove droplets, quickly inserted into the NMR tube, and immediately imaged over a span of about 5 minutes. This rapid transfer from the liquid water to the NMR instrument was necessary to avoid excessive drying of the sample during measurement. Measurements were repeated by reimmersing the sample in DI water, waiting at least 30 minutes, and then repeating the transfer and measurement process.

## **2.4 Results and Discussion**

Protonic conductivity is the foremost criteria for fuel cell proton exchange membranes. Without sufficient protonic conductivity, a membrane will never be applicable to hydrogen/air or direct methanol fuel cells. For membranes with low conductivity, the thickness may be decreased to reduce the resistive (Ohmic) losses in a fuel cell, but this technique can only be exploited to a certain extent. When the thickness is decreased, the reactant flux across the membrane increases (hydrogen or methanol and oxygen) and the mechanical properties decline, leading to shortened lifetime and reduced durability. An intrinsic copolymer protonic conductivity of at least 0.03 S/cm (as measured in 30°C in liquid water) is postulated to produce high performance proton exchange membranes and the resulting membrane electrode assemblies.

The protonic conductivity of various membranes in this study is correlated with ion exchange capacity in Figure 2-6.

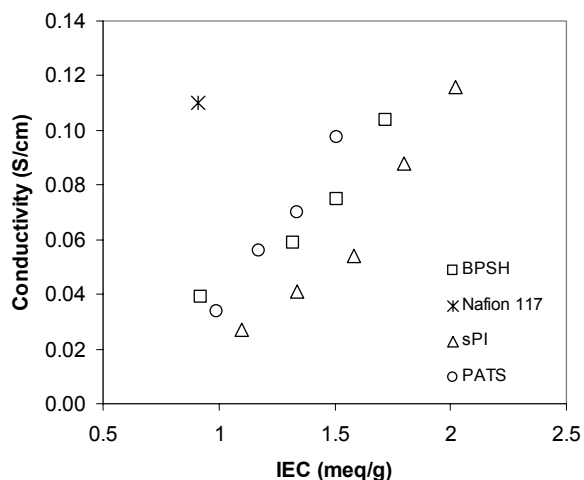


**Figure 2-6: Protonic Conductivity of Nafion, PATS, BPSH, and Sulfonated Polyimide on an Ion Exchange Capacity Basis**

One notes that Nafion has a much higher conductivity than the other systems even though it contains less ions on a mass basis. Many reports have referred to the high acidity of the perfluorosulfonic acid of Nafion compared to the arylsulfonic acid of the other copolymers as a rationale for such behavior. This is certainly a reasonable assumption and has driven researchers to explore the role of strongly acidic functional groups such as sulfonimide moieties in proton exchange membranes.<sup>97</sup>

---

97. (a) Koppel, I.A., R.W. Taft, F. Anvia, S.Z. Zhu, L.Q. Hu, K.S. Sung, D.D. DesMarteau, L.M. Yagupolskii, Y.L. Yagupolskii, N.V. Ingatev, N.V. Kondratenko, A.Y. Volkonskii, V.M. Vlasov, R. Notario, P.C. Maria, *J. Am. Chem. Soc.* **1994**, 116, 3047-3057; (b) Paddison, S.J., L.R. Pratt, T. Zawodzinski, D.W. Reagor, *Fluid Phase Equilibria* **1998**, 151, 235; (c) Eikerling, M., S.J. Paddison, T.A. Zawodzinski, *J. New Mat. For Elect. Sys.* **2002**, 5(1), 15.

DesMarteau et al. have compared Nafion and a structurally similar bis[(perfluoroalkyl) sulfonyl]imide-based ionomer.<sup>98</sup> There was not an increase in proton conductivity produced by incorporation of the sulfonimide moiety in their copolymer, in lieu of the perfluorosulfonic acid moiety. In fact, their sulfonimide-based copolymer gave similar results in all respects to Nafion. Allcock et al. has explored sulfonated poly(phosphazene)s with either sulfonic acid<sup>99</sup> or sulfonimide<sup>100</sup> proton conducting substituents. Like DesMarteau, this group did not observe a significant increase in conductivity for the sulfonimide-based copolymers. Despite the acidity difference in model compounds, no direct evidence has been provided for the sulfonimide moiety producing increased conductivity over sulfonic acid when incorporated in proton exchange membranes, but this strategy still remains under investigation.

Aside from Nafion, all of the copolymers in Figure 2 utilize sulfonic acid (or more succinctly, arylsulfonic acid) as the proton conducting functional group. What is striking about the conductivity data in Figure 6 is that the different families of copolymers give different conductivity when the copolymers are compared on an ion exchange capacity basis. BPSH and PATS copolymers have very similar conductivity when compared on an ion exchange capacity basis, most likely due to their very similar chemical structure, but sulfonated polyimides show consistently lower protonic conductivity over all ion exchange capacities. Since all these copolymers use essentially the same proton conductor, this observation cannot be a result of the acidity of the ion-conducting moiety. Another factor, either chemical or morphological, must

---

98. Savett, S.C., J.R. Atkins, C.R. Sides, J.L. Harris, B.H. Thomas, S.E. Creager, W.T. Pennington, and D.D. DesMarteau, *J. Electrochem. Soc.* **2002**, 149(12), A1527.

99. Allcock H.R., R.J. Fitzpatrick, L. Salvati, *Chem. Mater.* **1991**, 3, 1120-1132.

100. Hofmann, M.A., C.M. Ambler, A.E. Maher, E. Chalkova, X.Y. Zhou, S.N. Lvov, H.R. Allcock, *Macromolecules* **2002**, 35, 6490-6493.

influence the conductivity of the copolymers aside from the acidity of the ion conducting group. It is the goal of this paper to determine the fundamental factors that control the properties of each series of copolymers.

The phenomenon of electro-osmotic drag is associated with proton transport in aqueous media. As protons are conducted through a water-containing membrane, a certain number of water molecules are transported in concert with the protons.<sup>101</sup> The number of water molecules conducted across the membrane for every proton is termed the electro-osmotic drag coefficient expressed as the number of water molecules per proton ( $n \text{ H}_2\text{O}/\text{H}^+$ ).

The electro-osmotic drag coefficients at 60°C for fully hydrated membranes in a DMFC geometry are reported in Figure 2-7. Nafion and BPSH data has been reported earlier,<sup>102</sup> and it has been reproduced here for comparative purposes in light of the new results on sulfonated polyimide copolymers.

---

101. (a) Kreuer, K.D., *Solid State Ionics* **1997**, 94(1-4) 55-62. (b) Kreuer, K.D., *Chem. of Matls.* **1996**, 8(3) 610-614.

102. (a) Hickner, M., F. Wang, H. Shobha, N. Gunduz, J.B. Mechem, J.E. McGrath, AIChE 2000 Fall National Meeting, Los Angeles, CA, November, 12-17, 2000; (b) M. Hickner, F. Wang, Y.S. Kim, T.A. Zawodzinski, J.E. McGrath, B. Pivovar "Electro-osmotic Drag and Methanol Flux in Sulfonated Poly(Arylene Ether Sulfone) Copolymers: Elucidating Morphology from Transport," *J. Electrochem. Soc.* **2003**, in progress.

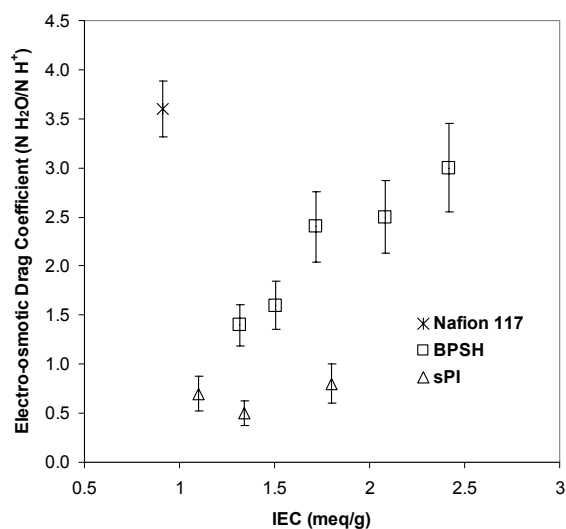


**Figure 2-7: Electro-osmotic Drag Coefficients at 60°C for Fully Hydrated Nafion, BPSH, and Sulfonated Polyimide Membranes**

The electro-osmotic drag coefficient of the wholly aromatic copolymers (BPSH and sPI) is much lower than Nafion 117 over the entire range of ion exchange capacities. The electro-osmotic drag coefficient is a measure of how mobile the water is in a particular system. In Nafion, the water moves relatively easily under the influence of the proton as indicated by its large electro-osmotic drag coefficient, whereas in BPSH and sPI copolymers, the water is not as susceptible to viscous drag created by the movement of the protons through the ionic domains.

Lower electro-osmotic drag in these materials would be reasonable if either the bulk water uptake, or lambda value (number of water molecules per sulfonic acid moiety) were considerably lower in the wholly aromatic systems than in Nafion, but in fact the water uptake of BPSH and sulfonated polyimides is similar to Nafion or in some cases greater than Nafion117. Table 2-1 shows the water uptake on a mass percent basis and a lambda basis for the copolymers in this study.

**Table 2-1: Water Uptake and Lambda Values for the Copolymers**

	IEC (meq/g)	Water Uptake (mass %)	$\lambda$ (H <sub>2</sub> O/SO <sub>3</sub> H)
Nafion 117	0.9	19	12
BPSH 30	1.3	29	12
BPSH 40	1.7	56	18
BPSH 50	2.0	124	34
BPSH 60	2.4	190	44
PATS 20	0.8	19	13
PATS 30	1.2	54	26
PATS 40	1.5	86	77
sPI 40	1.1	29	15
sPI 50	1.3	38	16
sPI 60	1.8	57	18

As Table 2-1 illustrates, most copolymers show more water uptake on a mass percent and lambda basis as compared to Nafion 117. The markedly decreased electro-osmotic drag coefficients in the wholly aromatic systems at comparable or greater water uptakes indicates that the hydrophilic domains where transport occurs are distinctly different in these materials than in Nafion.

The methanol permeability of these copolymers displays similar trends to both conductivity and electro-osmotic drag as reported in Figure 2-8.

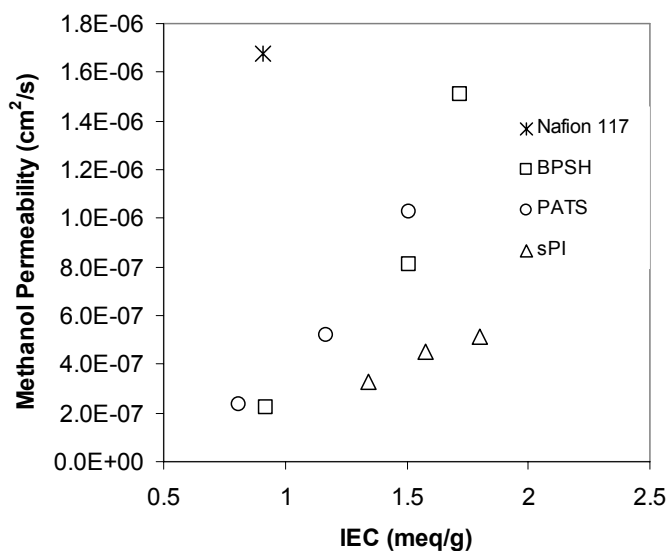


**Figure 2-8: Methanol Permeability of Nafion, BPSH, PATS, and Sulfonated Polyimide Copolymers**

Again, Nafion, even with its low ion content, has high methanol permeability particularly when compared to the other copolymers on an ion exchange capacity basis. The low methanol permeability of the wholly aromatic systems makes them desirable for direct methanol fuel cell systems. The technical feasibility of these membranes as proton exchange membranes for direct methanol fuel cells has been addressed elsewhere.<sup>103</sup>

Considering all of the transport properties presented in this paper and the similar trends observed in the case of proton conductivity, electro-osmotic drag, and methanol permeability, one may conclude that these transport properties are coupled. This observation has been made

---

103. (a) Hickner, M., B. Pivovar, F. Wang, T. Zawodzinski, J.E. McGrath, "Transport of methanol and protons in proton exchange membranes," The 201st Meeting of The Electrochemical Society, Inc., Philadelphia, PA, May 12-17, 2002; (b) Pivovar, B., M. Hickner, J. McGrath, P. Zelenay, T. Zawodzinski, "Problems with Membrane Electrode Assemblies for non-Nafion Based Membranes," The 200<sup>th</sup> Meeting of the Electrochemical society, Inc., San Francisco, CA, Sept 2-7, 2001.

previously,<sup>104</sup> however, no satisfactory explanation has so far been provided as to why seemingly different issues such as protonic conductivity, electro-osmotic drag, and methanol permeability should be associated in these systems.

It has been proposed<sup>85</sup> that the state of absorbed water in Nafion and BPSH copolymer membranes as determined by moderately pressurized dynamic scanning calorimetry and <sup>1</sup>H NMR T<sub>2</sub> relaxations plays a large role in determining proton conductivity, methanol permeability, and electro-osmotic drag. The results presented here extend the previous study by including new copolymer structures and quantifying the state of absorbed water by its self-diffusion coefficient (D<sub>H<sub>2</sub>O</sub>) as determined by <sup>1</sup>H pulsed-field gradient NMR. The self-diffusion coefficients of each copolymer (fully hydrated, 30°C) are shown in Figure 2-9 on the basis of ion exchange capacity in the same fashion as the previous transport results.

---

104. (a) Pivovar, B., PhD dissertation, Electrochemical Selectivity and Electro-osmosis in Direct Methanol Fuel Cell Electrolytes. University of Minnesota, Minneapolis, MN, 2000; (b) Pivovar, B., W. Smyrl, E. Cussler, *Journal of Membrane Science* **2003**, in progress.

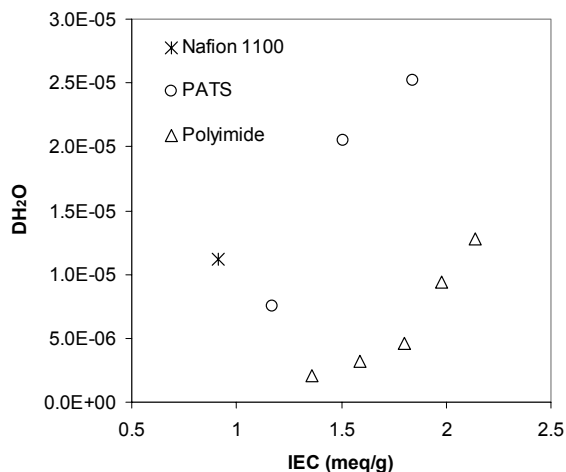


**Figure 2-9: Water Self-Diffusion Coefficients for Nafion, PATS, and Sulfonated Polyimide Membranes - Fully Hydrated Samples at 30°C**

The water self-diffusion coefficients help to quantify the state of absorbed water in each system. More loosely bound water yields a higher self-diffusion coefficient, while more tightly bound water yields a lower self-diffusion coefficient. This technique is not able to separate the different states of water into tightly bound, loosely bound, and free water as is possible with DSC and <sup>1</sup>H NMR T<sub>2</sub> relaxations, but rather the self diffusion coefficient gives an overall average of the distribution of the states of water. This average behavior of water over all states may be more applicable when discussing bulk transport properties of the membranes.

The features of Figure 2-9 are strikingly similar to the other data presented in this study for protonic conductivity, electro-osmotic drag, and methanol permeability. Nafion has a high water self-diffusion coefficient especially in light of its low ion content, which is an indication of a large amount of loosely bound and/or free water. Nafion also displays the largest protonic conductivity, electro-osmotic drag, and methanol permeability on an ion exchange capacity

basis. On the other hand, the sulfonated polyimide membranes display the lowest water self-diffusion coefficient (an indication of a large fraction of tightly bound water) and has the lowest conductivity, electro-osmotic drag, and methanol permeability of all of the copolymers in this study even though its water uptake is higher than Nafion and comparable to PATS. These results strengthen the connection between the state of absorbed water and the membrane transport properties in these types of systems.

The water self-diffusion coefficient and other transport properties of the membrane as determined by the state of water are proposed to be highly dependent on the local morphological structure of the ionic domains. The ionic domain morphology in turn relies on the detailed chemical structure of the copolymer. The chemical structure of Nafion and BPSH are again contrasted in Figure 2-10.

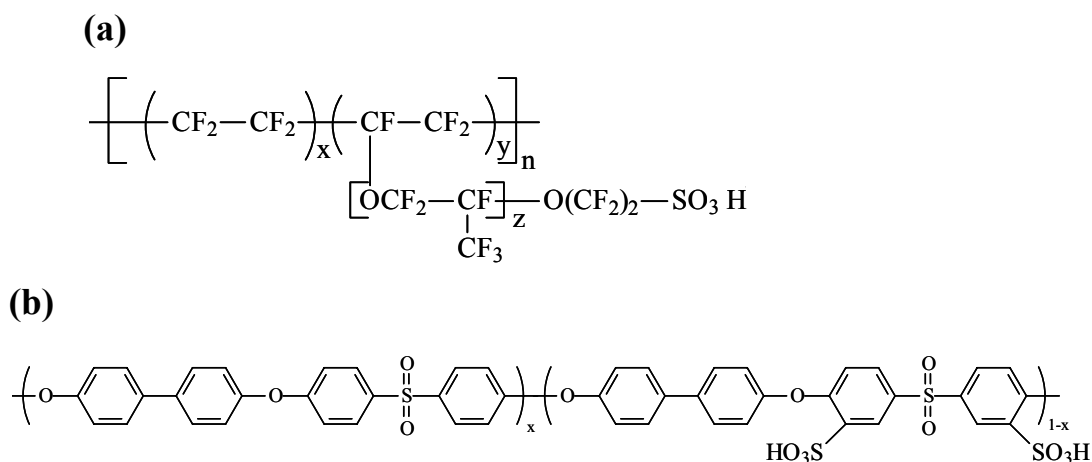


**Figure 2-10: Chemical Structure of (a) Nafion and (b) BPSH**

Two features of the chemical structure of the copolymers stand out in comparison to one another. Firstly, the ionic group in Nafion is located at the end of a long, flexible, perfluoroether side chain, while the ionic groups of BPSH are connected directly to the backbone. Also, the very hydrophobic tetrafluoroethylene backbone of Nafion itself is rather flexible as compared to the relatively stiff poly(arylene ether) backbone of BPSH (as supported by stress-strain results<sup>105</sup>) or the yet stiffer polyimide backbone as shown in Figure 2-4. These two features, ionic group location and backbone stiffness play a large role in determining how well the ionic groups can organize into hydrophilic domains. Ionic organization or clustering in Nafion may be rather facile because the ionic groups are on the end of the side chains without the surrounding unsulfonated polymer structure to disrupt ionic organization. In addition, there is a strong driving force for the strongly hydrophilic sulfonic acid groups to phase separate from the extremely hydrophobic tetrafluoroethylene-based backbone. These two factors lead to a high concentration of ionic groups in the ion rich domains of Nafion. For the ionic groups to associate in BPSH and other aromatic systems with the sulfonic acid moiety tethered directly to the backbone, a considerable backbone motion is needed to accommodate ionic clustering. It is possible that these ionic clusters will include other parts of the copolymer chain than just the ionic moieties leading to a lower concentration of ionic groups in what would be considered an ion rich domain. Also, the backbones of the aromatic copolymers in this work are not as strongly hydrophobic as the tetrafluoroethylene-based backbone of Nafion. The driving force for phase separation between hydrophobic and hydrophilic moieties is not as strong in these aromatic systems.

---

105. Kim, Y., F. Wang, M. Hickner, T. Zawodzinski, J.E. McGrath, *J. Membr. Sci.* **2003**, 212, 263-282.

The extent of phase separation is a useful concept to describe the differences between the copolymers in this work. Extent of phase separation is intended to suggest how well defined and how strongly phase separated the hydrophilic regions and hydrophobic regions of the morphology are in each system. Nafion probably has a very high extent of phase separation leading to distinct differences between ion rich and ion poor domains. The sulfonated polyimide would have a low extent of phase separation where the interface between the two phases is less distinct. The other copolymers (PATS and BPSH) would lie somewhere between the two extremes. Block and graft architectures could certainly produce new systems of interest.

In Nafion, the ionic groups are strongly segregated from the hydrophobic regions of the copolymer. When this type of morphology absorbs water, the water is proposed to be concentrated in well-defined pores and tends to be “free” or more loosely bound within the ionic domains. In BPSH (and even more so in sulfonated polyimides), the boundaries between ionic and nonionic phases are less distinct. When water is absorbed into this morphology, the water may become more tightly bound within the copolymer morphology and leads to suppressed transport properties.

A pictorial model for this type of ionic clustering, which depends on chain stiffness and ionic moiety location, was proposed earlier.<sup>102</sup> The proposed model is suggested to be valid for even stiffer systems such as the sulfonated polyimide. In the polyimide copolymer, the phase separation of ionic and nonionic domains is even less distinct than the sulfonated poly(arylene ether sulfone) copolymers and the water is more tightly bound within the morphology as a result. The transport data can be generalized on the basis of the expected extent of phase separation or

how well the ionic groups can be expected to organize into highly concentrated domains. A schematic of the transport data on the basis of ion exchange capacity and extent of phase separation is shown in Figure 2-11.

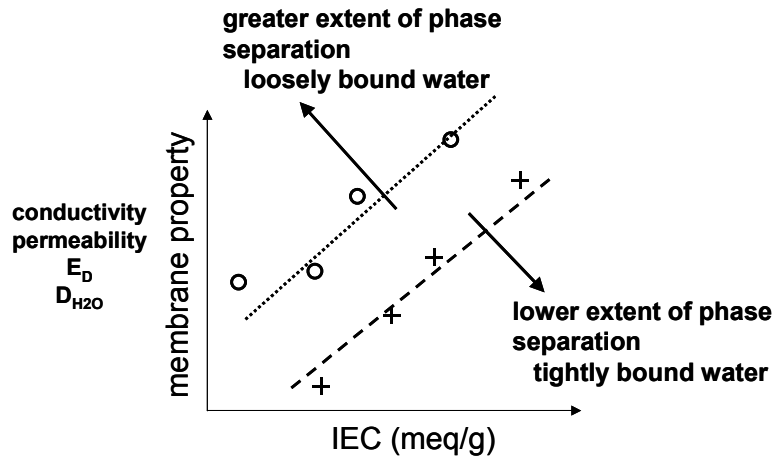


**Figure 2-11: Proposed Model Relating Extent of Phase Separation to Membrane Transport Properties**

Figure 2-11 suggests what transport properties may be expected when two families of copolymers with different chemical structures are compared on an ion exchange capacity (IEC) basis. More highly phase separated copolymers are predicted to yield increased formation of free and loosely bound water and thus enhanced transport. Less phase separated structures, where the ionic groups are not as well clustered, create more tightly bound water within their morphology and this in turn decreases the species transport through the membrane.

The effect of ion exchange capacity within a family of copolymers is easily understood. Increased ion content increases hydrophilicity and the amount of water absorbed within a given system. More water absorbed into a similar morphology creates a larger fraction of loosely bound water, which enhances the transport properties as ion exchange capacity increases. The state of water arguments compliment the simple picture of adding more ionic groups to the sample copolymer backbone, but the concept becomes especially important when comparing copolymers from different families where the state of water can be drastically different in each system regardless of the total bulk water uptake or lambda value.

## **2.5 Conclusions**

All experimental transport properties investigated including protonic conductivity, electro-osmotic drag, methanol permeability, and water diffusion coefficient were suppressed in wholly aromatic copolymer membranes compared to Nafion when considered on an ion exchange capacity basis. A consistent trend was observed with Nafion having the highest transport, sulfonated polyimide being the lowest, and BPSH and PATS in between the two extremes. Within a copolymer family, the transport property increased monotonically with increasing ion exchange capacity.

Comparing the transport properties of families of copolymers with dissimilar chemical structures has proven difficult, if not impossible, when only the total water uptake on a mass (or lambda) basis is considered. One must take into account the state of water (eg. free, loosely bound, and strongly (non-freezable) bound) in the copolymer membrane. This research has provided data

for the transport of protons, water, and methanol for systematic series of wholly aromatic copolymers and Nafion. The transport properties of all of the copolymers followed a logical order according to copolymer family when ion conductor location and backbone chain stiffness are considered. In Nafion, less stiff backbone chains and ionic groups located on the end of long, flexible side chains allowed the ionic groups to phase separate strongly from the very hydrophobic matrix and create a large fraction of loosely bound water when the copolymer membrane was swollen with water. In the case of wholly aromatic copolymers such as sulfonated poly(arylene ether sulfone) and sulfonated polyimide copolymers, the hydrophilic and hydrophobic domains were less sharply phase separated. This morphological situation created a larger fraction of tightly bound strongly interacting water within the copolymer structure and greatly suppressed the transport of protons, methanol, and water through the proton exchange membrane.

Other factors besides ion conductor location, ionic moiety location, and chain stiffness certainly play a role in determining the extent of phase separation of an ion containing copolymer. BPSH copolymers have proven to be sensitive to processing variables such as hydrothermal treatment<sup>76</sup> where the transport properties of the membrane were dependent on the thermal history of the membrane. In light of the results in this work, the phenomena observed in Reference 76 up to the hydrogel temperature was probably due the higher processing temperatures leading to a higher degree of phase separation thereby creating more loosely bound water within the copolymer microphase morphology and thus enhancing transport.

Another factor, which may play into the extent of phase separation between hydrophilic and hydrophobic regions of the copolymer, could be the difference in hydrophilicity between the ionic group and the polymer backbone. It is reasonable to assume that a more hydrophilic backbone would not be as prone to phase separation from the extremely hydrophilic ionic groups. A more hydrophilic structure in the backbone would tend to associate to a greater degree with absorbed water and cause that water to be more tightly bound within the copolymer membrane structure. On the other hand, a strongly hydrophobic backbone, such as that of Nafion, would be expected to produce a very phase-separated morphology and thus more loosely bound water.

Given the various factors that determine the phase separation characteristics of ion containing copolymers, we suggest that ionic moiety location and chain stiffness play a dominant role in determining the transport properties of proton exchange membranes. This interpretation of the membrane transport data gives some insight as to what chemical structures could prove to be desirable for improved proton exchange membranes for a given fuel cell application. For instance, a hydrogen/air proton exchange membrane may require maximum conductivity. For high conductivity one would desire as much loosely bound water as possible which is the result of a highly phase separated structure where the ionic groups are closely associated. In a direct methanol fuel cell, low methanol permeability may be the most desirable membrane characteristic. This would be accomplished by designing a membrane that did not have a high degree of phase separation and thus a large fraction of tightly bound water contained in its morphological structure.

# CHAPTER 3. ELECTRO-OSMOTIC DRAG AND METHANOL FLUX IN SULFONATED POLY(ARYLENE ETHER SULFONE) COPOLYMERS: ELUCIDATING MORPHOLOGY FROM TRANSPORT

## 3.1 Abstract

Progress in characterizing a new class of proton exchange membranes for application in direct methanol fuel cells is reported. The new membranes are directly copolymerized sulfonated wholly aromatic poly(arylene ether sulfones) and their synthesis and several physical properties have been reported previously by this group. Specifically, this paper focuses on the electro-osmotic drag and methanol transport of these new membranes. All membranes investigated showed a lower electro-osmotic drag coefficient than Nafion<sup>®</sup> 117 between 30°C and 80°C. Methanol transport was studied using a limiting crossover current method in a direct methanol fuel cell. Convective velocities for fluid transport through the membrane were determined and their impact on methanol flux was analyzed. The convective velocities observed in the experimental membranes were lower than those in Nafion. It is hypothesized that the microphase-separated morphology (ion clustering) of the membranes has a large influence on both the electro-osmotic drag and methanol flux, primarily by influencing the state of absorbed water. A morphological model that accounts for the differences observed in the electro-osmotic drag difference between the experimental membranes and Nafion is proposed.

keywords: direct methanol fuel cell, proton exchange membrane, limiting crossover current, electro-osmotic drag, methanol transport

### **3.2 Introduction**

Fuel cells are well recognized as an attractive energy source for next generation automobiles, stationary power, and portable power. Accompanying this interest in the technological application of fuel cells, a considerable research effort has been focused on understanding fundamental aspects and developing new materials to increase the performance of fuel cells. The VT group is primarily involved in the investigation of the proton exchange membrane (PEM) and the synthesis of new copolymer electrolytes for both hydrogen/air and direct methanol fuel cells (DMFC). This publication will center on two important properties for direct methanol fuel cells, namely electro-osmotic drag and methanol permeability, for one series of promising membrane candidates.

DMFC systems are typically operated with a liquid feed, water management, both on a local scale (in the catalyst layers) and on a global scale (system-wide), is an important consideration. In liquid feed DMFC operation, the anode is principally saturated with liquid methanol solution, so the attention is focused on the sources of water at the cathode. Various sources of water at the DMFC cathode are shown in Figure 3-1.



and absorbs more water as the equivalent weight decreases (ion exchange capacity increases), and thus shows a higher electro-osmotic drag coefficient. Ren and Gottesfeld also showed that the electro-osmotic drag coefficient increased with temperature.

In typical fuel cell electrolytes such as Nafion, where electro-osmotic drag coefficients range from 1 to 4 water molecules per proton, the electro-osmotic drag contribution to the water flux at the cathode can be substantial. In most practical operating systems, some fraction of the water in the cathode exhaust must be collected and recycled to the system instead of being released to the atmosphere. This process can place large parasitic losses on the system and lower the overall efficiency of the device. The amount of water required to be recycled is closely related to the electro-osmotic drag coefficient of the electrolyte, therefore membranes with lower electro-osmotic drag coefficients are desirable.<sup>108</sup>

Nafion has a relatively high electro-osmotic drag coefficient and current Nafion technology (Nafion 117, 1100 equivalent weight, and 0.007 inches or 178  $\mu\text{m}$  thick) is considered limited for DFMC applications because of its high methanol permeability. The methanol crossover from anode to cathode hampers fuel cell operation by causing lower cell voltages and decreased efficiency. Fuel cell operating strategies have been developed for combating methanol crossover, but a new membrane with lower intrinsic methanol permeability would be very desirable to realize gains in performance and greater dynamic operating ability. There has been and continues to be research on other types of polymer electrolytes with lower methanol permeability, but this lower permeability often comes at the expense of conductivity. The BPSH membranes presented in this study are interesting because they display significantly lower

methanol crossover without sacrificing protonic conductivity and have shown good performance in DMFCs.<sup>109</sup>

Limiting crossover current measurements in a DMFC have been used to characterize membrane methanol permeability. While absolute methanol permeability is not the focus of this paper, the characteristics of methanol transport are. In particular, the flux of methanol through the membrane is used to analytically differentiate between the proposed phase separation characteristics of Nafion and the experimental membranes. Additionally, by comparing the electro-osmotic drag coefficients of Nafion 117 and ion exchange capacities of sulfonated poly(arylene ether sulfone) copolymers, some inferences about each membrane's micro or nanophase morphology may be made.

### 3.3 Theory

Ren et al. reported a method for determining the methanol crossover of a DMFC membrane (membrane electrode assembly) in fuel cell hardware.<sup>110</sup> This method allows facile determination of methanol crossover in the standard DMFC hardware with the addition of an external power supply. MEA preparation techniques used in this study are reported in the Experimental section of this document. The experimental schematic is shown in Figure 3-2.

---

109. Pivovar, B.S., M. Hickner, J. McGrath, P. Zelenay, T. Zawodzinski, "Problems with membrane electrode assemblies for non-Nafion based membranes," The 200<sup>th</sup> Meeting of the Electrochemical Society, Inc., San Francisco, CA, September 2-7, 2001.

110. Ren, X., T.E. Springer, T.A. Zawodzinski and S. Gottesfeld, *J. Electrochem. Soc.* **2000**, 147(2), 466.

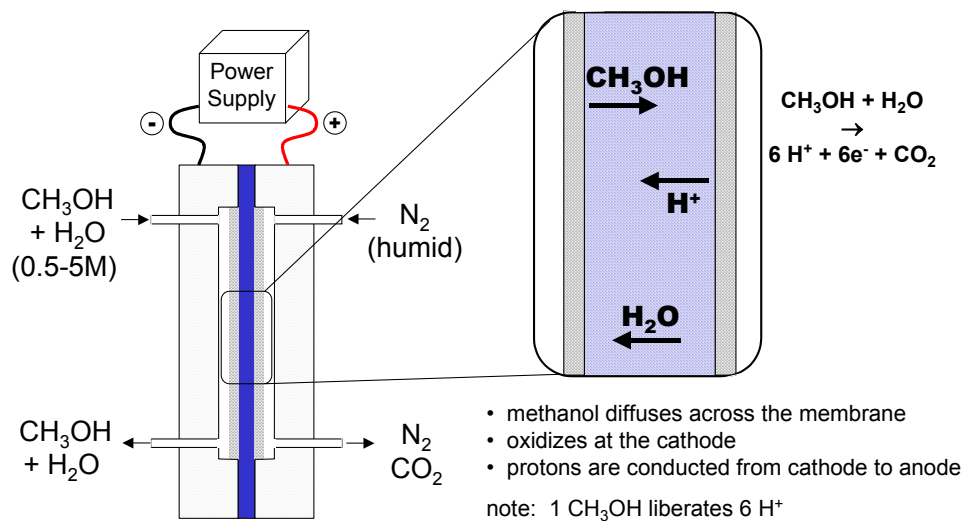
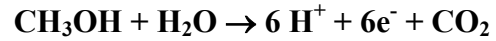


**Figure 3-2: Methanol Crossover Measurements Using Limiting Current in a DMFC**

A methanol/water solution of known concentration was introduced to the anode compartment (in fuel cell configuration) with a high flow rate to minimize concentration depletion (1.8 mL/min. in a 5cm<sup>2</sup> cell). The cathode compartment is fed with humidified nitrogen at 500 standard cm<sup>3</sup>/min. Unlike typical DMFC operation, where methanol is oxidized at the fuel cell anode and power is generated within the cell, a power supply is connected to the fuel cell in the opposite orientation forcing current to flow backward through the cell with respect to normal fuel cell orientation. In this configuration, what is traditionally considered the fuel cell ‘anode’ becomes the counter electrode (cathode), and the fuel cell ‘cathode’ is the working electrode (anode). Methanol diffuses through the ‘anode’ catalyst layer, across the membrane, and is oxidized at the fuel cell ‘cathode’ according the reaction:

**Equation 3-1**



The protons are then driven back across the membrane by the applied potential where they react at the fuel cell anode to produce hydrogen.

Methanol flux ( $j_{\text{CH}_3\text{OH}}$ ) through the membrane by diffusion is described by Fick's Law

**Equation 3-2**

$$j = -D\nabla c$$

Equation 3-3 is the 1-dimensional form of Fick's Law as it applies to this problem

**Equation 3-3**

$$j_{\text{CH}_3\text{OH}} = -D \frac{dc_{\text{CH}_3\text{OH}}}{dz}$$

Equation 3-3 is integrated over the limits 0 to  $\ell$  with respect to position ( $z$ ). and  $H \cdot c_0$  to  $H \cdot c_1$  with respect to methanol concentration ( $c_{\text{CH}_3\text{OH}}$ ). The solubility or partition coefficient,  $H$  is introduced with the concentration term to account for the partitioning of methanol between the solution and the membrane. The permeability of a species is its diffusion coefficient times its solubility, so the product,  $DH$ , in this work is the methanol permeability of the membrane. If  $c_0$  is the feed concentration of methanol into the cell at  $z = 0$ ,  $c_1$  is the concentration at  $z = \ell$ , which is zero for the limiting crossover current geometry. After integration, the resulting flux is described by Equation 3-4,

**Equation 3-4**

$$j_{CH_3OH} = \left( \frac{DH}{l} \right) (c_o)$$

where the flux is only a function of the methanol feed concentration ( $c_o$ ), thickness of the membrane ( $l$ ), and methanol permeability ( $DH$ ). Cussler<sup>111</sup> outlined this solution to the simple membrane separated cell first proposed by Barnes in 1934 and later simplified by Robinson and Stokes in 1960. The analysis assumes that the membrane is at steady-state, permeability is independent of concentration, there is no liquid phase mass transfer resistance, and also neglects water flux and membrane porosity and tortuosity.

From the stoichiometry shown in Equation 3-1, methanol permeability ( $DH_{LC}$ ) can be computed from the resulting current as measured in a fuel cell during a crossover current experiment according to Equation 3-5:

**Equation 3-5**

$$DH_{LC} = \frac{I_x \cdot l}{F \cdot c_o \cdot 6}$$

If the transport of methanol through the membrane in the limiting crossover current experiment was a purely diffusive process, the methanol permeability would not change with concentration. However, the opposing flux of both protons and water (through electro-osmotic drag) must be

---

111. E.L. Cussler, Diffusion Mass Transfer in Fluid Systems, 2nd Ed. Cambridge University Press, New York, 1997.

considered in this measurement. A schematic of the species transport within a sulfonic acid lined, hydrated membrane pore is shown in Figure 3-3.

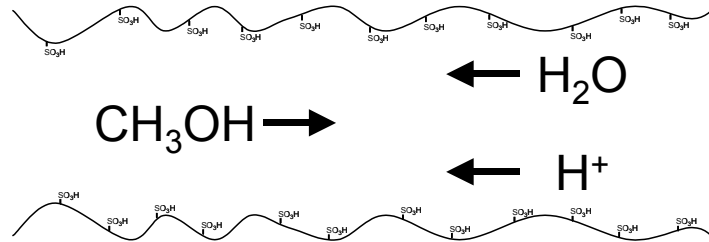


**Figure 3-3: A Model for the Opposing Movement of Species Through a Pore in the Limiting Crossover Current Experiment**

Once an opposing velocity is introduced into the system, Equation 3-4 is no longer valid. An additional term incorporating the convective velocity introduced by the opposing movement of protons and water must be added to the equation. Equation 3-6 shows the additional concentration-dependent term needed to account for this counter flux.

**Equation 3-6**

$$j_{CH_3OH} = -D \frac{dc_{CH_3OH}}{dz} - c_{CH_3OH} v_o$$

Notice the sign of the extra term is negative since the convective velocity opposes methanol diffusion and decreases the apparent flux of methanol across the membrane. This results in a flux consisting of a diffusive contribution and a convective contribution, in a treatment similar to

that of modeling work by Yang and Pintauro.<sup>112</sup> However, our expression is simplified because methanol is an uncharged species, hence no migration contribution, and there is no hydration contribution at steady-state. Also, unlike Yang and Pintauro, our equation assumes all species within the membrane are equivalent, i.e. no radial dependence of properties for species within the membrane, so that the values determined are effective permeability and convective velocity, neglecting both membrane porosity and tortuosity. Equation 3-6 is integrated over concentration and position with the same boundary conditions as Equation 3-4 to yield Equation 3-7.

**Equation 3-7**

$$j_{CH_3OH} = \frac{Hc_o v_o}{\exp\left(\frac{v_o l}{D}\right) - 1}$$

The convective velocity,  $v_o$ , can be determined by fitting Equation 3-7 to the experimentally determined methanol flux. This approach is similar to the work of Mayer and Woermann who added a fitting parameter to account for the apparent lower calculated fluxes of larger molecules.<sup>113</sup>

An electro-osmotic drag coefficient ( $E_D$ ) can also be estimated from measured or calculated properties using Equation 3-8. Based on the limiting crossover current density, water molar volume, and experimentally determined convective velocity, one can compute an estimate of the electro-osmotic drag coefficient assuming no back diffusion of water. This calculated electro-

---

112. Yang, Y., P.N. Pintauro, *AIChE Journal* **2000**, 46(6), 1177-1190.

113. Mayer, K., D. Woermann, *J. Membr. Sci.* **1997**, 127, 35-45.

osmotic drag coefficient,  $E_{Dcalc}$ , can then be compared to experimentally determined electro-osmotic drag coefficient,  $E_D$ .

**Equation 3-8**

$$E_{Dcalc} = \frac{v_o \cdot F}{I_x \cdot \bar{V}_{H_2O}}$$

where  $v_o$  is the convective velocity,  $F$  is Faraday's constant,  $I_x$  is the limiting crossover current, and  $\bar{V}_{H_2O}$  is the molar volume of water.

It is proposed that the convective velocity ( $v_o$ ), and electro-osmotic drag coefficient ( $E_D$ ) give information about the state of water and the morphological arrangement of the ionic domains within the membrane.

## 3.4 Experimental

### 3.4.1 Materials

Wang et al.<sup>114</sup> have reported the novel synthesis of a sulfonated poly(arylene ether sulfone) copolymers where the direct copolymerization of sulfonated monomers was employed in order to define the precise location and concentration of sulfonic acid units. The copolymer chemical structure is shown in Figure 3-4.

---

114. Wang, F., M. Hickner, Y. Kim, T. Zawodzinski, J.E. McGrath, *J. Membr. Sci.* **2002**, 197, 231-242.

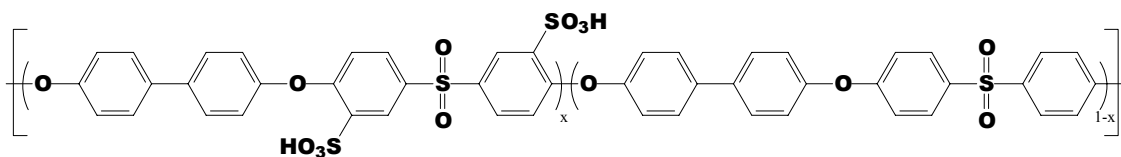


**Figure 3-4: Chemical Structure of Sulfonated Poly(arylene ether sulfone) Copolymers**

One may note that these polymers have been abbreviated BPSH XX (biphenol sulfone,  $H^+$  form), where XX represents the molar percent of the disulfonated monomer. These copolymers have proven through repeated fuel cell testing to have potential advantages such as lower methanol crossover and electro-osmotic drag in DMFCs.<sup>115</sup>

The membranes were prepared by first dissolving the salt form copolymer (mixed  $K^+$  and  $Na^+$ ) in N,N-dimethylacetamide at about 5% weight/volume. The polymer solutions were stirred for a minimum of 72 hours and then cast onto level, aluminum molds placed in a vacuum oven. Full vacuum was applied and the temperature was raised to 50°C for 24 hours, 100°C for 24 hours and finally to 160°C for 12 hours to eliminate the solvent before cooling and removal from the molds. Membranes were converted to the acid form by boiling in dilute sulfuric acid for 2 hours followed by boiling in deionized water for 2 hours to remove all residual acid (Method 2).<sup>116</sup> Membranes were stored in deionized water for at least one week before testing.

---

115. Pivovar, B.S., M. Hickner, F. Wang, J.E. McGrath, P. Zelenay, T. Zawodzinski, AIChE Topical Conference Proceedings, Spring National Meeting, New Orleans, LA, March 10-14, 2002.

Nafion membranes were prepared for MEA fabrication by previously reported methods.<sup>107</sup>

### 3.4.2 Electro-osmotic Drag

The method developed by Ren et al.<sup>117</sup> has been adopted to measure the electro-osmotic drag of proton exchange membranes in a liquid fed DMFC. This method is desirable because it mirrors the actual operation of a DMFC and does not require specialized instrumentation above the usual fuel cell testing equipment and an inexpensive carbon dioxide sensor. Membrane electrode assemblies for all membranes were prepared with standard Nafion-based electrodes using a direct painting method developed at Los Alamos National Laboratory.<sup>118</sup> Catalyst loadings were approximately 6 mg/cm<sup>2</sup> of platinum black on the cathode, and 9 mg/cm<sup>2</sup> of ruthenium/platinum black on the anode.

---

116. Kim Y.S., F. Wang, M. Hickner, S. McCartney, Y.T. Hong, T.A. Zawodzinski, J.E. McGrath, *J. Poly. Sci., B: Poly. Phys.* **2003**, 41(22).

117. X.M. Ren, W. Henderson, and S. Gottesfeld, *J. Electrochem. Soc.* **1997**, 144 (9), L267.

118. S.C. Thomas, X. Ren, S. Gottesfeld and P. Zelenay, *Electrochim. Acta* **2002**, **47**, 3741-748.

### 3.5 Results and Discussion

#### 3.5.1 The Effect of Ion Content on Electro-osmotic Drag

The electro-osmotic drag coefficient was measured at 60°C for various sulfonated BPSH copolymers and Nafion 117. Sulfonation levels between 30 and 60 mole % were studied because the properties of the membrane with this range of ionic content have found to be useful for fuel cells. The results for each membrane are plotted versus ion exchange capacity in Figure 3-5.

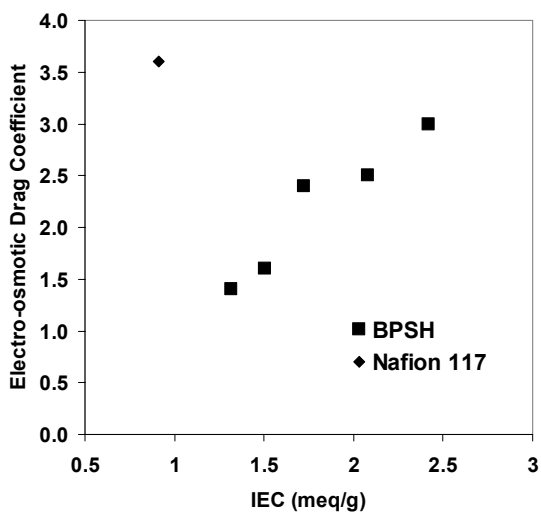


**Figure 3-5: Electro-osmotic Drag Coefficient versus Ion Exchange Capacity for BPSH and Nafion 117 Copolymers**

For the BPSH copolymer series, the electro-osmotic drag coefficient increases steadily with increasing sulfonated comonomer content. This is not surprising considering that the water

uptake and dimensional swelling of the membrane also increases with increasing sulfonate incorporation.

However, on the basis of ion content, the electro-osmotic drag coefficient of BPSH copolymers is much lower than Nafion 117. This phenomenon has been observed for conductivity and methanol permeability as well.<sup>119</sup> The low electro-osmotic drag coefficients of the BPSH membranes are somewhat unexpected given the high water uptake of the polymers (see Table 3-1). As an example, Nafion 117 absorbs 19 wt % water and has an electro-osmotic drag coefficient of 3.6, while BPSH 35 absorbs 40 wt % water and has an electro-osmotic coefficient of 1.2, which is 3 times lower than Nafion 117.

**Table 3-1: A Comparison of Selected BPSH Properties with Nafion 117**

	IEC (meq/g)	Conductivity (S/cm)*	Water uptake (%)*
Nafion 117	0.91	0.11	19
BPSH 30	1.32	0.06	29
BSPH 35	1.51	0.08	40
BPSH 40	1.69	0.10	56
BPSH 50	2.07	0.15	124
BPSH 60	2.42	0.31	190

\*Conductivity and water uptake at 30°C in liquid water

Note that while the conductivity and water uptake of the BPSH copolymers (especially BPSH-35 and BPSH-40) are similar to that of Nafion 1100, the chemical structure of BPSH copolymers is distinctly different than that of Nafion shown in Figure 3-6.

119. Hickner, M., F. Wang, Y.S. Kim, T.A. Zawodzinski, J.E. McGrath, "Influencing the transport of water, methanol, and protons through a fuel cell ion exchange membrane," *AIChE Topical Conference Proceedings*, Spring National Meeting, New Orleans, LA. March 10-14,2002.

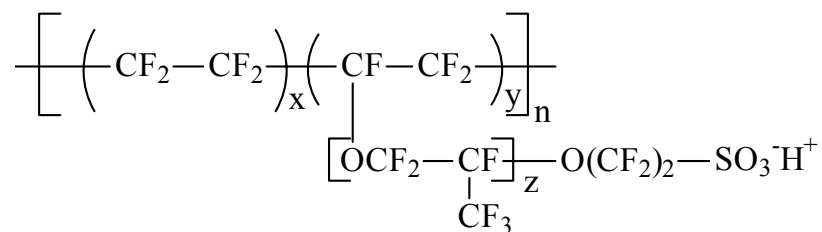


**Figure 3-6: Chemical Structure of Nafion**

The important differences to recognize between the two copolymers are the nature of the polymer backbone, the location, and acidity of the sulfonic acid moiety. Nafion's highly fluorinated backbone is a relatively flexible carbon-carbon bonded chain, with its highly acidic fluorosulfonic acid groups located on the end of perfluoroether side chains. Whereas the backbone of BPSH is a more rigid arylene ether sulfone chain, with somewhat less acidic arylsulfonic acid units tethered directly to the backbone.

The concept of a frustrated domain structure has been introduced to account for the differences in Nafion and BPSH morphology and physical properties.<sup>120</sup> The frustrated morphological structure in BPSH is a result of its relatively stiff backbone chain, which also has two weaker sulfonic acid groups (per sulfonated repeat unit) tethered closely to the backbone. These two factors may not allow BPSH copolymers to organize into sharply separated hydrophilic and hydrophobic domains. In order for the ionic groups to aggregate into clusters, a considerable

---

120. Hickner, M., F. Wang, Y.S. Kim, B. Pivovar, T.A. Zawodzinski, and J.E. McGrath, Abst. of Papers, 222nd ACS National Meeting, Chicago, IL, Aug. 26-30, 2001.

amount of closely attached copolymer may be required to move as well. This is different than Nafion where the sulfonic acid groups are attached to longer, flexible side chains, allowing easy clustering of ionic groups and sharper interfaces between hydrophilic and hydrophobic morphological regions. A more detailed model is discussed later in this paper.

In a parallel effort,<sup>121</sup> the state of water has been explored in fully hydrated BPSH and Nafion copolymers. Even though BPSH membranes absorb more water than Nafion, a larger fraction of the absorbed water is more tightly bound within the microphase-separated morphology in BPSH, as evidenced by nuclear magnetic resonance  $^1\text{H}$   $T_2$  relaxation and dynamic scanning calorimetry. It is proposed that the state of water in a proton exchange membrane may account for many of its transport properties.

### 3.5.2 The Influence of Temperature on Electro-osmotic Drag

Ren and Gottesfeld<sup>108</sup> showed for a variety of poly (perfluorosulfonic acid) membranes that the electro-osmotic drag increased with increasing temperature. This trend holds for BPSH copolymer membranes between 30°C and 80°C as shown in Figure 3-7.

---

121. Kim Y.S., L. Dong, M. Hickner, T.E. Glass, J.E. McGrath, *Macromolecules* **2003**, 36(17), 2003.

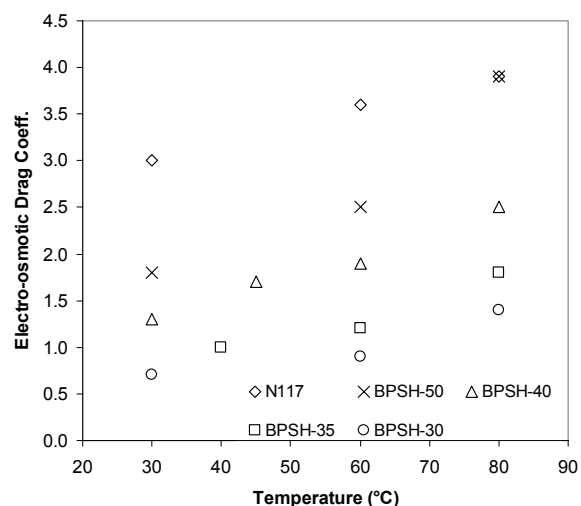


**Figure 3-7: Electro-osmotic Coefficient versus Temperature**

One interesting feature of this plot is that the electro-osmotic drag coefficients of all the BPSH copolymers are lower than Nafion 117 for temperatures below 60°C. At 80°C, the electro-osmotic drag of BPSH-50 matches that of Nafion, while the electro-osmotic drag of BPSH-40, BPSH-35, and BPSH-30 remains below that of Nafion across the entire temperature range investigated.

For Nafion 117, BPSH-40, BPSH-35, and BPSH-30 there is a modest, regular increase in electro-osmotic drag coefficient with increasing temperature from 30°C to 80°C. This orderly increase in electro-osmotic drag coefficient coincides with the increase in swelling (and water uptake) of the membrane with increased temperature. For these four copolymers, the volume fraction of the hydrophobic matrix is great enough to constrain the hydrophilic domains (see

atomic force microscopy results in Ref. 114) and no large swelling or morphological changes occur below 80°C.<sup>122</sup>

In the case of BPSH-50, there is again a modest increase in electro-osmotic drag coefficient at temperatures between 30°C and 60°C. However, at 80°C there is a larger than expected increase in electro-osmotic drag coefficient. Because BPSH-50 contains more sulfonated groups than the other BPSH copolymers, there may not be enough of a hydrophobic matrix to contain the hydrophilic domains. Atomic force microscopy supports the assertion that BPSH-50 copolymers are near the limit of hydrophilic domain percolation, where a large increase in swelling is observed.<sup>114</sup> Thus at 80°C, there could be a significant morphological change that affects the electro-osmotic drag coefficient of the membrane causing a discontinuity in the regular increase of electro-osmotic drag coefficient with temperature. The morphological stability of these BPSH copolymers was investigated as a function of hydrothermal treatment temperature<sup>122</sup> and it was found that BPSH-50 undergoes an irreversible morphological change at 80°C. The morphological change as reported in Ref. 122 is accompanied by increased swelling and increased water uptake, resulting in more loosely bound (or free) water, and thus a higher than expected electro-osmotic drag coefficient at 80°C.

---

122. Kim Y.S., L. Dong, M. Hickner, B.S. Pivovar, J.E. McGrath, *Polymer* **2003**, 44(19), 5729-5736.

### 3.5.3 Limiting Crossover Current and Convective Velocity

Methanol crossover in direct methanol fuel cells is one of the critical parameters that determines cell performance. Measurements of limiting crossover current are not only valuable because they offer a convenient method for determining membrane methanol permeability, but careful observation of limiting crossover current at different methanol feed concentrations can help illustrate the varying transport behaviors of various proton exchange membranes.

To examine the effect of convective velocity on methanol transport, the methanol flux versus feed concentration is plotted in Figure 3-8 for a limiting current experiment on Nafion 117 at 80°C. The dashed line is the linear relationship between flux and concentration that would be expected if only diffusion was occurring.

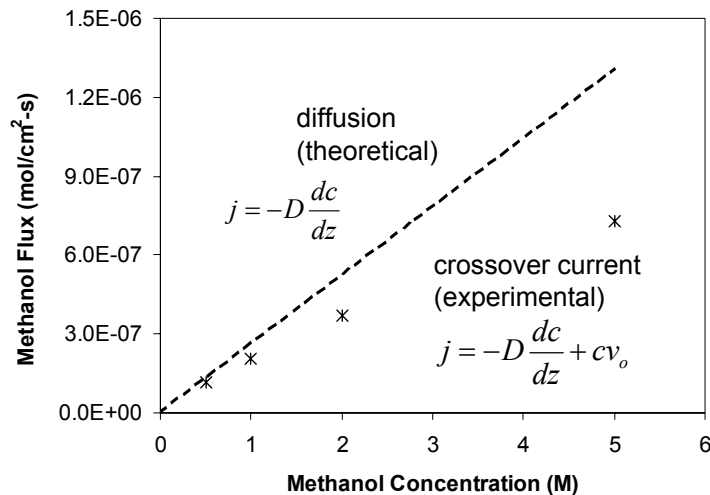
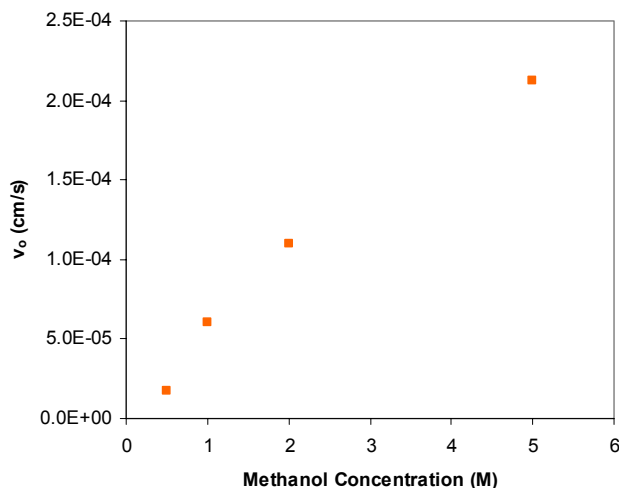


Figure 3-8: Flux versus Concentration for N117 at 80°C

At methanol concentrations less than 5M, the methanol permeability in these membranes was determined not to be a function of concentration (flux is proportional to concentration). Methanol permeability determined from free standing film measurements as a function of concentration confirms this assumption.<sup>119</sup> Therefore, the dashed line is what would be expected from a pure diffusive process: a linear relationship between flux and concentration (Equation 3-4). The dashed line in Figure 3-8 was computed from the resulting diffusion coefficient when the concentration was extrapolated to 0M methanol feed.

The flux versus concentration plot for the limiting current experiment under these conditions shows a clear departure from diffusion at high methanol feed concentrations due to the opposing convective velocity in the limiting crossover current geometry. Using Equation 3-7, the convective velocity,  $v_o$ , was computed as a function of concentration. Figure 3-9 shows the convective velocities determined by fitting the above limiting current data.



**Figure 3-9: Convective Velocities for Nafion 117 at 80°C**

Figure 3-8 and Figure 3-9 taken together show that the convective velocity developed by the movement of water and protons has a large influence on the transport behavior of methanol.

When the feed concentration in the limiting crossover current was increased, the protonic current increased, with the result being a larger convective velocity and a larger departure from a diffusion process for the methanol flux.

To study the differences in methanol transport between Nafion and the BPSH copolymers, the convective velocity for each copolymer was determined as a function of methanol feed concentration. The convective velocities were derived from experimentally measured limiting crossover current experiments as outlined above. A comparison of the convective velocities is shown in Figure 3-10.

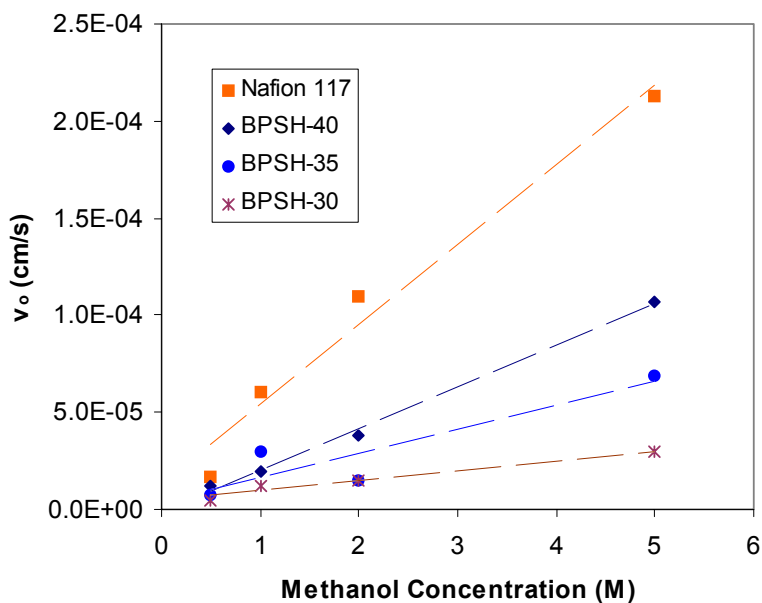


**Figure 3-10: Convective Velocities for Limiting Current Experiments with 5 M Methanol**

The best-fit lines shown in Figure 10 are simply an aid to show the trend. They have no implied meaning.

The lower convective velocities in BPSH copolymers indicate (along with electro-osmotic drag evidence) that there is a different hydrophilic domain structure in these copolymers than in Nafion. Our hypothesis is that the domain structure of BPSH copolymers is more diffuse with water closely associated with the polymer instead of existing in regions of more bulk-like water as with Nafion. The convective velocity followed the expected trend as the ionic content of the BPSH membrane decreased with BPSH-40 showing the greatest convective velocities, and

BPSH-30 the smallest convective velocities. This trend is understandable given the water uptake and electro-osmotic drag coefficient behavior of the copolymers.

We calculated electro-osmotic drag coefficients from the obtained convective velocities according to Equation 3-8. The values shown in Table 3-2 are electro-osmotic drag coefficients for the four membranes at four methanol concentrations (and the average for each membrane), as well as the experimentally determined  $E_D$ . Ideally, electro-osmotic drag coefficients could be determined by such a method, as it is faster and/or simpler than any of the commonly used techniques. It also provides data on methanol permeability, which is of interest for DMFCs. The measurement is performed in standard fuel cell hardware making further testing, such as AC impedance or high frequency resistance measurements for membrane conductivity, trivial.

**Table 3-2: Electro-osmotic Drag Coefficients ( $E_{Dcalc}$ ) Calculated Convective Velocity from Convective, Comparison to Experimentally Determined Electro-osmotic Drag Coefficient ( $E_{D exp}$ )**

Methanol Concentration (M)	Nafion	BPSH 30	BPSH 35	BPSH 40
0.5	1.4	1.4	1.4	1.4
1	2.8	1.9	3.0	1.1
2	2.8	1.2	0.7	1.2
5	2.8	1.0	1.7	1.6
<b><math>E_{Dcalc}</math> average</b>	<b>2.5</b>	<b>1.4</b>	<b>1.7</b>	<b>1.3</b>
$E_{D exp}$	3.9	1.4	1.8	2.5

All measurements performed at 80°C

While BPSH 30 and 35 showed good agreement between the average drag coefficient and the experimentally determined coefficient, Nafion and especially BPSH 40 showed poor agreement between the values calculated from convective velocities and those determined experimentally. The values for BPSH 30 and 35 show high variability, although the average values do give good agreement. The most surprising of these data are the low electro-osmotic drag coefficients obtained for BPSH 40, calling into question the use of this technique for even qualitative purposes. Many of the assumptions made including treating the membrane as a homogeneous medium (treating every proton, methanol and water molecule as equivalent), neglecting diffusion of water and methanol depletion in the feed stream and not addressing porosity or tortuosity of the membrane may lead to errors in the calculations, beyond experimental uncertainty. The use of an appropriate model to explain these results is needed to improve understanding of this system. However, with further investigations or in situations where other methods for determining electro-osmotic drag do not exist, the estimates provided from convective velocity measurements may prove useful.

Both electro-osmotic drag ( $E_D$ ) and convective velocity ( $v_o$ ) were determined experimentally for a systematic series of membranes. Electro-osmotic drag and convective velocity data gave complimentary information about the state of water in the membrane. When these two measurements are coupled, a broad picture of the domain morphology of the membrane can be developed. However, it may not always be possible to make both measurements for all membrane systems of interest. By measuring one parameter (either  $E_D$  or  $v_o$ ) and a few key physical properties of the membrane, the other parameter may be approximated to expand the information on the morphology of the membrane or for incorporation into a transport model.

It is worth noting, the convective velocity, here, was measured using a limiting current experiment where the convective velocity opposed the flux of methanol through the membrane. In an actual operating fuel cell the convective velocity occurs in the same direction as the flux of unreacted methanol from the anode to the cathode. The convective velocity in the membrane is an important factor in the methanol flux to the cathode especially at high current densities. Membranes with low convective velocity are important for systems that demand the absolute minimum methanol crossover.

#### 3.5.4 Qualitative Membrane Morphology Model

While there is still debate over the exact solid-state structure of Nafion, the commonly accepted microphase model of Nafion is a highly phase separated structure with distinct hydrophilic and hydrophobic domains on the nanometer size scale. The first model involving an inverted micellar arrangement of sulfonic acid groups was proposed by Gierke et al. in 1981.<sup>123</sup> Morphological models based on scattering data have been proposed over the last twenty years, and many inquiries point towards some sort of tube-like structure for the geometry of these domains.<sup>124</sup> Water absorbed by the membrane is almost exclusively contained in sulfonic acid lined channels, which leads to a large amount of loosely bound and bulk-like water.<sup>125</sup> In

---

123. T.D. Gierke, G.E. Munn, and F.C. Wilson, *J. Polym. Sci.: Polymer Physics* **1981**, 19(11), 1687-704.

124. (a) Rubatat, L., A.L. Rollet, G. Gebel, O. Diat, *Macromolecules* **2002**, 35, 40-50-4055; (b) Rubatat, L., O. Diat, G. Gebel, *Advances in Materials for Proton Exchange Membrane Fuel Cell Systems*, Pacific, Grove, Ca, Feb. 23-26, 2003.

125. K.D. Kreuer, *J. Membr. Sci.* **2001**, 185, 29-39.

addition, the extent of phase separation between hydrophilic and hydrophobic domains is very high and the borders between hydrophilic and hydrophobic regions are well-defined. Sauer et al.<sup>126</sup> have characterized the domain structure of Nafion 1100 by AFM and have concluded that the hydrophilic domains are about 10 nm in diameter for small levels of hydration. The atomic force microscopy results are in reasonable agreement with small angle X-ray scattering data that has shown the ionic clusters to be between 3.5 and 5.5 nm.<sup>123, 124, 127</sup> These are the range of generally accepted values for the characteristic ionic features in Nafion, even though the scattering results are still open to debate.<sup>127</sup> Pintauro et al.<sup>128</sup> has supported this model of Nafion with a dielectric model of hydrated pores on the order of a few to several nanometers.

Given only the lower observed electro-osmotic drag coefficients of BPSH membranes especially in light of the explanations given in this paper, one would be tempted to conclude that the diameter of the hydrophilic pores should be smaller than those of Nafion. However, AFM evidence suggests that BPSH copolymers actually have an ionic domain size that is larger (c.a. 25 nm domains for BPSH 40) than Nafion 117.<sup>114</sup> Therefore, another explanation is needed. Our hypothesis is that the microphase separated domain structure of BPSH copolymers is more diffuse than that of Nafion. Ionic clusters are not as well organized in BPSH copolymers and water absorption does not occur in a reverse micellar manner as with Nafion and care must be taken in differentiating between pores that contribute to species transport and ionic domains. Nafion's large degree of phase separation with tightly clustered ionic groups yields membranes

---

126. R.S. McLean, M. Doyle, B.B. Sauer, *Macromolecules* **2000**, 33, 6541.

127. Elliot, J.A., S. Hanna, A.M.S. Elliot, G.E. Cooley, *Macromolecules* **2000**, 33, 4161.

128. (a) P.N. Pintauro, M.W. Verbrugge, *J. Membr. Sci.* **1989** 44, 197-212; (b) A.G. Guzman-Garcia, P.N. Pintauro, M. Verbrugge, et al. *AIChE Journal* **1990**, 36(7), 1061-74.

with a large quantity of loosely bound or free water. The extent of phase separation in BPSH is lower than Nafion and the interface between hydrophilic and hydrophobic domains are somewhat less distinct as compared to the sharply defined hydrophilic and hydrophobic domains of Nafion. This type of morphology causes the absorbed water to become more tightly bound within the copolymer morphology. A model suggesting some differences between the domain structures of both copolymers are illustrated in

Figure 3-11.

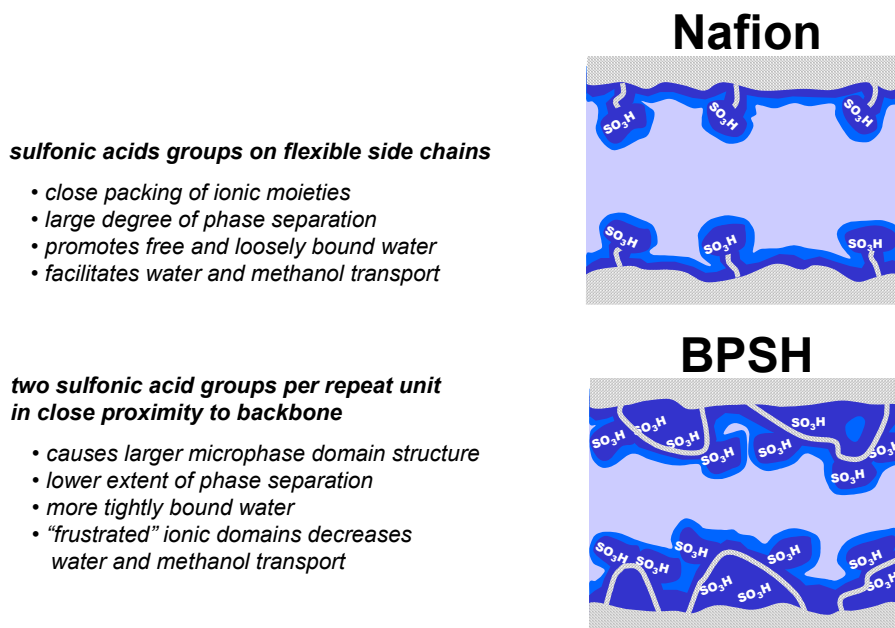


**Figure 3-11: A Domain Model of Nafion and BPSH Copolymer Membranes**

In the figure, lighter shades of blue represent water that is more loosely bound. The highly phase separated nature of Nafion is suggested to cause the water absorbed in the membrane to be more loosely bound in the hydrophilic pores and results in high electro-osmotic drag. The association between a water molecule and BPSH is stronger than the association between a water molecule and Nafion. Nafion has a distinct two-phase structure with regions that contain principally water

that is loosely bound within the structure and regions that contain principally copolymer. The BPSH membranes afford more of a continuum, where regions of water and copolymer exist, however, these regions are much less distinct and the transitions between the water-rich and copolymer-rich areas are gradual. This increases the local viscosity of water in BPSH membranes, making the water molecules less susceptible to electro-osmotic drag induced by a protonic current.

Because the hydrophilic structure of BPSH copolymers is more diffuse and the hydrophilic and hydrophobic domains are not as highly organized as in Nafion, the BPSH membranes are more susceptible to excessive swelling, especially at high sulfonic acid content, at high temperatures as shown by the rapid increase in electro-osmotic drag of BPSH 50 at 80°C. In this case, the hydrophobic matrix of the copolymer is insufficient to constrain the increased swelling of the hydrophilic phase. In the BPSH-40 copolymer a large increase in electro-osmosis is not seen at 80°C, so one can conclude that at this ion content (and subsequently lower ionic contents), the hydrophobic matrix is sufficiently intact as to not allow large swelling of the hydrophilic domains at temperatures up to 80°C.

### **3.6 Conclusions**

A systematic increase in electro-osmotic drag coefficient is exhibited with increasing sulfonation for the BPSH series, as has been shown for other families of ionomers.<sup>108</sup> Surprisingly, even BPSH 60 with a water uptake of 190 wt % has an electro-osmotic drag coefficient of only 3.0, while Nafion 117 with a water uptake of 19 wt % has an electro-osmotic drag coefficient of 3.6

under full hydration at 60°C. Our earlier results showed,<sup>121</sup> the water contained in BPSH membranes is not as mobile as the water in Nafion, and as a result, it is proposed that there is less viscous drag of the water molecules in BPSH copolymers, which manifests itself as lower observed electro-osmotic drag coefficients.

The transport properties of the BPSH membranes were further explored by measuring the limiting crossover current in a direct methanol fuel cell as a function of methanol feed concentration. In these experiments, methanol diffusion across the membrane is opposed by water flux in response to proton transport. Consequently, the flux of methanol across the membrane is not a linear function of concentration as in diffusion cell experiments. A new flux equation to describe the transport of methanol was written to account for this opposing convective velocity. It was observed that the convective velocities from 0.5M to 5M methanol feed in Nafion are much greater than those in the BPSH copolymers. The convective velocity of the BPSH copolymers decreased with ion exchange capacity in a similar fashion to electro-osmotic drag. From the experimentally observed convective velocity, an electro-osmotic drag coefficient could be computed. These computed electro-osmotic drag coefficients compared well with experimentally determined values for two of the membrane samples, but more work needs to be done in this area.

To account for the electro-osmosis and convective velocity results, a model was proposed for the morphological differences between Nafion and BPSH copolymers. It is concluded that the stiffer backbone chains and closely tethered sulfonic acid groups of BPSH copolymers may not allow a high degree of phase separation (or ionic clustering) compared to Nafion. The more diffuse

hydrophilic domains promote closer association between the copolymer and the water molecules. This dramatically different morphology and increased ionic content (IEC) is likely responsible for the different temperature dependence of properties of BPSH copolymers compared to Nafion as evidenced in the larger than expected increase in electro-osmotic drag coefficient from 60°C to 80°C for the BPSH-50 copolymer which is probably near or at the percolation limit of the hydrophilic domains. Both the amount of unsulfonated, hydrophobic matrix and any crystallinity in the hydrophobic phase would be expected to influence the membrane's response to temperature.

The results in this paper and insight gained are important to the future development of proton exchange membranes. With the BPSH copolymers, the chemical structure (ion content and location of the ion conductors) and thus the membrane microphase separated morphology can be closely controlled. This facilitates a systematic study on the influence of membrane morphology on membrane transport properties. Extending the ideas in this work further, it is possible that yet more diffuse domain structures (or even a homogenous membrane) may display further reduced electro-osmotic drag and convective velocities. The latter could be connected to reduced methanol permeation and higher selectivity for proton conduction over methanol permeation. Developing proton exchange membranes with low methanol permeability and reasonable protonic conductivity will facilitate improvement in direct methanol fuel cell performance.

### 3.7 List of Symbols

$E_D$	Electro-osmotic Drag Coefficient ( $N H_2O/H^+$ )
$F$	Faraday's Constant (96485 Coulombs/mole of charge)
$MW_{H_2O}$	Molar Mass of Water (18.01 g/mole)
$\bar{V}_{H_2O}$	Molar Volume of Water (moles/cm <sup>3</sup> )
$DH_{LC}$	Permeability as Determined by Limiting Current (cm <sup>2</sup> /s)
$I_x$	Limiting Crossover Current (A/cm <sup>2</sup> )
$l$	Membrane Thickness (cm)
$c_o$	Methanol Feed Concentration (g/cm <sup>3</sup> )
$j_{CH_3OH}$	Methanol Flux (g/cm <sup>2</sup> -s)
$D$	Methanol Diffusion Coefficient in Membrane (cm <sup>2</sup> /s)
$H$	Partition Coefficient of Methanol Between Membrane and Solution
$DH$	Membrane Permeability (cm <sup>2</sup> /s)
$c_{CH_3OH}$	Methanol Concentration (g/cm <sup>3</sup> )
$v_o$	Convective Velocity – experimentally determined (cm/s)
$v_{calc}$	Convective Velocity – calculated from membrane properties (cm/s)

# CHAPTER 4. THE STATE OF WATER AND TRANSPORT PROPERTIES IN ORGANIC/INORGANIC COMPOSITE PROTON EXCHANGE MEMBRANES

## 4.1 Abstract

Many research efforts have shown that blending inorganic additives such as phosphotungstic acid or zirconium hydrogen phosphate with sulfonated organic polymers such as Nafion, sulfonated poly(sulfone), sulfonated poly(ether ketone), and other copolymers is a promising strategy for producing high performance proton exchange membranes, particularly for high temperature hydrogen/air fuel cell applications. The reported benefits of organic/inorganic composite membranes include increased conductivity at low relative humidity and high temperatures, increased mechanical strength, and lower water swelling. Several sulfonated polymer/inorganic composite systems have been investigated, but there has been little information on the transport properties of these organic/inorganic composites aside from protonic conductivity and in addition, there has been little data on how the inorganic additives function in the composites. This paper suggests the mechanisms of how the inorganic additives function in these composite systems. The argument is based on the inorganic filler influencing the state of water within the membrane and the state of water in turn affecting the transport properties such as protonic conductivity, methanol permeability, electro-osmotic drag, and water self-diffusion coefficient. Specifically, the effect of two inorganic fillers, phosphotungstic acid, and zirconium hydrogen phosphate, on the transport properties of sulfonated poly(arylene ether

sulfone) (BPSH) copolymer membranes are discussed. It was found that the water-self diffusion coefficient of the organic/inorganic composites correlated with the transport properties. Addition of phosphotungstic acid increased the water-self diffusion coefficient while the zirconium hydrogen phosphate decreased the water-self diffusion coefficient and the resulting transport properties. Results are reported for fully hydrated membranes, but these observations may have broad applicability for both direct methanol and low relative humidity hydrogen/air fuel cell systems as will be discussed.

key words: heteropoly acid, zirconium hydrogen phosphate, proton exchange membrane, organic/inorganic composite, fuel cell

## 4.2 Introduction

Organic/inorganic composite proton exchange membranes have become an important topic in fuel cell research.<sup>129</sup> Inorganic compounds are attractive because they may be more conductive than sulfonated polymers, especially at low water contents. However, these inorganic compounds do not form robust membranes due to their brittle nature. Efficient blending of these inorganic additives with polymers, particularly sulfonic acid containing polymers, is needed to generate film-forming tough, ductile proton exchange membranes (PEM) that can be fabricated into a fuel cell membrane electrode assembly (MEA). It has been shown that even with water-

---

129. (a) Arimura, T., D. Ostrovskii, T. Okada, G. Xie, *Solid State Ionics* **1999**, 118, 1-10; (b) Genova-Dimitrova, P., B. Baradie, D. Foscallo, C. Poinsignon, J.Y. Sanchez, *J. Membr. Sci.* **2001**, 185, 59-71; (c) Zaidi, S.M.J., S.D. Mikhailenko, G.P. Robertson, M.D. Guiver, S. Kaliaguine, *J. Membr. Sci.* **2000**, 173, 17-34.

soluble inorganic additives such as phosphotungstic acid, complexation with sulfonated copolymers reduces their extraction from the membrane matrix.<sup>130</sup>

Desirable membrane properties have been shown in composites employing phosphotungstic acid and zirconium hydrogen phosphate as the inorganic phase, and Nafion or other sulfonated copolymers as the organic phase. Research groups at UConn<sup>131</sup> have shown that phosphotungstic acid (and other heteropolyacid)/Nafion composites can give very good fuel cell performance under moderately dry hydrogen/air conditions. Phosphotungstic acid is a highly proton conducting water-soluble heteropoly acid.<sup>132</sup> It displays good protonic conductivity when hydrated, but is unsuitable as a proton exchange membrane alone because of its water solubility and inability to form robust membranes. Alberti et al.<sup>133</sup> demonstrated attractive properties in proton exchange membranes with zirconium hydrogen phosphate (and other zirconium compounds) as the inorganic component and sulfonated PEEK as the organic component. Zirconium hydrogen phosphate is a water-insoluble inorganic compound that shows some surface proton conductivity in its layered form.

Most research dealing with organic/inorganic composites has focused on characterizing the proton exchange membrane properties that are important to fuel cells, namely protonic

---

130. Kim, Y., F. Wang, M. Hickner, T. Zawodzinski, J.E. McGrath, *J. Membr. Sci.* **2003**, 212, 263-282.

131. (a) Lin, J.C., H.R. Kuntz, M.B. Cutlip, J.M. Fenton, *Hazardous and Industrial Wastes* **1999**, 31, 656-662; (b) Lin, J.C., H.R. Kuntz, J.M. Fenton, *Proceedings of the Electrochemical Society Power Sources for the New Millennium* **2001**, 2000-22, 48-63.

132. Pourcelly, G., C. Gavach, in: P. Colomban (Ed.), *Proton Conductors: Solids, Membranes and Gels – Materials and Devices*, Cambridge University Press, New York, 1992, 294-310.

133. (a) Alberti, G., M. Casciola, R. Palombari, *J. Membr. Sci.* **2000**, 172, 233-239; (b) Alberti, G., U. Constantino, M. Casciola, S. Ferroni, L. Massinelli, P. Staiti, *Solid State Ionics* **2001**, 145, 249-255.

conductivity. Little information has been presented on the other transport properties of these composite membranes and little data has been given to justify the mechanism of how these inorganic compounds influence the transport within a proton exchange membrane. The aim of this work is to provide data that demonstrates how the transport properties of a composite proton exchange membrane with either phosphotungstic acid or zirconium hydrogen phosphate differs from a pure sulfonated copolymer (poly(arylene ether sulfone) or BPSH shown in Figure 4-1) and develops a detailed argument that accounts for the major differences observed between the composite systems.

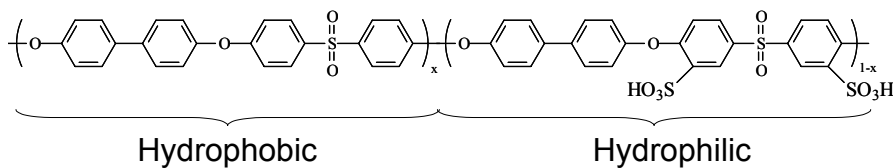


**Figure 4-1: Chemical Structure of BPSH Copolymers Containing Hydrophobic and Hydrophilic Units**

## 4.3 Experimental

### 4.3.1 Membrane Preparation

BPSH copolymers were synthesized by direct polymerization of sulfonated monomers as described earlier in detail.<sup>134</sup> Tough, ductile membranes were solution cast from the as polymerized sodium/potassium cation sulfonate form on aluminum molds in a heated vacuum oven. Once filtered through a 0.4  $\mu\text{m}$  PTFE syringe filter, cast copolymer solutions of 5 % (wt./vol.) in N,N-dimethylacetamide (DMAc) were held under full vacuum at 40°C for 24 hours, then 100°C for 24 hours, and finally 150°C for 12 hours, before being removed from the oven. The membranes were converted to the acid (proton) form by boiling in 0.5 M sulfuric acid ( $\text{H}_2\text{SO}_4$ ) for 2 hours. The membranes were rinsed well then boiled in deionized (DI) water for 2 hours to remove any residual sulfuric acid, which was described previously as Method 2.<sup>135</sup> The membranes underwent a final rinse in DI water and were then stored in DI water for at least one week before testing.

BPSH/phosphotungstic acid composite membranes were cast from acid form copolymer. Once the acid form copolymer was dissolved in DMAc (5% wt./vol.) to form a clear solutions, the desired amount of phosphotungstic acid was added to the polymer/DMAc solution and allowed

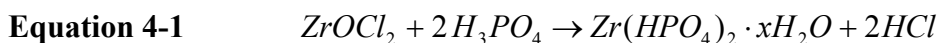
---

134. Wang, F., M. Hickner, Y. Kim, T. Zawodzinski, J.E. McGrath, *J. Membr. Sci.* **2002**, 197, 231-242.

135. Kim, Y.S., F. Wang, M. Hickner, S. McCartney, Y.T. Hong, T.A. Zawodzinski, J.E. McGrath, *J. Poly. Sci., B: Poly. Phys.* **2003**, 41(22).

to stir for another 24 hours. The casting and acid conversion procedure remained the same as above.<sup>136</sup>

BPSH/zirconium hydrogen phosphate membranes were prepared from an already cast and converted (as described above) acid form BPSH membrane using an optimized procedure already in the literature.<sup>136</sup> To form the zirconium hydrogen phosphate composite, the acid form BPSH membrane was immersed in boiling water for 1 hour, then immediately transferred to an 80°C zirconyl chloride ( $ZrOCl_2$ ) solution of desired  $ZrOCl_2$  concentration. The  $ZrOCl_2$  solutions were prepared by diluting a stock  $ZrOCl_2$  solution (30%  $ZrOCl_2$  in HCl from Aldrich) with DI water. The concentration of  $ZrOCl_2$  determined the final zirconium hydrogen phosphate content of the composite. The membranes were removed from the  $ZrOCl_2$  solution after 6 hours, quickly rinsed with DI  $H_2O$  to remove any surface  $ZrOCl_2$ , then immersed in 1.5M phosphoric acid ( $H_3PO_4$ ) (a large excess for reaction with the  $ZrOCl_2$ ) for 24 hours at room temperature. The  $H_3PO_4$  diffused into the membrane and reacted with the  $ZrOCl_2$  imbibed in the membrane to form zirconium hydrogen phosphate,  $Zr(HPO_4)_2$  (and its associated waters of hydration), according to Equation 4-1.



After immersion for 24 hours in 1.5 M  $H_3PO_4$ , the membranes were then rinsed well with DI water and boiled in DI water for 2 hours to remove any residual reactants. The composite

---

136. Grot, W.G., G. Rajendran, US 5,919,583 to E.I. du Pont de Nemours and Company, 1999.

membranes were then re-acidified according to the method above to ensure full conversion to the acid form. All membranes were stored in DI water for at least 1 week before testing.

#### 4.3.2 Water Uptake

The water uptake of the membranes was determined by a simple weight-difference approach. The membranes were first immersed in deionized water at room temperature for 24 hours. The wet membranes were then blotted dry to remove surface droplets and quickly weighed. After 3 - 5 measurements to ensure repeatability of the blotting process, the membranes were dried under full vacuum at 80-100°C for at least 24 hours and weighed again. The water uptake of the membranes was calculated according to Equation 4-2 where  $mass_{dry}$  and  $mass_{wet}$  refer to the mass of the wet membrane and the mass of the dry membrane, respectively.

#### Equation 4-2

$$water\ uptake = \frac{mass_{wet} - mass_{dry}}{mass_{dry}}$$

#### 4.3.3 Protonic Conductivity

Protonic conductivity at 30°C under full hydration (in liquid water) was determined using a Solartron 1260 Impedance/Gain-Phase Analyzer over the frequency range of 10 Hz - 1 MHz. The cell geometry was chosen to ensure that the membrane resistance dominated the response of

the system.<sup>137</sup> The resistance of the film was taken at the frequency which produced the minimum imaginary response. The conductivity of the membrane can be calculated from the measured resistance and the geometry of the cell according to Equation 4-3.

**Equation 4-3**

$$\sigma = \frac{l}{Z' A}$$

Where  $\sigma$  is the protonic conductivity,  $l$  is the length between the electrodes,  $A$  is the cross sectional area available for proton transport, and  $Z'$  is the real impedance response.

#### 4.3.4 Atomic Force Microscopy

Tapping mode atomic force microscopy (TM-AFM) was performed with a Digital Instruments Dimension 3000, using the micro-fabricated cantilevers with a force constant of approximately 40 N/m. The ratio of amplitudes used in feedback control was adjusted to 0.6 of the free air amplitude. The samples were imaged in a relative humidity of about 35%.

#### 4.3.5 Methanol Permeability

Methanol permeability of the membranes was determined using a standard membrane-separated diffusion cell as shown in Figure 4-2.

---

137. Zawodzinski, T.A., M. Neeman, L. O. Sillerud and S. Gottesfeld. *J. Phys. Chem.* **1991**, 95, 6040-6044.

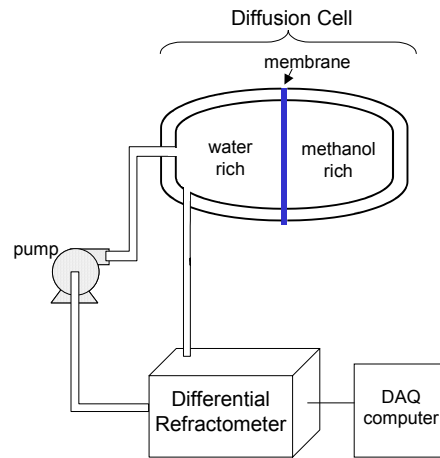


**Figure 4-2: Membrane Separated Cell**

A methanol/water solution was introduced to one compartment while pure water filled the compartment connected to the recirculating pump, differential refractometer, and data acquisition computer to conduct the measurement. Once both compartments were filled, the methanol diffused from the methanol rich compartment through the membrane and into the water rich compartment, thus raising the concentration of the methanol in the left-hand compartment which was followed by refractive index, and lowering the concentration in the right-hand compartment. The permeability of the membrane could be calculated from the rate of change of concentration for each side.

Cussler<sup>138</sup> outlined the mathematical solution to the simple membrane separated cell first proposed by Barnes in 1934 and later simplified by Robinson and Stokes in 1960. This analysis assumes that the membrane reaches steady-state very quickly, there is no liquid mass transfer resistance, and it also neglects the water flux. First, a mass balance is written for each compartment.

**Equation 4-4**

$$V_L \frac{dc_{CH_3OH,L}}{dt} = Aj$$

**Equation 4-5**

$$V_R \frac{dc_{CH_3OH,R}}{dt} = Aj$$

$V_R$  and  $V_L$  are the volumes of the left and right-hand sides, and  $A$  is the area of the membrane exposed for diffusion. Equation 4-4 is subtracted from Equation 4-5 to yield

**Equation 4-6**

$$\frac{d}{dt}(c_{CH_3OH,R} - c_{CH_3OH,L}) = DH\chi(c_{CH_3OH,L} - c_{CH_3OH,R})$$

where  $\chi$  is a cell constant that incorporates the geometrical characteristics of the cell and the membrane as shown in Equation 4-7.

---

138. E.L. Cussler, Diffusion Mass Transfer in Fluid Systems, 2nd Ed. Cambridge University Press, New York, 1997.

**Equation 4-7**

$$\chi = \frac{AH}{l} \left( \frac{1}{V_L} + \frac{1}{V_R} \right)$$

If Equation 4-6 is integrated subject to the initial condition at  $t = 0$

$$c_{CH_3OH,R} - c_{CH_3OH,L} = c_{CH_3OH,R}^o - c_{CH_3OH,L}^o$$

then

**Equation 4-8**

$$\frac{c_{CH_3OH,R} - c_{CH_3OH,L}}{c_{CH_3OH,R}^o - c_{CH_3OH,L}^o} = e^{-DH\chi t}$$

taking the natural log of both sides, and simplifying

**Equation 4-9**

$$-DH_{FS} \cdot \chi \cdot t = \ln \left( \frac{\Delta c_{CH_3OH}}{\Delta c_{CH_3OH}^o} \right)$$

Therefore a plot of  $\ln[(c_{1,R}-c_{1,L}) / (c_{1,R}^o-c_{1,L}^o)]$  versus  $t$  should yield a straight line with slope  $-DH\chi$ .

Once  $\chi$  was determined by measuring the geometry of the cell, the methanol permeability (DH) of the membrane could be calculated.

### 4.3.6 Water Self-Diffusion Coefficient

Water self-diffusion coefficients ( $D_{\text{H}_2\text{O}}$ ) were determined using a Varian Inova 400 MHz (for protons) nuclear magnetic resonance (NMR) spectrometer with a 60 G/cm gradient diffusion probe. The diffusion coefficients for water were determined using a standard stimulated echo pulse sequence as shown in Figure 4-3.<sup>139</sup> A total of 16 points were collected at decreasing gradient strengths and the signal-to-noise ratio was enhanced by coadding 4 scans.

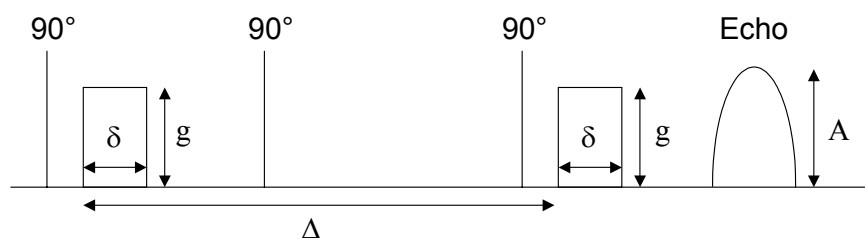


**Figure 4-3: NMR Stimulated Echo Pulse Sequence**

The measurement is conducted by observing the NMR signal intensity ( $A$ ) as a function of the gradient strength ( $g$ ). The diffusion coefficient is determined by fitting the data to Equation 4-10.<sup>140</sup>

**Equation 4-10**

$$A(g) = A(0) \exp[-\gamma^2 D g^2 \delta^2 (\Delta - \delta/3)]$$

---

139. Tanner, J.E., *J. Chem. Phys.* **1970**, 52, 2523.

140. Stejskal, E.O., J.E. Tanner, *J. Chem. Phys.* **1965**, 42, 288.

where  $\gamma$  is the gyromagnetic ratio ( $26752 \text{ radG}^{-1}\text{s}^{-1}$  for protons),  $D$  is the diffusion coefficient,  $g$  is the gradient strength,  $\delta$  is the length of the gradient pulse, and  $\Delta$  is the time between gradient pulses.

Membrane samples of approximately 5 mm by 15 mm by 150  $\mu\text{m}$  were equilibrated in liquid water for at least 24 hours. The samples were removed from the liquid water, blotted dry, quickly inserted into the NMR tube and immediately imaged over a span of about 5 minutes. This rapid transfer from the liquid water to the NMR instrument was necessary to avoid excessive drying of the sample during measurement. Measurements were repeated by reimmersing the sample in DI water, waiting at least 30 minutes, and then repeating the transfer and measurement process.

#### **4.4 Results and Discussion**

Three systems are discussed in this work: pure BPSH copolymer, BPSH copolymer blended with phosphotungstic acid (using solution blending), or a BPSH/zirconium hydrogen phosphate composite formed by the in-situ precipitation technique as described above. These three systems were chosen because the inorganic components have been used in many organic/inorganic composite blends that have shown promise for application as proton exchange membranes in fuel cells. Moreover, the transport properties of pure BPSH copolymers have been well characterized by this group.

#### 4.4.1 Morphology

The three tapping mode, phase-image atomic force micrographs in Figure 4-4 show that all samples feature hydrophilic/hydrophobic domain morphologies represented by light and dark regions. In these tapping mode images the darker regions are taken as the hydrophilic phases that have a small amount of absorbed water and are lower in modulus than the non-water absorbing hydrophobic phases, which appear as the lighter regions.

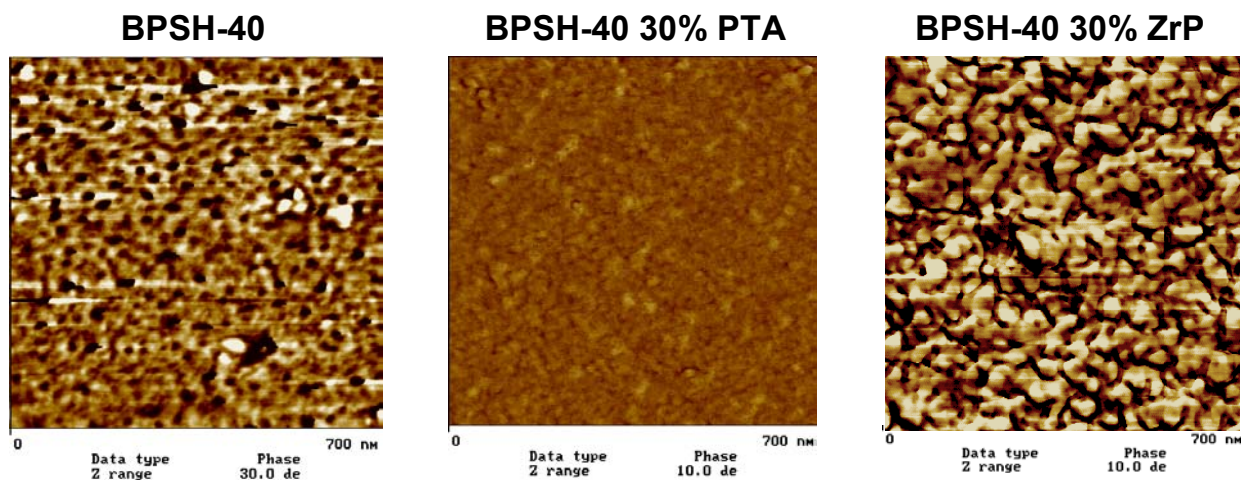


**Figure 4-4: Phase Mode Atomic Force Micrographs of BPSH 40, BPSH 40 with 30 wt % Phosphotungstic Acid (PTA), and BPSH 40 with 30 wt % Zirconium Hydrogen Phosphate (ZrP)**

Other than illustrating that each sample undergoes nanophase separation into hydrophilic (darker) and hydrophobic (lighter) domains, the AFM micrographs are quite different in appearance, but a visual inspection of the micrographs does not give any indication of the

transport properties of the sample. One is also not able to distinguish which sample may have the highest protonic conductivity or methanol permeability.

The atomic force micrographs cannot reveal detailed morphological information such as exact size or composition of each phase, but there is no detectable separation between organic and inorganic components in these images. The size features of the two transparent composites are on the same order as the size features of the pure copolymer.

Visual inspection of the membranes confirms that the inorganic additives are dispersed on a very small scale (less than 0.1  $\mu\text{m}$ ) because of the clarity of each sample. As shown in Figure 4-5, both phosphotungstic acid and zirconium hydrogen phosphate composites remain as transparent as the pure copolymer membrane. The zirconium hydrogen phosphate composites are slightly more yellow than the other samples, but they are just as transparent as the rest.

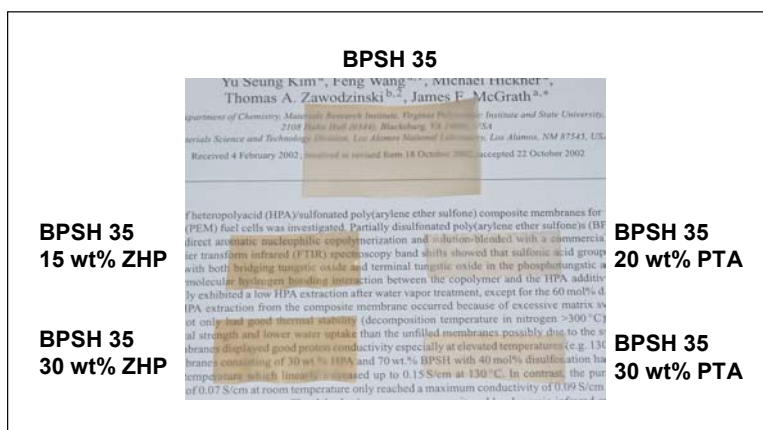


**Figure 4-5: Pure BPSH Copolymer, BPSH/Phosphotungstic Acid (PTA), and BPSH Zirconium Hydrogen Phosphate (ZHP) Composite Membranes: All Show Optical Clarity**

The small size scale of the dispersed inorganic phase indicates that the inorganic compound is well incorporated into the structure of the organic copolymer and gross phase separation between the organic and inorganic phases does not occur in these systems up to 30 weight percent of either inorganic additive.

#### 4.4.2 Water Uptake

Phosphotungstic acid/BPSH composites were somewhat surprisingly shown to have decreased water absorption as compared to the pure BPSH copolymer.<sup>130</sup> As shown in

Figure 4-6, the BPSH 40/30 wt % zirconium hydrogen phosphate composite also shows decreased water absorption, but the decrease is not as great as the phosphotungstic acid composite.

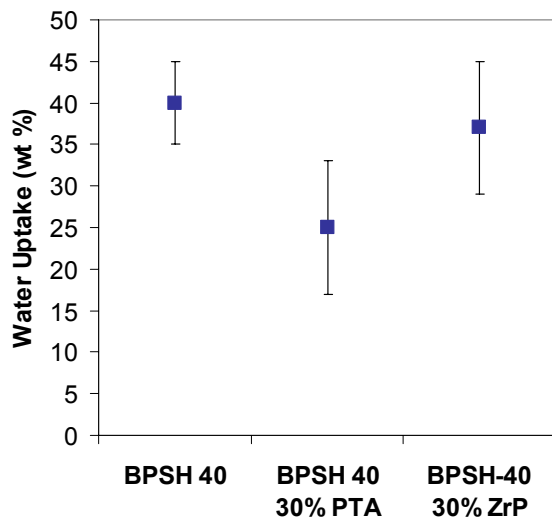


**Figure 4-6: Water Absorption of BPSH 40, BPSH 40 with 30 wt % Phosphotungstic Acid (PTA), and BPSH 40 with 30 wt % Zirconium Hydrogen Phosphate (ZrP)**

It is somewhat surprising that adding a water soluble additive such as phosphotungstic acid to a water-absorbing sulfonated copolymer would decrease the water uptake of the membrane. The decreased water absorption of the phosphotungstic acid composite is due to the strong association of the phosphotungstic acid with the sulfonic acid as evidenced by the sulfonic acid (from the sulfonated copolymer) and tungsten oxygen bond (from the phosphotungstic acid) wavenumber shifts in the FTIR spectra of the composite.<sup>130</sup> This association between organic and inorganic components must be stronger than the association of sulfonic acid with water,

therefore the water uptake of the composite system is decreased. There is no such detectable interaction between the zirconium hydrogen phosphate and the sulfonated copolymer. Because the zirconium hydrogen phosphate is formed in-situ in the hydrophilic domains of an already cast membrane, it is reasonable that the water uptake of this composite could be decreased simply by the zirconium hydrogen phosphate occupying space within the hydrophilic regions of the copolymer. If part of the volume of the hydrophilic pores is decreased, one could argue that there is less room for water and the bulk water uptake of the material decreases.

#### 4.4.3 Protonic Conductivity

The protonic conductivity of the two composites shows quite different behavior. Figure 4-7 shows that the conductivity of the phosphotungstic acid composite increases as compared to the pure copolymer (0.09 S/cm versus 0.08 S/cm, respectively) even though the water uptake of this composite decreased as described in the previous section. The water uptake of the BPSH/zirconium hydrogen phosphate composite is likewise decreased, but somewhat more conventionally the conductivity of this composite also decreased from 0.08 S/cm for the pure BPSH 40 copolymer to 0.07 S/cm for the BPSH 40/30 wt % zirconium hydrogen phosphate.

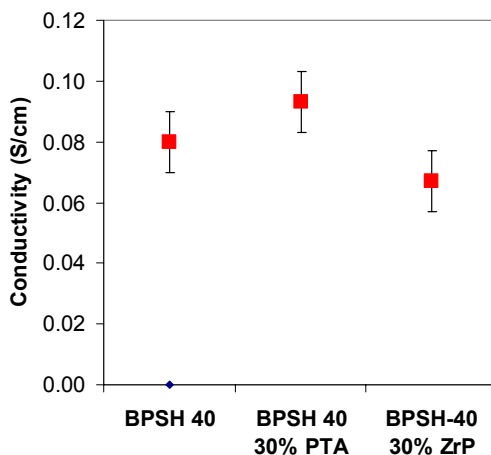


**Figure 4-7: Protonic Conductivity of BPSH 40, BPSH 40 with 30 wt % Phosphotungstic Acid (PTA), and BPSH 40 with 30 wt % Zirconium Hydrogen Phosphate (ZrP)**

Even though the water uptake is decreased in both composites, the additives appear to be affecting the protonic conductivity of the materials in an opposite manner. The conductivity increases in the case of phosphotungstic acid, while it decreases with the incorporation of zirconium hydrogen phosphate. The change in bulk water uptake of each sample is not sufficient to describe the observed change in conductivity. If only the bulk water uptake was considered, the protonic conductivity of each composite should decline. One may argue that the intrinsic conductivity of the inorganic compounds caused the observed change in conductivity for the composites. However, the maximum conductivity of phosphotungstic acid was reported to be  $1.8 \cdot 10^{-2}$  S/cm (when associated with 29 waters of hydration),<sup>141</sup> which is still lower than the conductivity of the pure copolymer. It stands to reason that adding a less conductive filler to a more conductive polymer would not increase the conductivity of the composite on a simple

---

141. Pourcelly, G., C. Gavach, Proton Conductors: Solids, Membranes and Gels - Materials and Devices, P. Colomban (Ed.), Cambridge University Press, New York, 1992, 294-310.

additive basis based on mass or volume fraction. There is clearly another phenomenon at work in these composites and further investigation of the other transport properties of these materials is warranted.

#### 4.4.4 Methanol Permeability

The transport in these composite systems was further investigated by measuring the methanol permeability of each material between the temperatures of 30°C and 80°C. The results are shown in Figure 4-8.

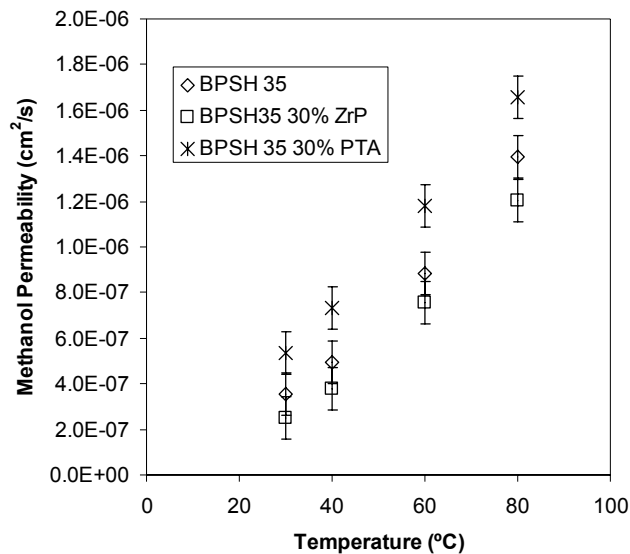


**Figure 4-8: Methanol Permeability of BPSH 35, BPSH 35 with 30 wt % Phosphotungstic Acid (PTA), and BPSH 35 with 30 wt % Zirconium Hydrogen Phosphate (ZrP) Between 30°C and 80°C**

Similar to the results for protonic conductivity, while the water uptake of both composites decreased as shown in Figure 1, the methanol permeability increased for the phosphotungstic acid composite and decreased for the zirconium hydrogen phosphate composite. On average the methanol permeability of the BPSH/phosphotungstic acid composite is 38 % greater than the pure copolymer membrane, while the methanol permeability of the BPSH/zirconium hydrogen phosphate composite is 20 % lower than the pure copolymer. As with protonic conductivity, the result for the BPSH/zirconium hydrogen phosphate composite is understandable by considering the bulk water uptake of the composite compared to the pure copolymer. A decrease in methanol permeability would certainly be consistent with a decrease in water uptake.

Methanol permeability does not rely on the same mechanisms as proton conductivity so even if the phosphotungstic acid contributes to conductivity of the sulfonated copolymer in the composite material in a synergistic manner, a decrease in water uptake and an increase in methanol permeability in the BPSH/phosphotungstic acid composite is not expected. One might expect that the water uptake and the methanol permeability would be closely related, but in the phosphotungstic acid composite materials, this is not the case. Merely considering the water uptake, protonic conductivity, and methanol permeability, there is no cohesive explanation of the dissimilar behavior of the phosphotungstic acid and zirconium hydrogen phosphate organic/inorganic composites.

Earlier, the state of water has been linked to the transport properties of sulfonated copolymer membranes.<sup>142</sup> The state of water in the organic/inorganic systems has been investigated by measuring the water self-diffusion coefficient using pulsed field gradient <sup>1</sup>H Nuclear Magnetic Resonance (NMR). In this measurement, more loosely bound water within the morphological structure of the copolymer is manifested as a greater water self-diffusion coefficient, while tightly bound water yields a lower water self-diffusion coefficient. The water self-diffusion coefficients of each composite system were measured in order to gauge the state of water in each system and these results are shown in Figure 4-9.

---

142. (a) Kim Y.S., L. Dong, M. Hickner, T.E. Glass, J.E. McGrath, *Macromolecules* **2003**, accepted; (b) Hickner, M.A., Y.S. Kim, L. Dong, B. Pivovar, J.E. McGrath "The Influence of Chemical Structure on the Transport Properties of Proton Exchange Membranes," *Macromolecules* **2003**, in progress.

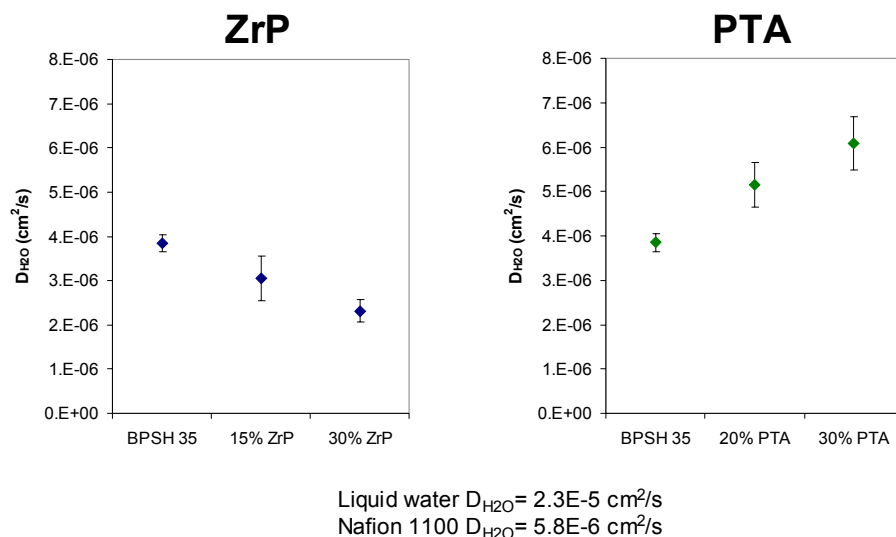


**Figure 4-9: Water Self-Diffusion Coefficient of BPSH 35, BPSH 35 with 30 wt % Phosphotungstic Acid (PTA), and BPSH 35 with 30 wt % Zirconium Hydrogen Phosphate (ZrP)**

The water self-diffusion coefficient decreases as zirconium hydrogen phosphate content in BPSH increases, indicating that increased zirconium hydrogen phosphate increases the amount of tightly bound water in the system or skews the distribution of absorbed water to the more tightly bound fraction. As has been established for pure copolymer systems, tightly bound water decreases the transport properties of the membrane<sup>142</sup> and is consistent with the conductivity and methanol permeability data in this work for the zirconium hydrogen phosphate composite. Contrary to the zirconium hydrogen phosphate composite, the phosphotungstic acid composite shows increasing water diffusion coefficient with increasing inorganic additive content. Increased water diffusion coefficient has been related to more loosely bound water and increased conductivity and methanol permeability. These results demonstrate again that the state of the absorbed water in the membrane, rather than the bulk water content of the membrane, is a more critical parameter influencing the transport properties.

The influence of the inorganic composites on the state of water within the composite membrane is based on the interaction (or lack thereof) of the inorganic additive with the sulfonic acid in the copolymer. Phosphotungstic acid has been shown to strongly interact with the sulfonic acid group of the copolymer.<sup>130</sup> This interaction decreases the water uptake of the composite by decreasing the solvation of the acid group, which frees a portion of the bound water in the membrane from association with the sulfonic acid to create more loosely bound water within the composite. Therefore a decrease in overall water uptake, but an increase in loosely bound water is suggested for the BPSH/phosphotungstic acid composite (as evidenced by water uptake and  $D_{H_2O}$  measurements). The zirconium hydrogen phosphate shows no such specific interaction with the sulfonic acid or any other part of the copolymer. The inorganic phase, because it is formed in-situ in the hydrophilic domains, may simply occupy space within the domain and therefore moderately decreases the water uptake of the zirconium hydrogen phosphate composite. This space-filling function creates more surface area for association with water (creating more tightly bound water), and also may block some of the pore diameter available for transport and water diffusion, which decreases the water self-diffusion coefficient and transport properties as reported in this work.

While the relationship between the water uptake and transport properties of the BPSH/zirconium hydrogen phosphate composite are easily understood, the properties of the BPSH/phosphotungstic acid composite are somewhat counterintuitive if only the bulk water uptake of the composites is considered. However these results are not contradictory once the effect of the state of water in the membrane is recognized. The comparison of transport

properties between a BPSH membrane and the BPSH/phosphotungstic acid composite is similar to the comparison of BPSH 35 and Nafion 117.<sup>142</sup> Nafion has a lower bulk water uptake than BPSH 35 (19 wt % and 30 wt %, respectively) and a lower lambda value, but its conductivity, methanol permeability, and electro-osmotic drag are greater than BPSH 35 as shown in Table 4-1.

**Table 4-1: Comparison of Nafion and BPSH 35 Water Uptake and Transport Properties – 30°C Fully Hydrated Membranes**

	Nafion 117	BPSH 35
Ion Exchange Capacity (meq/g)	0.9	1.5
Water Uptake (weight %)	19	40
Lambda (n H <sub>2</sub> O/SO <sub>3</sub> H)	12	15
Conductivity (S/cm)	0.11	0.06
Methanol Permeability (cm <sup>2</sup> /s)	1.7*10 <sup>-6</sup>	2.4*10 <sup>-7</sup>
Electro-osmotic Drag (n H <sub>2</sub> O/H <sup>+</sup> ) <sup>143</sup>	3	0.9

Similar to the arguments presented in this paper that were applied to BPSH 35 and BPSH/phosphotungstic acid composites, the differences in transport properties between Nafion 117 and BPSH 35 can only be accounted for by considering the state of water in each system. The water in BPSH 35 is much more tightly bound than the water in Nafion 117 as indicated by the water self-diffusion coefficient in each membrane (3.8\*10<sup>-6</sup> cm<sup>2</sup>/s and 5.8\*10<sup>-6</sup> cm<sup>2</sup>/s, respectively as reported in Figure 4-9).

---

143. Hickner, M., F. Wang, Y.S. Kim, T.A. Zawodzinski, J.E. McGrath, B. Pivovar “Electro-osmotic Drag and Methanol Flux in Sulfonated Poly(Arylene Ether Sulfone) Copolymers: Elucidating Morphology from Transport,” *J. Electrochem. Soc.* **2003**, in progress.

## 4.5 Conclusions

This paper provides evidence for the mechanism by which inorganic additives influence the transport properties of water-absorbing, sulfonated proton conducting copolymers and composites. The two inorganic compounds featured in this work showed decidedly different effects on the transport properties of BPSH copolymers. Zirconium hydrogen phosphate synthesized in-situ in an already cast membrane slightly decreased the water uptake of the composite and in turn, the conductivity, methanol permeability, and water self-diffusion coefficient were also reduced in this system. This result is not surprising, given that water uptake has been tied to all of these transport properties previously. When phosphotungstic acid was solution blended with acid form BPSH and cast into a membrane, the behavior of this composite was quite different. The water uptake of this composite membrane was also decreased, in fact even more so than the BPSH/zirconium hydrogen phosphate composite, but this composite's conductivity, methanol permeability, and water self-diffusion coefficient increased. This decrease in water uptake but increase in proton exchange membrane transport properties was unexpected given the conventional tie between water uptake and transport properties, but was consistent with state of water arguments.

The water self-diffusion coefficient gives a rationale for the different transport properties measured in each composite system. Earlier,<sup>142</sup> the water self-diffusion coefficient has been linked to the state of water, which in turn gives an indication of the transport properties of a proton exchange membrane. Lower water self-diffusion coefficients are a result of more tightly

bound water within the copolymer morphology, while greater water self-diffusion coefficients are evidence of more loosely bound and bulk water. Tighter bound water yields suppressed transport properties in these systems (conductivity, methanol permeability, etc.). This is exactly the phenomenon demonstrated in this paper. While the water uptake of the phosphotungstic acid-based composite is lower than the zirconium hydrogen phosphate composite, its conductivity and methanol permeability are significantly higher. These results are due to the difference in the state of water in each system as quantified by the water self-diffusion coefficient in the membranes.

Even though these results were demonstrated for a narrow range of material systems and experimental conditions, there are some general conclusions that can be drawn from this work that are suggested to be applicable to all (or many) sulfonated, water absorbing membranes. To increase the protonic conductivity (a top concern for hydrogen fuel cells) in these membranes, an appreciable amount of loosely bound water is needed. Morphological structures and materials that generate loosely bound water are advantageous for improving conductivity, however the increase of methanol permeability, electro-osmotic drag and other transport properties must be considered when more loosely bound water is present. To decrease the methanol permeability and electro-osmotic drag (a primary concern for direct methanol fuel cell systems) in these materials, the water absorbed into the proton exchange membrane must be more tightly bound. Along with an increase in tightly bound water will come a corresponding decrease in conductivity. It is this balance between conductivity and the other transport properties that must be carefully considered when designing a new proton exchange membrane for a specific fuel cell application.

# CHAPTER 5. TRANSPORT AND MECHANICAL PROPERTIES OF PROTON EXCHANGE MEMBRANES: EFFECT OF MOLECULAR WEIGHT

## 5.1 Abstract

Many classes of ion containing copolymers have been synthesized to serve as proton exchange membranes in fuel cells. These copolymers have been characterized in a multitude of ways that are relevant to their function as proton exchange membranes (water uptake, protonic conductivity, and methanol and gas permeability), however the molecular weight of the system of interest is not often stated in initial reports of polymer properties. It is a well-known principle in polymer science that molecular weight has a tremendous influence on the properties of a polymeric material. This study elucidates the influence of molecular weight on the properties of one class of proton exchange membranes, sulfonated poly(arylene thioether sulfone)s. It was found that the water uptake and methanol permeability of the lower molecular weight copolymer series were greater than the similar properties of the higher molecular weight copolymers. The lower molecular weight copolymers also had poorer mechanical properties. The protonic conductivity of the copolymer was not greatly affected by molecular weight.

Key words: molecular weight, gel permeation chromatography, proton exchange membrane, fuel cell

## 5.2 Introduction

It is widely recognized that the state of the art perfluorinated copolymer fuel cell proton exchange membrane (eg. Nafion) does not possess sufficient properties for all fuel cell applications such as liquid fed direct methanol fuel cells or high temperature operation of hydrogen/air fuel cells at low relative humidity. These shortfalls have spurred the development of alternative proton exchange membranes and many advances have been reported utilizing polyketone,<sup>144</sup> polyimide,<sup>145</sup> polybenzimidazole, and polysulfone<sup>146,147,148</sup> high performance polymeric backbones with attached sulfonic acid groups to provide protonic conductivity.

There have been two general synthetic schemes employed to produce most of the aforementioned proton exchange membranes. The first technique relies on post-sulfonating an existing polymer with fuming sulfuric acid, or other sulfur trioxide containing complexes.<sup>146,149</sup> Most practitioners of this scheme obtain their polymer feedstock from commercial sources for post-sulfonation. The advantage of this technique is that complicated polymerization reactions are avoided, but this method of making sulfonated polymers implies that one must use polymers that already exist on the market. One of the drawbacks of the post-sulfonation methodology to

---

144. Alberti, G., M. Casciola, L. Massinelli, B. Bauer, *J. Membr. Sci.* **2001**, 185, 73.

145. (a) Gunduz, N., T.Y. Inan, E. Yildiz, J.E. McGrath, *Polymeric Materials Science and Engineering* **2001**, 84, 911; (b) Genies, C., R. Mercier, B. Sillion, N. Cornet, G. Gebel, M. Pineri, *Polymer* **2001**, 42, 359; (c) Yin, Y., J. Fang, H. Kita, K. Okamoto, *Chemistry Letters* **2003**, 32(4), 328.

146. Nolte, R., K. Ledjeff, M. Bauer, R. Mulhaupt, *J. Membr. Sci.* **1993**, 83, 211.

147. Koter, S., P. Piotrowski, J. Kerres, *J. Membr. Sci.* **1999**, 153, 83-90.

148. Wang, F., M. Hickner, Y. Kim, T. Zawodzinski, J.E. McGrath, *J. Membr. Sci.* **2002**, 197, 231-242.

149. Poppe, D., H. Frey, K.D. Kreuer, A. Heinzl, R. Mulhaupt, *Macromolecules* **2002**, 35, 7936.

form ion-conducting polymers is that many of the polymers available commercially are synthesized with molecular weights that are conducive to injection molding, extrusion, and other polymer processes. The molecular weight of these polymers is often controlled during the polymerization reaction to be as low as possible for the intended application.

The other method for producing novel ion conducting polymers is the direct polymerization of sulfonated monomers to form a sulfonic acid containing copolymer.<sup>145,148</sup> This scheme, unlike the post-sulfonation route, requires the synthesis of a new monomer and copolymer. However, it affords much better control of all aspects of the macromolecular chemical structure including molecular weight, which is the focus of this study.

Considering all of the research that has been conducted in the last two decades on novel proton exchange membranes, there has been little (if any) reports on the molecular weight of the copolymers studied. Many fuel cell relevant properties have been measured such as water uptake, protonic conductivity, electro-osmotic drag, and others, but molecular weight still remains an unknown in many systems. Characterization of the molecular weight of ion containing copolymers is complicated by the “polyelectrolyte effect” where the ionic groups of the copolymer repel one another due to electrostatic forces and change the size of the molecule.<sup>150</sup> This causes problems for the traditional means of determining polymer molecular weight based on the size of the molecule in a dilute solution such as light scattering, gel

---

150. (a) Mukoyama, Y., N. Shimizu, T. Sakata, S. Mori, *J. Chromatogr* **1991**, 588, 195; (b) Chakrabarty, K., L-Y. Shao, R.A. Weiss, *Solution Properties, In Ionomers, Synthesis, Structure, Properties and Applications*, Eds. MR. Tant, K.A. Mauritz, G.L. Wilkes Blackie Academic and Professional, London 1997.

permeation chromatography (GPC) (size exclusion chromatography (SEC)), or intrinsic viscosity.

The polyelectrolyte effect has been effectively suppressed in GPC characterization of molecular weight by addition such electrolytes as lithium bromide (LiBr).<sup>151</sup> This additive typically employed in concentrations of about 0.05M in the mobile phase of the GPC, reduces the polyelectrolyte interaction with the GPC column and screens the electrostatic repulsion of the ionic moieties on the same copolymer chain. Suppression of these two factors allows a more accurate determination of the molecular weight of ion containing polymers such as the sulfonated copolymers for proton exchange membranes.

Sulfonated copolymers that show promising properties for use as proton exchange membranes develop a microphase-separated morphology consisting of ion rich domains and ion poor domains. In a simplified picture, the ion rich domains when swollen with water facilitate the transport of protons, water, and methanol through the membrane, while the ion poor domains constrain the swelling of the ion rich domains and provide mechanical integrity for the membrane. Due to molecular structure and the high level of sulfonation in these copolymers and their amorphous nature in the sulfonated form, there is little if any semicrystallinity in the membrane to help constrain the swelling of the membrane. There have been reports of a small amount of crystallinity in Nafion,<sup>152</sup> but not in most other sulfonated copolymers. In order for the ion poor domains to provide mechanical integrity for the membrane they must compose the

---

151. P.P. Nefedov, *Polymer Sci. U.S.S.R.* **1981**, 23, 1055.

152. Laporta, M., M. Pegoraro, L. Zanderighi, *Macromolecular Materials and Engineering* **2000**, 282, 22-29.

majority volume fraction within the copolymer morphology to form a continuous supporting phase. It has been reported previously by this group that once the ionic phase begins to show co-continuity (becomes the majority volume fraction) as elucidated by atomic force microscopy, the water absorption and dimensional swelling of the copolymer membrane increased dramatically.<sup>148</sup>

It is proposed that the molecular weight of the copolymer has a significant effect on the physical behavior of the membrane. As a membrane is swollen with water, the entanglements of polymer chains resist dimensional changes of the film. A low molecular weight copolymer with few entanglements would be more susceptible to swelling than the high molecular weight copolymer with many entanglements. The water absorption in turn affects the transport properties of the membrane in terms of protonic conductivity and methanol permeability. Two series of copolymers with the same chemical structure, but different molecular weights, were employed to show the effect of molecular weight on important proton exchange membrane properties and demonstrate that low molecular weight copolymers show increased transport characteristics and decreased mechanical properties as compared to their higher molecular weight counterparts.

## **5.3 Experimental**

### **5.3.1 Materials**

Poly(arylene thioether sulfone) random copolymers (PATs) were synthesized by the direct nucleophilic step copolymerization of a sulfonated dihalide with an unsulfonated dihalide and a

bis(mercaptodiphenyl thioether). General procedures of the copolymer synthesis have been outlined earlier<sup>148,153</sup> and in a recent preprint.<sup>154</sup> The PATS chemical structure is shown in Figure 5-1.

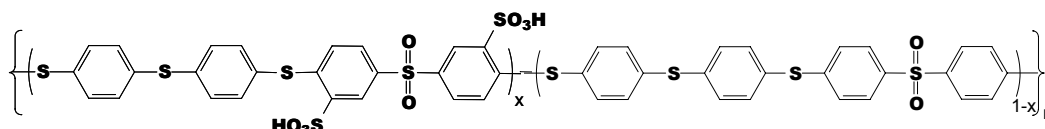


**Figure 5-1: Chemical Structure of the PATS Copolymer**

The number following the PATS acronym denotes the molar percent of sulfonated repeat units that are randomly distributed along the chain ( $x/100$  in Figure 5-1).

Tough, ductile membranes were solution cast from the potassium cation form copolymer onto aluminum molds in a heated vacuum oven. Once filtered through a 0.45  $\mu\text{m}$  PTFE syringe filter, cast polymer solutions of 5 % (wt./vol.) in *N,N*-dimethylacetamide (DMAc) were held under full vacuum at 40°C for 24 hours, then 100°C for 24 hours, and finally 150°C for 12 hours, and removed from the oven. The membranes were converted to the acid (proton) form by boiling in 0.5 M sulfuric acid ( $\text{H}_2\text{SO}_4$ ) for 2 hours. The membranes were rinsed well then boiled in deionized (DI) water for 2 hours to remove any residual sulfuric acid. The membranes

---

153. (a) Harrison, W.L., F. Wang, J.B. Mecham, V.A. Bhanu, M. Hill, Y.S. Kim, J.E. McGrath, *J. Polym. Sci. A* **2003**, 41, 2264-2276; (b) Liu, Y., A. Bhatnagar, Q. Ji, J.S. Riffle, J.E. McGrath, J.F. Geibel, T. Kashiwagi, *Polymer* **2000**, 41(13), 5137-5146.

154. K.B. Wiles, V.A. Bhanu, F. Wang, J.E. McGrath, *Polymer Preprints* **2002**, 43(2), 993-994.

underwent a final rinse in DI water and were then stored in DI water for at least one week before testing.

### 5.3.2 Molecular Weight Characterization

The molecular weight of the PATS copolymers was characterized by intrinsic viscosity (IV) in N-methylpyrrolidone (NMP) at 25°C using a Ubbelohde viscometer. Results were calculated as an average of the reduced and inherent viscosities after extrapolation to zero concentration.

Molecular weights were determined by using size exclusion chromatography (Waters 717 Autosampler, Waters 1515 isocratic HPLC pump, and Waters 2414 refractive index detector) operated at 60 C. The GPC apparatus had a column set with three columns (two Styragel HT 6E and one Styragel HT 3). The mobile phase was N-methylpyrrolidone (NMP) containing 0.05 M LiBr with a flow rate of 1.0 mL/min. The calibration was carried out using narrow molecular weight distribution polystyrene standards.

### 5.3.3 Dynamic Tensile Modulus

Dynamic Mechanical Analysis (DMA) was performed on a TA Instruments DMA 2980 with a submersion film tension clamp. The submersion clamp allows DMA experiments to be performed with the sample fully immersed in a liquid water environment.<sup>155</sup> The hydrated

---

155. Eichstadt, A.E., PhD Dissertation, Structure-property relationships and adhesion in polyimides of varying aliphatic content, Virginia Polytechnic Institute and State University, Blacksburg, VA 2002.

membrane sample was loaded into the submersion clamp geometry and a 1Hz oscillation was applied. The amplitude of the oscillation was increased until a constant modulus plateau was obtained over a period of 30 minutes. This plateau was recorded as the hydrated modulus of the membrane.

#### 5.3.4 Water Uptake

The water uptake of all membranes was determined by first soaking the membranes in 30°C water for at least one week after acidification. The water uptake of the membranes was determined by a simple weight-difference approach. Wet membranes were blotted dry to remove surface droplets and quickly weighed. After 3 - 5 measurements to ensure repeatability of the blotting process, the membranes were dried at 80-100°C under full vacuum for at least 24 hours and weighed again. The water uptake of the membranes was calculated according to Equation 5-1 where  $mass_{dry}$  and  $mass_{wet}$  refer to the mass of the wet membrane and the mass of the dry membrane, respectively.

**Equation 5-1**

$$water\ uptake\ \% = \frac{mass_{wet} - mass_{dry}}{mass_{dry}} \times 100$$

The lambda value ( $\lambda$ ), number of water molecules absorbed per sulfonic acid, can be determined from the mass water uptake and the ion exchange of the copolymer using Equation 5-2.

**Equation 5-2**

$$\lambda = \frac{mass_{wet} - mass_{dry} / MW_{H_2O}}{IEC \cdot mass_{dry}}$$

Where  $MW_{H_2O}$  is the molecular weight of water (18.01 g/mol), and IEC is the ion exchange capacity of the dry copolymer in equivalents per gram.

### 5.3.5 Protonic Conductivity

Protonic conductivity at 30°C under full hydration (in liquid water) was determined using a Solatron 1260 Impedance/Gain-Phase Analyzer over the frequency range of 10 Hz - 1 MHz. The cell geometry was chosen to ensure that the membrane resistance dominated the response of the system.<sup>156</sup> The resistance of the film was taken at the frequency which produced the minimum imaginary response. The conductivity of the membrane can be calculated from the measured resistance and the geometry of the cell according to Equation 5-3.

**Equation 5-3**

$$\sigma = \frac{l}{Z' A}$$

Where  $\sigma$  is the protonic conductivity,  $l$  is the length between the electrodes,  $A$  is the cross sectional area available for proton transport, and  $Z'$  is the real part of the impedance response.

---

156. Zawodzinski, T.A., M. Neeman, L. O. Sillerud and S. Gottesfeld. *J. Phys. Chem.* **1991**, 95, 6040-6044.

### 5.3.6 Methanol Permeability

The methanol permeability of each acid form membrane was determined in a standard membrane separated diffusion cell. This method has been reported previously by this group<sup>157</sup> and the numerical analysis of this experiment has been outlined by Cussler.<sup>158</sup>

### 5.3.7 Relative Selectivity

Selectivity in a proton exchange membrane may be defined as the membrane's protonic conductivity divided by its methanol permeability<sup>159</sup> as shown in Equation 5-4.

**Equation 5-4**

$$\beta = \frac{\sigma}{DH}$$

where  $\beta$  is the selectivity,  $\sigma$  is the protonic conductivity and  $DH$  is the methanol permeability.

Higher selectivity and has been related to lower electro-osmotic drag coefficients in proton

---

157. (a) Hickner, M., F. Wang, Y.S. Kim, T.A. Zawodzinski, J.E. McGrath, AIChE Topical Conference Proceedings **2002**, Spring National Meeting, March 10-14, New Orleans, LA; (b) Y. S. Kim, M. A. Hickner, L. Dong, B. S. Pivovar, and J. E. McGrath, *J. Membr. Sci.* **2003**, submitted.

158. E.L. Cussler, *Diffusion Mass Transfer in Fluid Systems*, 2nd Ed. Cambridge University Press, New York, 1997.

159. Pivovar, B.S., Y. Wang, E.L. Cussler, *J. Membr. Sci.* **1999**, 154, 155-162.

exchange membranes.<sup>160</sup> Relative selectivity is defined as the selectivity of the membrane of interest divided by the selectivity of Nafion, Equation 5-5.

**Equation 5-5**

$$\text{relative selectivity} = \frac{\beta_m}{\beta_{\text{Nafion}}}$$

A membrane with relative selectivity greater than 1 is thus potentially a better direct methanol fuel cell proton exchange membrane than Nafion.

#### 5.4 Results and Discussion

Two activated aryl dihalides, one with chlorine leaving groups and the other with fluorine leaving groups, were utilized in a similar copolymerization scheme to form two series of PATS copolymers with different molecular weights. The more reactive difluoro-based dihalide gave higher molecular weight than a dichloro dihalide. From this point forward in this paper, the two series will be simply denoted as either the low molecular weight (low MW) or high molecular weight (high MW) series. Intrinsic viscosity (IV), number average molecular weights ( $M_n$ ), and weight average molecular weights ( $M_w$ ) for each copolymer obtained via GPC are given in Table 5-1.

---

160. (a) Pivovar, B., PhD dissertation, Electrochemical Selectivity and Electro-osmosis in Direct Methanol Fuel Cell Electrolytes. University of Minnesota, Minneapolis, MN, 2000; (b) Pivovar, B., E. Cussler, *Journal of Membrane Science* **2003**, in progress.

**Table 5-1: Intrinsic Viscosity and Molecular Weight for Low MW and High MW PATS Copolymers**

	IEC (meq/g)	IV (dL/g)*	M <sub>n</sub> , M <sub>w</sub> (kg/mole) <sup>+</sup>
PATS 20 low MW	0.81	0.69	23, 68
PATS 30 low MW	1.17	0.61	19, 58
PATS 40 low MW	1.51	0.76	20, 61
PATS 20 high MW	0.81	1.30	25, 104
PATS 30 high MW	1.17	0.98	26, 127
PATS 40 high MW	1.51	1.20	28, 151

\* 25°C, NMP

<sup>+</sup> NMP with 0.05M LiBr versus calibration against polystyrene standards

As can be seen from Table 5-1, the low MW PATS copolymers derived from the less reactive dichloro aryl dihalide have consistently lower IV and molecular weights (especially M<sub>w</sub>) than the series of high MW PATS copolymers synthesized utilizing the difluoro dihalide. Endgroups could play a role in membrane properties, with the low MW copolymers having a larger number of endgroups than the high MW copolymers, but the effects of endgroups were not considered in this work.

Protonic conductivity is the foremost requirement for proton exchange membranes. If a membrane shows poor conductivity performance, it will not function well in a proton exchange membrane fuel cell. The protonic conductivity of the acid form of both PATS series was measured and the results reported in Figure 5-2.

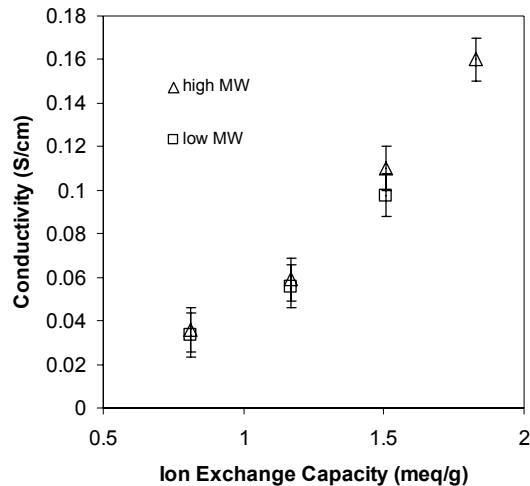


**Figure 5-2: Protonic Conductivity of High MW and Low MW PATS Copolymers**

The protonic conductivity of the low MW PATS 50 copolymer (IEC of 1.8 meq/g) could not be measured because of its extremely poor mechanical properties when hydrated. Within the inherent experimental error and repeatability of the measurement, the conductivity of the two series of PATS copolymers is comparable. This is a reasonable result considering the two series have the same chemical structure and the same number of ionic groups on an ion exchange capacity basis.

Cast membranes in the acid form were measured for water uptake for liquid water at 30°C. The results are shown in Figure 5-3.

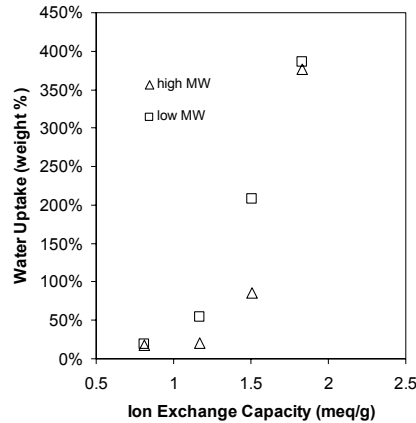


**Figure 5-3: Water Uptake of High MW and Low MW PATS Copolymers**

At the extremes of sulfonation (20%, IEC 0.71 meq/g and 50%, IEC 1.81 meq/g) the water uptake of the two series of copolymers is strikingly similar, about 19% and 380%, respectively. For PATS 30 samples, high MW membranes absorb 20% water, while the PATS 30 low MW membranes absorb significantly more water at 54%. Similarly, the PATS 40 high MW membranes absorbed 86% water, while the low MW PATS 40 samples absorbed 208% water.

At 20% sulfonation, the volume fraction of ion poor domains is high and the molecular weight of the copolymer does not seem to have a large influence on the swelling properties of the copolymer membrane. At the high level of sulfonation, the volume fraction of the ionic poor domains starts to become the minority phase in both series of copolymers and can no longer constrain the swelling of the ion rich domains regardless of molecular weight.

As was proposed in the introduction, the lower molecular weight PATS copolymers absorb more water on a weight basis than the higher molecular weight copolymers. It is interesting that even though the two series of copolymers have different water uptake, their conductivities are similar.

The lower water content of the high MW PATS series is sufficient as to not impede conductivity, but the extra water absorbed in the low MW PATS copolymers does not enhance conductivity or cause a decrease in conductivity by excessive swelling and separation of the ionic groups.

The water uptake observations demonstrate that at very low and very high levels of sulfonation, the molecular weight of the copolymer has little effect on the water uptake and swelling of the membrane. It is at the intermediate levels of sulfonation (30% and 40%) where the molecular weight is critical to control water uptake. The low and high levels of sulfonation are interesting from a polymer science and fundamental materials property perspective, but they are not necessarily suitable to fuel cell applications. The protonic conductivity of the PATS 20 copolymers is too low to be useful for proton exchange membranes, and the PATS 50 copolymers' mechanical properties are not sufficient for membrane electrode assembly fabrication or long-term use in the fuel cell. Most copolymers under investigation for applications in fuel cells fall in the range of ion contents of the PATS 30 (IEC = 1.17 meq/g) and PATS 40 (IEC = 1.51 meq/g) copolymers.

From the water uptake and ion exchange capacity data, the lambda value for each sample was determined (Table 5-2).

**Table 5-2: Lambda Values for High MW and Low MW PATS Copolymer Membranes - 30°C in Liquid Water**

	IEC (meq/g)	Water Uptake (weight %)	Lambda (N H <sub>2</sub> O/SO <sub>3</sub> H)
PATS 20 low MW	0.81	19	13
PATS 30 low MW	1.17	54	26
PATS 40 low MW	1.51	208	77
PATS 50 low MW	1.84	386	117
PATS 20 high MW	0.81	18	12
PATS 30 high MW	1.17	20	9
PATS 40 high MW	1.51	86	32
PATS 50 high MW	1.84	377	114

Again, this table shows that at the low and high levels of sulfonation (20 and 50%), the water uptake of the high MW and low MW copolymers is similar. However, the lambda values are drastically different for PATS 30 and 40 samples. When the lambda values are taken in context with the protonic conductivity (Figure 5-2), these results demonstrate that for a given ion exchange capacity, the conductivity does not vary greatly over a wide range of lambda values.

The methanol permeability of both series of PATS copolymers was measured in a classical diffusion cell experiment and the results are shown in Figure 5-4.

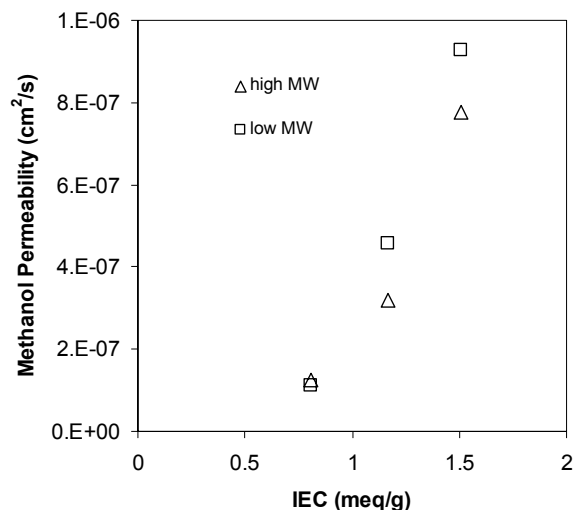


**Figure 5-4: Methanol Permeability of High MW and Low MW PATS Copolymer Membranes - Fully Hydrated Membranes at 30°C**

Similar to the results for water uptake, at 20% sulfonation the methanol permeability of both the high MW and low MW series is similar. Again, because the volume fraction of ion poor domains is so large at 20% sulfonation, molecular weight does not play a significant role in determining the transport properties of the membrane and both series of molecular weights show similar methanol permeability. As sulfonation is increased, the low MW PATS copolymers show significantly higher methanol permeability than the analogous high MW copolymers which is expected given the water uptake results. Low MW PATS 30 has a 45% greater permeability than the high MW PATS 30 specimen ( $4.6 \times 10^{-7} \text{ cm}^2/\text{s}$  versus  $3.2 \times 10^{-7} \text{ cm}^2/\text{s}$ ). The increase in permeability between low MW and high MW PATS 40 was 20% ( $9.3 \times 10^{-7} \text{ cm}^2/\text{s}$  versus  $7.8 \times 10^{-7}$

cm<sup>2</sup>/s). The permeability of the 50% copolymers for each series was not measured in the diffusion cell because the mechanical properties of the membranes were extremely poor.

As a result of the similar conductivity of the two series of PATS copolymers and the higher methanol permeability of the low MW series, the selectivity of the low MW series is lower than the high MW PATS copolymers. The relative selectivity of each series of copolymers as compared to Nafion (relative selectivity of Nafion is 1) is shown in

Figure 5-5.

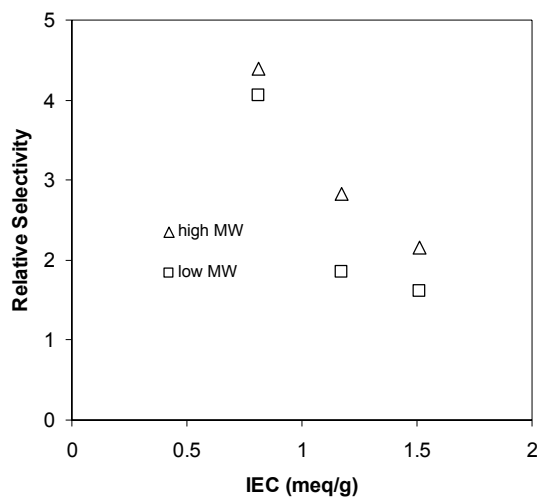


**Figure 5-5: Selectivity of High MW and Low MW PATS Copolymers**

This result shows that higher molecular weight copolymers are more desirable than low molecular weight copolymer for direct methanol fuel cell applications because of their higher (or equal) relative selectivity over all levels of sulfonation. Many of the commercially available

poly(sulfone) or poly(ketone) copolymers that have been used for post-sulfonation reactions to form proton exchange membranes are lower molecular weight than may be desirable for fuel cell applications. This creates the need for mechanical reinforcement or crosslinking in many post-sulfonated systems.<sup>161</sup> The water absorption and dimensional swelling of these lower molecular weight copolymers is large and causes the methanol permeability to increase (and selectivity decrease) as compared to their high molecular weight counterparts.

In addition to transport properties, mechanical properties are also a key consideration when designing new proton exchange membranes. Mechanically robust membranes are important during both the MEA fabrication and operation of a direct methanol fuel cell. The membrane must provide a support for the catalyst layer and be able to withstand the mechanical clamping and pressure gradients that exist during operation of the fuel cell. Strength and ductility of the membranes in the dry state is important during membrane handling and MEA fabrication, but during their use in fuel cells the membranes are partially or completely hydrated which greatly influences their mechanical properties. In-situ dynamic mechanical analysis (DMA) was used to allow the dynamic tensile modulus of the membrane to be probed while the membrane is submerged in liquid water.<sup>155</sup> This experimental method allows one to determine the modulus of the membrane in an environment that is very similar to a direct methanol fuel cell. It has been shown previously that absorbed water greatly affects the modulus of proton exchange membranes.<sup>162</sup> The dynamic modulus of fully hydrated, submerged PATS membranes was

---

161. (a) Kerres, J., W. Zhang, A. Ullrich, C.M. Tang, M. Hein, V. Gogel, T. Frey, L. Jorissen, *Desalination* **2002**, 147, 173; (b) Guo, Q., P.N. Pintauro, H. Tang, S. O'Connor, *J. Membr. Sci.* **1999**, 154, 175.

162. Hickner, M., Y. Kim, F. Wang, T. Zawodzinski, J.E. McGrath, "Proton exchange membrane nanocomposites," Proceedings of the American Society for Composites, Sixteenth Technical Conference, M.W. Hyer and A.C. Loos, Ed., September 9-12, 2001, 323-336.

measured by in-situ dynamic mechanical analysis (DMA). The results for the high and low molecular weight PATS copolymer series are compared in Figure 5-6.

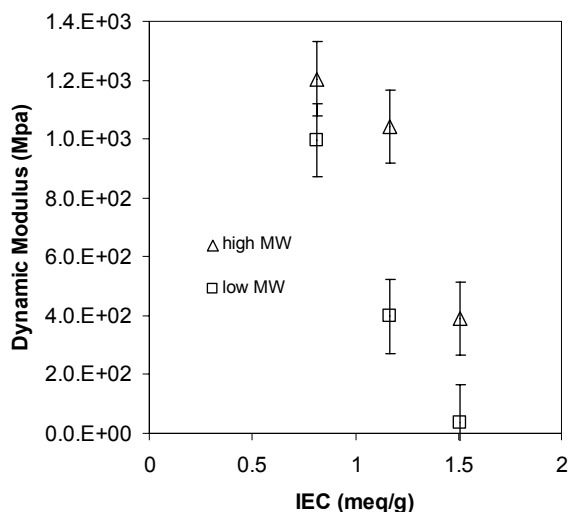


**Figure 5-6: Dynamic Tensile Modulus of High MW and Low MW PATS Copolymer Membranes**

The mechanical properties of the copolymers show a distinct difference between the high MW and low MW PATS materials. Over all levels of sulfonation, the low MW copolymers have a lower tensile modulus than the high MW series. This result is expected when the molecular weight (especially  $M_w$ ) and water uptake of each series is considered as reported above. Additionally, the gap between the two series is greater at the 30% and 40% levels of sulfonation than at 20% sulfonation (PATS 50 copolymers were not measured due to their poor mechanical properties and problems with loading these membranes into the DMA). Again, at low ion

contents the molecular weight has less of an effect on the properties of the proton exchange membrane than at the higher ion contents. The ion poor domains can be thought of as physical crosslinks which constrain the ion rich domains during water absorption. At 20% sulfonation there is a large volume fraction of ion poor domains that tends to hold the membrane together and thus high molecular weight (and more chain entanglements) is not required to provide mechanical integrity. As the level of sulfonation increases, the amount of physical crosslinks declines and the molecular weight of the chains becomes important to provide mechanical integrity for the membrane.

## **5.5 Conclusions**

The effect of molecular weight on the proton exchange membrane properties of protonic conductivity, water uptake, methanol permeability, relative selectivity, and hydrated modulus was demonstrated using two analogous series of copolymers. The copolymers were synthesized using two different dihalide monomers to achieve consistently lower molecular weights with the dichloro dihalide (as evidenced by intrinsic viscosity and GPC) versus the difluoro dihalide over the entire range of sulfonation.

It was demonstrated that the protonic conductivity of the two series of copolymers was strikingly similar even though their water uptake and  $\lambda$  values were considerably different at higher levels of sulfonation. The methanol permeability of the low molecular weight series was greater than the high molecular weight series above 20% sulfonation. As with water uptake, there was little difference between the high MW and low MW PATS copolymers at 20% sulfonation. Due

to the difference in methanol permeability, the relative selectivity of the low MW copolymers was lower than the higher molecular weight series. In addition to the transport properties of the two series, the hydrated modulus of the lower MW copolymers was lower than the higher MW series. This may have an impact on the processing and fuel cell durability of the membrane electrode assembly.

Both high and low molecular weight series copolymer membranes had similar water uptake, methanol permeability, and hydrated modulus at 20% sulfonation. At this low level of sulfonation, the volume fraction of ion poor domains is large and molecular weight does not have as strong an influence on membrane properties as when the sulfonation level is increased. Additionally, the 50% PATS copolymers had similar water uptake. This is a result of the ion rich domains beginning to dominate the behavior of the system, and the molecular weight of the high MW series being insufficient to constrain the swelling of the domains.

PATS copolymers were utilized for this study because of the ability to control the molecular weight of the polymer backbone during the copolymer synthesis. The results of this study can be extended to post-sulfonated copolymer systems. Because the base polymer in post-sulfonation reactions is often low molecular weight (for injection molding) the resulting proton exchange membrane properties of these types of materials can be compromised. In order to produce a copolymer-based proton exchange membrane with the most desirable properties in terms of mechanical properties and methanol permeability, the molecular weight of the backbone should be as high as possible. Additionally, this study demonstrates that the molecular weight of the sulfonated copolymer is a critical parameter that determines the behavior of the resulting proton

exchange membrane. There are numerous studies of new proton exchange membrane copolymers, but characterization of the molecular weight of these materials is still rather rare. Increased efforts to understand the relationship between molecular weight and membrane properties will help to further development of alternative proton exchange membranes.

# CHAPTER 6. FABRICATING HIGH PERFORMANCE MEMBRANE ELECTRODE ASSEMBLIES FROM NON- NAFION PROTON EXCHANGE MEMBRANES

## 6.1 Abstract

Efforts on commercialization of proton exchange membrane fuel cells has made evident that perfluorinated copolymer systems such as Nafion<sup>®</sup> do not have the most desirable properties for direct methanol fuel cells. Specifically, its methanol permeability is too high and new membrane materials are required to meet the technical challenge of decreased methanol crossover while maintaining sufficient protonic conductivity. Many research efforts have produced promising alternate proton exchange membranes based on sulfonated polysulfones, polyketones, polyimides, and polyphosphazenes with very low methanol permeability, but synthesizing a membrane with high conductivity and low methanol permeability is only the first step. A high performance proton exchange membrane material must be fabricated into high performance membrane electrode assemblies (MEAs) to achieve optimum fuel cell performance. This paper outlines some of the issues associated with producing MEAs from membranes other than Nafion, by comparing the properties of free-standing membranes and MEAs made from those membranes. Two approaches are proposed for increasing the performance of MEAs based on non-Nafion membranes.

## 6.2 Introduction

Direct methanol fuel cells are increasingly becoming a viable energy source for portable devices such as mobile telephones, notebook computers, soldier power, and other “portable power” applications. One of the primary performance inhibitors for direct methanol fuel cells is methanol crossover. Methanol crossover occurs when methanol (typically in the form of a methanol/water solution) fed to the anode catalyst is not completely oxidized in the catalyst layer. The unreacted methanol crosses the proton exchange membrane and is then oxidized at the cathode, which both reduces the fuel efficiency of the system and creates a mixed cathode potential, resulting in lowered voltage efficiency of the cell. Employing a proton exchange membrane with reduced methanol permeability (or more exactly reducing the methanol flux to the cathode) can combat these two losses, loss of methanol fuel, and mixed cathode potential.

It is useful here to make the distinction between methanol permeability and methanol flux, and similarly membrane conductivity and membrane resistance. Methanol permeability is an intrinsic property of the material and is independent of membrane thickness or methanol concentration. Methanol flux, on the other hand, is a function of membrane permeability, thickness, and concentration gradient. This comparison can most easily be illustrated by considering the 1-dimensionalized, integrated form of Fick’s Law shown in Equation 6-1 as it applies to membrane diffusion.

**Equation 6-1**

$$j = \frac{DH}{t}(c_1 - c_2)$$

Where  $j$  is the methanol flux,  $DH$  is the membrane methanol permeability,  $t$  is the membrane thickness, and  $(c_1 - c_2)$  is the methanol concentration difference across the membrane.

Researchers designing novel membranes are most interested in the intrinsic methanol permeability of a material ( $DH$ ), while the methanol crossover is more important for fuel cell operation. In a direct methanol fuel cell apparatus, the methanol crossover is also influenced by current density, gas diffusion layer, and flow rate of methanol in addition to the membrane effects discussed above. The same parallel can be applied to the membrane conductivity and the membrane resistance. Proton exchange membrane protonic conductivity is an intrinsic property of the ion conducting polymer which is independent of thickness, while the membrane resistance (measured as “high frequency resistance” in a fuel cell) is dependent on both the membrane conductivity, membrane thickness and area. The relationship between conductivity and resistance is shown in Equation 6-2. Note that resistance measurements are often normalized for area ( $R-A$  in Equation 6-2).

**Equation 6-2**

$$R = \frac{t}{\sigma A}$$

Where  $R$  is the resistance,  $t$  is the membrane thickness,  $\sigma$  is the membrane conductivity, and  $A$  is the cross-sectional area for conduction. Current DMFC technology utilizes rather thick Nafion 117 (7 mil, 0.007 inches, 178  $\mu\text{m}$ ) to reduce the methanol crossover. Nafion 1135 and Nafion 112 are the standard Nafion membranes for hydrogen/air fuel cells because thinner membranes are desirable from a cell resistance perspective, but the thicker 117 membrane is required in

DMFCs to partially control the methanol crossover encountered in current systems. Increasing the thickness of the membrane eases the problem of methanol crossover, but it undesirably increases the resistance of the cell in DMFC systems. It is this balance between methanol flux and cell resistance that must be considered when optimizing any new membrane for use in a DMFC.

Aside from just the membrane properties, one must consider the properties of the full membrane electrode assembly. Much work has been done to describe the electrochemical performance of the catalysts,<sup>163</sup> but there has been comparatively little work on describing the fundamental processes in the catalyst layer itself and even less research has focused on the attachment of catalyst layers to new (e.g. non-Nafion containing) proton exchange membranes.

Various nomenclatures have been developed to describe membrane electrode assemblies and the various components of a fuel cell that lie between the anode and cathode bipolar plates. In this paper, the membrane electrode assembly refers to the proton exchange membrane bonded to the catalyst layers that are typically a composite of ion conducting polymer and the catalyst. The catalyst can either be metal or metal supported on carbon black depending on the application. The gas diffusion layers lie between the catalyst layers and the bipolar plate. Gas diffusion layers are hot pressed onto the MEA or mechanically clamped to the MEA using the compression of the fuel cell hardware. The bipolar plates are typically graphite or highly filled graphite/polymer composites and contain the gas flow fields for reactant delivery to the MEA.

---

163. (a) Thompsett, D., "Catalysts for the proton exchange membrane fuel cell," Fuel Cell Technology Handbook 2003, ed. Hoogers, Gregor, CRC Press LLC, Boca Raton, FL; (b) Thomas, S.C., X. Ren, S. Gottesfeld, P. Zelenay, *Electrochimica Acta* **2002**, 47(22-23), 3741-3748.

The membrane electrode assembly and gas diffusion layers, from bipolar plate to bipolar plate can be pictured as a set of resistances in series, with a resistance corresponding to each component and each interface. A model depicting these resistances is shown in Figure 6-1.

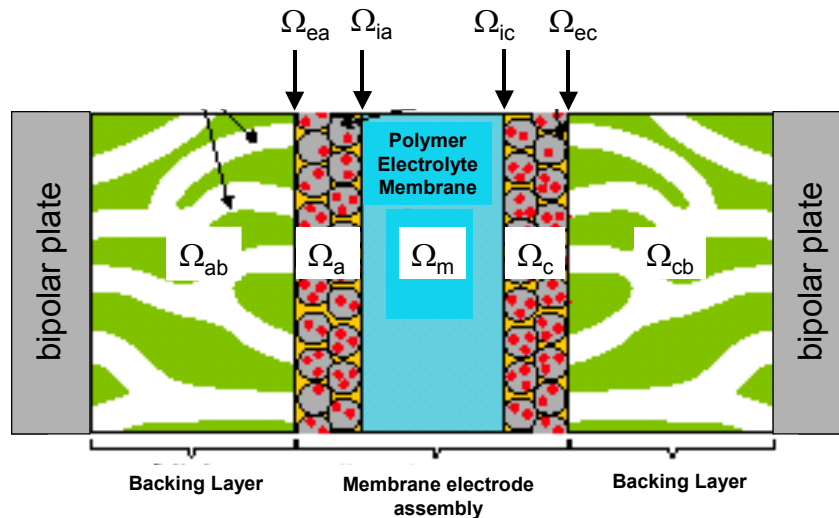


**Figure 6-1: Membrane Electrode Assembly and Gas Diffusion Layer Resistances of Components and Interfaces**

Within this simple schematic of a membrane electrode assembly there are two types of conducting materials, electronic conducting and protonic conducting, and two types of interfaces, the interface between an electronic conductor and an electronic conductor, and the interface between an electronic conductor and a protonic conductor. The catalyst layers, being mixed protonic and electronic conductors are special cases that will be described shortly.

In the high frequency resistance measurement of a fuel cell, an impedance measurement is made at a frequency usually between 2,000 and 8,000 Hertz. The frequency is chosen so the imaginary component of the impedance is minimized (current and voltage signals are nearly in-phase). Using impedance analysis, the resistance in Ohms of the entire MEA between the bipolar plates is measured and the result can be normalized on the basis of area with the units  $\Omega\text{-cm}^2$ . All of the materials and interfaces labeled in Figure 6-1 contribute to the overall resistance measured in this technique. Throughout this work the bipolar plates, gas diffusion backing layers, and catalyst layers remain constant, so their material resistances ( $\Omega_{\text{plates}}$ ,  $\Omega_{\text{ab}}$ ,  $\Omega_{\text{ac}}$ ,  $\Omega_{\text{cb}}$ ) and interfacial resistances ( $\Omega_{\text{ea}}$  and  $\Omega_{\text{ec}}$ ) remain constant. Of interest here is the resistance of the membrane ( $\Omega_{\text{m}}$ ) itself and the interfacial resistance between the membrane and the catalyst layers ( $\Omega_{\text{ia}}$ ,  $\Omega_{\text{ic}}$ ). High performance MEAs would have a high frequency resistance that is representative of  $\Omega_{\text{m}}$  and minimizes the interfacial resistances  $\Omega_{\text{ia}}$  and  $\Omega_{\text{ic}}$ .

The membrane resistance tends to dominate the system in the high frequency resistance measurements because of the intrinsically low conductivity of protonic conducting polymers as compared to the other components in the system. In the course of novel proton exchange membrane development, a large emphasis is placed on protonic conductivity of the polymer itself. Protonic conductivity is the first and perhaps most important property, but not the only requirement of new proton exchange membranes. The membrane must also be robust mechanically, stable chemically, and be amenable to MEA fabrication. As is becoming more evident,<sup>164</sup> the interfacial resistance between the membrane and the catalyst layer is critically

---

164. Pivovar, B.S., "The role of membrane thickness and interfaces on DMFC performance," Proceedings of the 202<sup>nd</sup> Meeting of the Electrochemical Society, Salt Lake City, UT, Oct. 20-25, 2002.

important when new membranes are incorporated into fuel cells. A well-designed proton exchange membrane should not only have high protonic conductivity, but it should also bond well to the electrode. Characterization of the membrane/electrode interface remains relatively undeveloped when dealing with non-Nafion membranes.

One can envision two general strategies to decrease the interfacial resistance between the proton exchange membrane and the electrode; either the electrode can be optimized to bond to the membrane, or the membrane must be optimized to bond with a standard electrode. Much work has been done to optimize the electrocatalytic activity of Nafion-based electrodes, so the later strategy was chosen as the focus of this work. It is noted that the first strategy remains relatively untested. Very few if any reports of novel ion conducting polymers in the electrode exist in the literature.

It is the goal of this communication to demonstrate that both intrinsic membrane properties and the catalyst layer/membrane interface must be given consideration during the design and development of novel proton exchange membranes and subsequent demonstration as membrane electrode assemblies. Our focus is on increasing the compatibility between the proton exchange membrane and a Nafion-based catalyst layer as described in the paragraph above. We will describe two copolymers with similar membrane properties in terms of methanol permeability and proton conductivity, but show different fuel cell performance due to their differing affinity for Nafion-based catalyst layers.

## 6.3 Experimental

### 6.3.1 Materials and Membrane Preparation

Nafion 117 (1100 equivalent weight, 0.007 mils thick) membranes were obtained from Los Alamos National Laboratory. Nafion's chemical structure is shown in Figure 6-2.

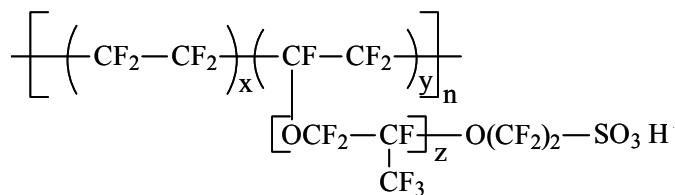


**Figure 6-2: Chemical Structure of Nafion**

The membranes were prepared for measurement by standard preparation methods described elsewhere.<sup>165</sup>

Poly(arylene ether sulfone) copolymers (BPSH) were synthesized by direct copolymerization of sulfonated monomers as described in detail in Ref. 166, and their chemical structure is shown in Figure 6-3.

---

165. Zawodzinski, T.A., C. Deroin, S. Radzinski, J. Sherman, V.T. Smith, T.E. Springer, and S. Gottesfeld, *J. Electrochem. Soc.* **1993**, 140,1041.

166. Wang, F., M. Hickner, Y.S. Kim, T.A. Zawodzinski, J.E. McGrath, *J. Membr. Sci.* **2002**, 197, 231-242.

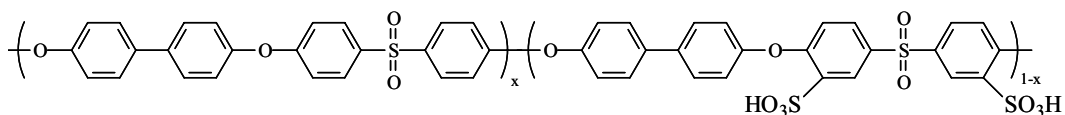


**Figure 6-3: Chemical Structure of BPSH**

Tough, ductile membranes were solution cast from the potassium cation form copolymer on aluminum molds in a heated vacuum oven. Once filtered through a 0.45  $\mu\text{m}$  PTFE syringe filter, cast polymer solutions of 5 % (weight/volume) in N,N-dimethylacetamide (DMAc) were held under full vacuum at 40°C for 24 hours, then 100°C for 24 hours, and finally 150°C for 12 hours, then removed from the oven. The membranes were converted to the acid (proton) form by boiling in 0.5 M sulfuric acid ( $\text{H}_2\text{SO}_4$ ) for 2 hours. The membranes were rinsed well then boiled in deionized (DI) water for 2 hours to remove any residual sulfuric acid. The membranes underwent a final rinse in DI water and were then stored in DI water for at least one week before testing.

Sulfonated bisphenol-AF poly(arylene ether sulfone) copolymers (6F) were synthesized using a similar methodology to the BPSH copolymers as described elsewhere.<sup>167</sup> Bisphenol-AF, the hexfluoroisopropylidene analog of bisphenol-A, was substituted for the biphenol of BPSH in the step growth polymerization scheme to achieve the 6F structure shown in Figure 6-4.

---

167. W.L. Harrison, F. Wang, J.B. Mechem, V.A. Bhanu, M. Hill, Y.S. Kim, J.E. McGrath, *J. Polym. Sci. A* **2003**, 41, 2264-2276.

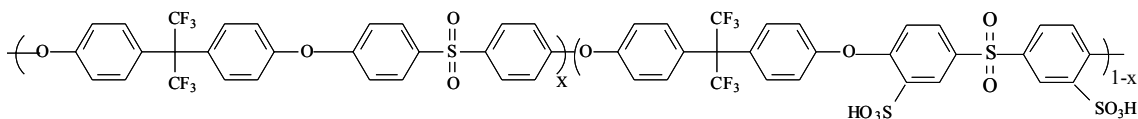


**Figure 6-4: Chemical Structure of Bisphenol AF-Based Poly(Arylene Ether Sulfone) Copolymer (6F)**

These membranes were solution cast from DMAc and converted to the acid form in an analogous manner to the BPSH membranes.

### 6.3.2 Free-Standing Membrane Conductivity

Protonic conductivity at 80°C under full hydration (in liquid water) was determined using a Solatron 1260 Impedance/Gain-Phase Analyzer over the frequency range of 10 Hz - 1 MHz. The cell geometry was chosen to ensure that the membrane resistance dominated the response of the system.<sup>168</sup> The resistance of the film was taken at the frequency which produced the minimum imaginary response. The conductivity of the membrane can be calculated from the measured resistance and the geometry of the cell according to Equation 6-3.

---

168. Zawodzinski, T.A., M. Neeman, L. O. Sillerud and S. Gottesfeld. *J. Phys. Chem.* **1991**, 95, 6040-6044.

**Equation 6-3**

$$\sigma_m = \frac{l}{Z' A}$$

Where  $\sigma_m$  is the protonic conductivity of the membrane,  $l$  is the path length between the electrodes,  $A$  is the cross sectional area available for proton transport, and  $Z'$  is the real part of the impedance response.

Free-standing membrane conductivity was determined at 80°C at 100% relative humidity using a sealed pressure vessel.<sup>169</sup> The conductivity cell (with external leads through the vessel) was suspended above liquid water in a saturated liquid water environment while the entire vessel was evacuated then equilibrated at 80°C for at least 4 hours. The impedance analysis described above was then performed.

### 6.3.3 Free-Standing Membrane Methanol Permeability

The methanol permeability of each acid form membrane was determined in a standard membrane separated diffusion cell. This method has been reported previously by this group<sup>170</sup> and the numerical analysis of this experiment has been outlined by Cussler.<sup>171</sup> The free-standing membrane methanol permeability will be denoted as  $DH_m$ .

---

169. Kim, Y., F. Wang, M. Hickner, T. Zawodzinski, J.E. McGrath, *J. Membr. Sci.* **2003**, 212, 263-282.

170. (a) Hickner, M., F. Wang, Y.S. Kim, T.A. Zawodzinski, J.E. McGrath, AICHE Topical Conference Proceedings, Spring National Meeting, March 10-14, New Orleans, LA. 2002; (b) Y. S. Kim, M. A. Hickner, L. Dong, B. S. Pivovar, and J. E. McGrath, *J. Membr. Sci.* **2003**, submitted.

### 6.3.4 Membrane Electrode Assembly Fabrication

Direct methanol fuel cell (DMFC) membrane electrode assemblies (MEA) for all membranes were prepared with standard Nafion 1100-based electrodes using a direct painting method developed at Los Alamos National Laboratory.<sup>172</sup> Catalyst loadings were approximately 6 mg/cm<sup>2</sup> of platinum black on the cathode, and 9 mg/cm<sup>2</sup> of ruthenium/platinum black on the anode.

DMFC performance of the MEAs was tested using standard serpentine channel 5cm<sup>2</sup> Fuel Cell Technologies (Albuquerque, NM) fuel cell hardware with E-Tek (De Nora North America, Inc., Somerset, NJ) ELAT<sup>®</sup> gas diffusion backings, which were mechanically clamped to the MEA in the fuel cell hardware. Methanol (typically diluted to 0.5M with Millipore 18.5 MΩ water) was supplied to the anode compartment at a flow rate of 1.8 mL/min. Air humidified to 10°C above cell temperature was introduced to the cathode at a flowrate of 300-500 cm<sup>3</sup>/min. The anode and cathode cell outlets were maintained at ambient pressure. All tests were conducted at Los Alamos National Laboratory at an elevation of 7,200 feet above sea level.

---

171. E.L. Cussler, *Diffusion Mass Transfer in Fluid Systems*, 2nd Ed. Cambridge University Press, New York, 1997.

172. Thomas, S.C., X. Ren, S. Gottesfeld and P. Zelenay, *Electrochim. Acta* **2002**, **47**, 3741- 3748.

Hydrogen/air MEAs were fabricated using a decal transfer technique as described previously.<sup>173</sup> Catalysts were standard E-Tek 20% Platinum on XC-72 with loadings of 0.2 mg Pt/cm<sup>2</sup> on both the anode and the cathode. MEAs were tested using standard serpentine channel 5cm<sup>2</sup> Fuel Cell Technologies (Albuquerque, NM) fuel cell hardware with E-Tek (De Nora North America, Inc., Somerset, NJ) ELAT<sup>®</sup> gas diffusion backings mechanically clamped to the MEA in the fuel cell hardware. Air (humidified to 10°C above cell temperature) was supplied to the cathode at 500 cm<sup>3</sup>/min and hydrogen (humidified to 10°C above cell temperature) was supplied to the anode at 200 cm<sup>3</sup>/min regardless of current density. Backpressure of 30 psig was maintained in both anode and cathode compartments.

### 6.3.5 Fuel Cell Protonic Conductivity as Determined by High Frequency Resistance

The high frequency resistance (HFR) of each MEA was determined using a National Instruments data acquisition system to drive the external program input on an Agilent electronic load incorporated in the Fuel Cell Technologies test stand. Single frequency impedance measurements were performed at 5 kHz where the imaginary impedance response of the system is small. The impedance response at this frequency is assumed to reflect only the membrane ohmic resistance and contact resistances of the membrane/electrode interface.<sup>174</sup>

---

173. Wilson, M.S., J.A. Valerio, S. Gotesfeld, *Electrochim. Acta* **1995**, 40, 355.

174. Springer, T.E., T.A. Zawodzinski, M.S. Wilson, S. Gotesfeld, *J. Electrochem. Soc.* **1996**, 143(2), 587.

From the HFR (in units of  $\Omega\text{-cm}^2$ ) data, the conductivity of the MEA can be computed as shown in Equation 6-4.

**Equation 6-4** 
$$\sigma_{MEA} = \frac{l}{HFR}$$

Where  $\sigma_{MEA}$  is the conductivity of the MEA,  $l$  is the thickness of the membrane, and HFR is the high frequency resistance. The MEA conductivity as determined from the fuel cell high frequency resistance is compared to the membrane conductivity by computing the % loss between membrane and MEA conductivity as shown in Equation 6-5.

**Equation 6-5** 
$$\% \text{ LOSS} = \frac{(\sigma_m - \sigma_{MEA})}{\sigma_m} \times 100$$

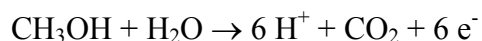
where  $\sigma_m$  is the membrane conductivity from free standing membrane measurements and  $\sigma_{MEA}$  is the conductivity of the MEA computed from HFR.

### 6.3.6 Limiting Current Method for Determining Fuel Cell Methanol Permeability

A method for determining the methanol crossover of a DMFC membrane in fuel cell hardware was reported by Ren et al.<sup>175</sup> This method allows facile determination of methanol crossover in the standard DMFC hardware with the addition of an external power supply.

A methanol/water solution of known concentration was introduced to the anode compartment (in fuel cell configuration) with a high flow rate to minimize concentration depletion down the flow channel (1.8 mL/min. in a 5cm<sup>2</sup> cell). The cathode compartment is fed with humidified nitrogen at 500 standard cm<sup>3</sup>/min and both anode and cathode compartments are maintained at ambient pressure. Unlike typical DMFC operation, where methanol is oxidized at the fuel cell anode and power is generated within the cell, a power supply is connected to the fuel cell in the opposite orientation forcing current to flow backward through the cell with respect to normal fuel cell orientation. In this configuration, what is traditionally considered the fuel cell anode becomes the counter electrode, and the fuel cell cathode is the working electrode. Methanol diffuses through the anode catalyst layer, across the membrane, and is oxidized at the fuel cell cathode (although in this experiment, the fuel cell cathode is the electrochemical anode) according the reaction:

**Equation 6-6**



The protons are then driven back across the membrane by the applied potential where they react at the fuel cell anode to produce hydrogen.

---

175. X. Ren, T.E. Springer, T.A. Zawodzinski and S. Gottesfeld, *J. Electrochem. Soc.* **2000**, 147(2), 466.

From the stoichiometry shown in Equation 6-6, the methanol permeability of the MEA ( $DH_{MEA}$ ) can be computed from the resulting current as measured in a fuel cell during a crossover current experiment according to Equation 6-7:

**Equation 6-7**

$$DH_{MEA} = \frac{I_x \cdot l}{F \cdot c_o \cdot 6}$$

Where  $I_x$  is the measured crossover current,  $l$  is the membrane thickness,  $F$  is Faraday's constant, and  $c_o$  is the methanol feed concentration. The factor of 6 arises in the denominator because each methanol molecule oxidized yields 6 protons (and the corresponding 6  $e^-$  which are measured by the power supply).

### 6.3.7 Electrochemical Selectivity

Electrochemical selectivity in a proton exchange membrane is defined as a membrane's protonic conductivity divided by its methanol permeability<sup>176</sup> as shown in Equation 6-8.

**Equation 6-8**

$$\beta_m = \frac{\sigma_m}{DH_m}$$

---

176. Pivovar, B.S., Y. Wang, E.L. Cussler, *J. Membr. Sci.* **1999**, 154, 155-162.

where  $\beta$  is the selectivity,  $\sigma$  is the protonic conductivity and DH is the methanol permeability.

Relative selectivity may be defined as the selectivity of the membrane of interest divided by the selectivity of Nafion, Equation 6-9.

**Equation 6-9**

$$\text{relative selectivity} = \frac{\beta_m}{\beta_{\text{Nafion}}}$$

A membrane with relative selectivity greater than 1 is potentially a better direct methanol fuel cell proton exchange membrane than Nafion. Selectivity and relative selectivity can also be computed from the conductivity and permeability as determined by MEA measurements, however, only free-standing membrane selectivities are presented in this work.

## 6.4 Results

### 6.4.1 Methanol Permeability

The issues concerning the production of high performance MEAs from high performance membranes can best be illustrated by comparing free-standing membrane data with data obtained in a fuel cell on an MEA composed of the novel membrane and standard, painted-on, Nafion-based catalyst layers. The two membrane properties that have the greatest impact on DMFC performance, methanol permeability and conductivity, are highlighted in this study.

The methanol permeability of free-standing membranes ( $DM_m$  from a membrane-separated diffusion cell) and MEAs ( $DH_{MEA}$  from crossover current measurements) was measured over the temperature range of 30 to 80°C. The results for diffusion cell and crossover current experiments are shown in Figure 6-5.

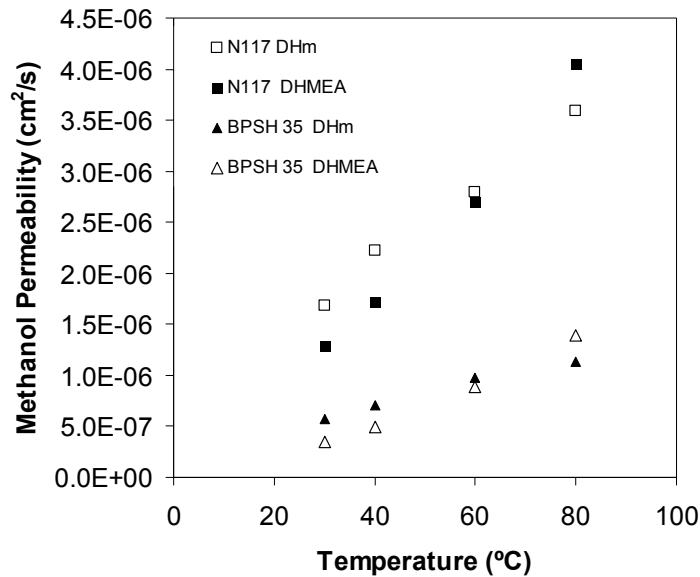


**Figure 6-5: Comparison of Methanol Permeability For Free-standing Membranes and Membrane Electrode Assemblies**

The methanol permeability of an MEA is surprisingly similar to that of a free-standing membrane. In free-standing membrane measurements, the only resistance to methanol diffusion

comes from the membrane. In the crossover current measurement, the methanol must diffuse through the anode gas diffusion layer, anode catalyst layer, and the membrane before it is oxidized in the cathode catalyst layer. The gas diffusion layer or the cathode catalyst layer could contribute resistance to methanol diffusion in addition to the membrane therefore decreasing the apparent methanol permeability of the membrane in an MEA configuration. However, because the permeability is similar for free-standing membranes and MEAs, it can be concluded that the gas diffusion layers and electrodes do not provide a large barrier for methanol diffusion at the low current densities encountered in limiting current experiments. At higher current densities, where large amounts of methanol are consumed at the anode, the gas diffusion layer could provide significant resistance to methanol transport.

Once the permeability of a free-standing membrane is known, the thickness of the membrane to be used in a DMFC can be tailored to give a specific crossover rate or flux of methanol to the cathode, since the losses in the cathode are a result of crossover rate rather than methanol permeability. For instance, if the methanol permeability of an experimental membrane is half that of Nafion and the conductivity is equivalent, the membrane can be half as thick while still providing the same crossover rate and half the cell resistance. If the experimental membrane is the same thickness as Nafion, it can be predicted that the crossover rate of methanol will be half that of Nafion while still giving the same cell resistance.

A lower crossover rate of methanol to the cathode can be expected to boost the open circuit voltage and increase the voltage across the entire range of current densities because the mixed potential losses at the cathode are decreased. In various regimes of DMFC operation the

resistive losses may be come more important than the crossover losses. In this case, a thinner membrane would be desired to decrease the resistance of the cell even though the crossover may be slightly increased. At other design points (typically at high voltages) the crossover losses become more important than the resistive losses and a thicker membrane with less crossover is desirable.

#### 6.4.2 Protonic Conductivity

Aside from methanol permeability, the other major membrane parameter that governs DMFC performance is protonic conductivity. The protonic conductivity of a membrane must be at a sufficient level as to not cause drastic Ohmic losses within the cell. Despite its high methanol permeability, Nafion has proven to be a popular proton exchange membrane in direct methanol fuel cells because of its high conductivity in well-hydrated systems. The conductivity of a series of membranes for stand-alone membrane measurements and MEAs at 80°C and full hydration (0.5 CH<sub>3</sub>OH feed to fuel cell) is listed in Table 6-1.

**Table 6-1: Membrane and MEA Conductivities for BPSH and Nafion Copolymers**

	Membrane conductivity $\sigma_m$ (S/cm)	HFR ( $\Omega\text{-cm}^2$ )	MEA conductivity $\sigma_{MEA}$ (S/cm)	% Loss
N117	0.17	0.17	0.11	40
BPSH 30	0.10	0.31	0.05	48
BPSH 35	0.13	0.23	0.05	63
BPSH 40	0.16	0.21	0.07	59
BPSH 50	0.23	0.15	0.08	68

80°C fully hydrated membranes

There is a noted disparity in the conductivity of the membrane versus the computed conductivity of an MEA as determined by high frequency resistance measurements. Taking Nafion as a control, the decrease in conductivity between the membrane and the MEA can be accounted for by the bulk resistance of the gas diffusion layers, the interface between the gas diffusion layer and the catalyst layer, and the interface between the catalyst layer and the membrane. The only variable that changes in Table 6-1 between each MEA is the catalyst layer/membrane interface. In the BPSH series of copolymers there is, on average, a 60% loss in conductivity as compared to a 40% loss in conductivity for the Nafion membrane. The large drop in measured MEA conductivity when a non-Nafion membrane is utilized with Nafion containing catalyst layers is attributed to poor electrochemical contact at the membrane/electrode interface where protons must be shuttled from Nafion in the anode to the BPSH membrane and back into the Nafion in the cathode.

The exact origin of the increased interfacial resistance between Nafion-based catalyst layers and non-Nafion membranes remains unknown, but it is reasonable to assume that Nafion, being a highly fluorinated tetrafluoroethylene-based material would tend to not bond intimately with a poly(arylene ether sulfone) copolymer such as BPSH. What bonding does occur could be a result of the hydrogen bonding via sulfonic acid groups in each system. It is proposed that in order to create a durable, high-performance membrane electrode assembly, both good mechanical bonding and electrochemical bonding must occur. The catalyst layer must adhere well to the membrane substrate and not debond over the life of the fuel cell, and the proton transport from anode catalyst layer to membrane to cathode catalyst layer must be facile.

To promote electrochemical bonding between the copolymer membrane and a Nafion-based catalyst layer, a partially fluorinated analog of BPSH, sulfonated bisphenol AF poly(arylene ether sulfone), abbreviated 6F, has been synthesized as is described in the Experimental section.<sup>167</sup>

The methanol permeability and protonic conductivity, and thus the relative selectivity of the 6F copolymers is strikingly similar to the BPSH copolymers in free-standing film measurements on an ion exchange capacity basis as shown in Figure 6-6.

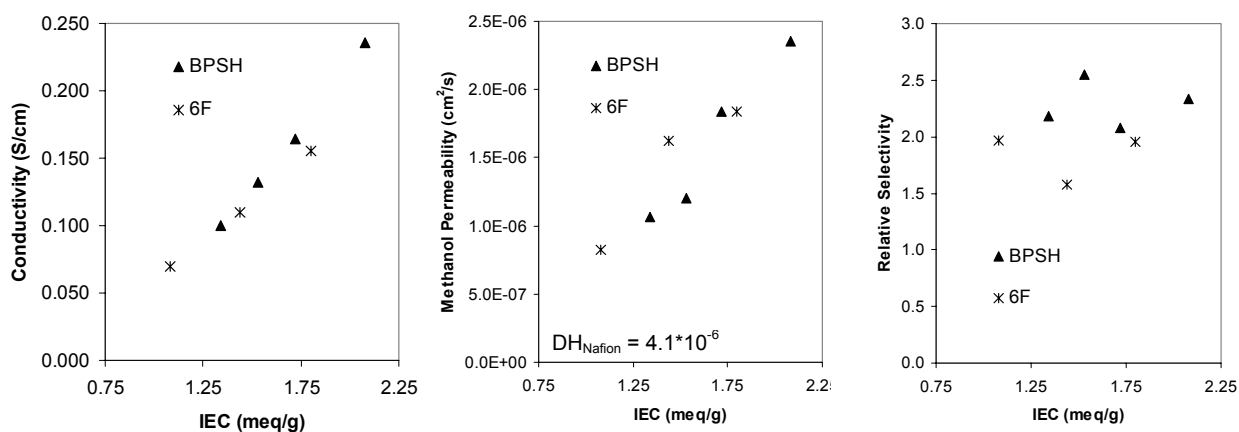


**Figure 6-6: Comparison of Methanol Permeability, Protonic Conductivity, and Relative Selectivity for BPSH and 6F Copolymers – 80°C in Liquid Water**

It is evident from the free-standing film data, that the introduction of a small amount of fluorine in the backbone of the 6F copolymers does not have a great effect on the membrane properties as compared to BPSH when the change in ion exchange capacity is taken into account. In fact, the

free-standing membrane relative selectivity of BPSH membranes is slightly greater than the 6F copolymers, so one may assume that their performance would be better in direct methanol fuel cells.

The performance of 6F copolymers was also measured in MEAs with Nafion-based electrodes. A comparison of the protonic conductivity in membranes and MEAs is shown in Table 6-2.

**Table 6-2: Membrane and MEA Conductivities for 6F Copolymers**

	Membrane conductivity (S/cm)	HFR ( $\Omega\text{-cm}^2$ )	MEA conductivity (S/cm)	% Loss
N117	0.17	0.17	0.11	40
6F 30	0.07	0.29	0.03	59
6F 40	0.11	0.09	0.07	33
6F 50	0.16	0.07	0.09	44

80°C fully hydrated membranes

For this series of copolymers there is considerably less change in conductivity between the free-standing membranes and the MEAs. On average, a 45% loss is observed for the 6F copolymers as compared to a 60% loss as shown in Table 6-1 for the BPSH copolymers. The exact nature of the improvement of the 6F copolymers as compared to the BPSH copolymers is unknown, but it is reasonable to assume that a moderately fluorinated copolymer would have better mechanical and electrochemical contact with the highly fluorinated Nafion. Contact could be enhanced between Nafion and a fluorinated copolymer due to partial fluorine enrichment at the surface of each material.

The improved electrochemical contact between 6F membranes and Nafion electrodes over the BPSH/Nafion system as characterized by high frequency resistance measurements is supported by the direct methanol fuel cell performance of each system. Representative polarization curves under standard DMFC conditions are shown in Figure 6-7.

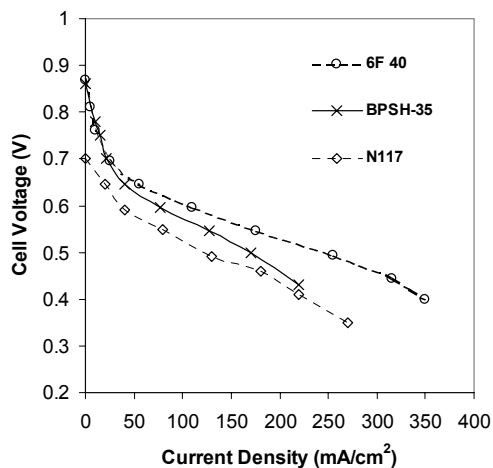


**Figure 6-7: DMFC Polarization Curves for Nafion 117, BPSH, and 6F MEAs – 80°C 0.5M CH<sub>3</sub>OH**

The open circuit voltage of both BPSH 35 and 6F 40 were significantly greater than Nafion (N117) due to these membranes' lower methanol crossover. The BPSH 35 curve dropped precipitously through the activation portion of the curve and its Ohmic slope was steep yielding performance that is equivalent that of Nafion at 220 mA/cm<sup>2</sup> at about 0.4 V. The voltage of the 6F 40 sample also declined quickly through the activation region, but the Ohmic losses in this MEA were not as severe as in BPSH 35 and its performance was greater across the entire range of current. The conductivity of the two experimental membranes is similar, in fact the conductivity of BPSH 35 is greater than the conductivity of 6F 40 (0.13 S/cm and 0.11 S/cm,

respectively - Table 6-1 and Table 6-2), but the interfacial resistance was lower in the 6F system, which produced better performing DMFC MEAs as shown in Figure 6-7.

Most of this work has been focused towards DMFCs, but the same interfacial resistance arguments are valid for hydrogen/air fuel cells. Large interfacial resistances were observed when Nafion catalyst layers are hot pressed onto non-Nafion membranes as shown in Table 6-3.

**Table 6-3: Comparison of Membrane Conductivities and Hydrogen/Air High Frequency Resistance for BPSH Copolymers and Nafion**

	Membrane conductivity (S/cm)	HFR ( $\Omega\text{-cm}^2$ )	MEA conductivity (S/cm)	% Loss
N1135	0.15	0.11	0.81	46
BPSH 30	0.08	0.21	0.03	58
BPSH 35	0.10	0.15	0.04	57
BPSH 50	0.17	0.11	0.06	63

80°C membranes equilibrated at 100% relative humidity

As demonstrated above for direct methanol fuel cells (Table 6-1), hydrogen/air MEAs composed of a Nafion electrode hot pressed onto a BPSH membrane yielded higher resistive losses than a Nafion electrode hot pressed onto a Nafion membrane as shown in Table 6-3. By visual inspection, the hot press method produced a good mechanical bond between the BPSH membrane and the electrode. In fact, after electrode attachment, the MEAs were acidified under boiling conditions without delamination of the electrode from the membrane. The increased resistive losses in the BPSH membrane/Nafion electrode MEAs are attributed to the poor interface between dissimilar polymers. Future work will be directed towards optimizing the

copolymer composition to promote electrochemical interface between the membrane and Nafion-based electrodes for hydrogen/air fuel cell systems.

It is surmised that increased interfacial resistance in both DMFC and hydrogen/air fuel cell systems has been one of the primary obstacles in novel proton exchange membrane development and fuel cell MEA demonstration. Many new membranes have shown promise in free-standing membrane tests (high conductivity and low methanol permeability), but have lacked the complimentary results in fuel cell tests. Some of these new sulfonated copolymers suffer from life-time issues such as oxidative degradation and embrittlement as with polystyrene sulfonic acid, but initially poor fuel cell results due to interfacial resistance issues with standard, Nafion-based electrodes (or lack of understanding of the interfacial resistance problem) has turned attention away from some other potentially attractive alternative proton exchange membranes. During MEA testing of novel proton exchange membranes the interaction between the electrode and the membrane must be well-characterized and the interfacial resistance issues understood to get a true evaluation of a the membrane's potential performance. In addition to this study, Pivovar et al. have reported another method for separating the interfacial and the bulk conductivity issues in MEAs with non-Nafion membranes.<sup>164</sup> Clearly, more investigations along this vein are needed.

In addition to the initial lower performance encountered with BPSH membrane/Nafion electrode MEAs reported above, there are indications that the long-term degradation of these cells is more rapid than Nafion membrane/Nafion electrode or 6F membrane/Nafion electrode systems. The bonding interaction between the membrane and the electrode was studied electrochemically in

this work, but the increased resistance could also be a sign of poor mechanical adhesion between the components. The degradation of the mechanical interface could cause decreases in cell performance and greatly shortened lifetimes. Increasing the affinity of the membrane for the electrode as with the 6F membranes is expected to improve the lifetime performance of the DMFC.

Two strategies are proposed to combat the interfacial electrochemical resistance that exists between Nafion-based electrodes and non-Nafion proton exchange membranes. One strategy involves changing the chemistry of the membrane to increase the compatibility with the Nafion electrode. If a membrane can be modified to increase its compatibility with the Nafion in the electrode without sacrificing protonic conductivity or methanol permeability, it is reasonable to expect that the electrochemical interfacial resistance between the electrode and the membrane will decrease.

This work probed the “membrane modification” strategy by employing the synthesis of the 6F copolymer. The 6F copolymer was similar to BPSH on a chemical structure basis and yielded comparable free-standing membrane properties in terms of protonic conductivity and methanol permeability. Its fluorine content promoted compatibility with the fluorinated structure of Nafion. As a result, the desirable transport properties of BPSH were maintained (low methanol permeability and sufficient protonic conductivity) while the electrochemical contact with the Nafion electrode was enhanced as evidenced by high frequency resistance measurements.

The second proposed strategy to decrease the interfacial resistance between the membrane and the composite electrode is to replace the Nafion in the electrode with an ion conducting polymer that is more compatible with the membrane copolymer. Having similar polymers in the membrane and electrode (not necessarily the same) is anticipated to decrease the electrochemical interfacial resistance between the layers of the MEA. However, there are significant challenges to replacing Nafion in the electrode by employing an “electrode modification” approach. Nafion, for all of its drawbacks as a membrane material in direct methanol fuel cells, tends to have properties that are desirable as an ion conducting polymer in the electrode. Its high methanol and gas permeability impart good mass transport within the structure electrode and Nafion’s electrochemical and degradative stability resist reaction with the platinum electrocatalyst under strongly oxidizing or reducing conditions. Commercial Nafion solutions (or more correctly dispersions) used to fabricate MEAs using a variety of common techniques, seem to generate the correct porosity, ionic conductivity, and water management properties for good-performing electrodes that have been optimized over the last 30 years.

There have been very few if any attempts at replacing Nafion in the catalyst layer reported in the literature. The delicate balance between ionic conductivity, electrical conductivity, and porosity seems to be hard to reproduce with polymers other than Nafion. For instance, an ion conducting polymer with low methanol permeability may produce an excellent proton exchange membrane, but when placed in the anode its low methanol permeability may decrease methanol diffusion to the catalytic sites and performance at high current densities would suffer. In addition, a novel electrode ion conducting polymer may interact more strongly with the platinum catalyst and

hinder its electrochemical activity. Mass transport, electrochemical activity, stability, and processing issues exist if Nafion is to be supplanted from the composite electrode.

## **6.5 Conclusions**

This study compared the methanol permeability and protonic conductivity of free-standing membranes to the properties of MEAs in direct methanol fuel cells. It was observed that the MEAs showed similar methanol permeability to that of the membranes. This implied that the membrane itself dominated the methanol crossover rate in an MEA while the electrodes and gas diffusion layers did not provide significant additional resistance to methanol transport.

Oppositely, it was shown that the conductivity of a free-standing membrane as measured by electrochemical impedance spectroscopy was much greater than the conductivity of an analogous MEA as computed from fuel cell high frequency resistance. The gas diffusion layers, catalyst layers, and interfaces accounted for some of the decrease in conductivity from membranes to MEAs, but the important observation was that the conductivity drop was larger for BPSH MEAs than for Nafion MEAs where both systems utilized Nafion electrodes. The only variable that changed between the BPSH and Nafion MEAs was the membrane/electrode interface. Increased interfacial resistance between the Nafion-based electrode and the BPSH membrane resulted in poorer fuel cell performance than would otherwise be expected from the stand-alone membrane properties.

To lower the interfacial resistance at the membrane/electrode interface, a fluorine containing sulfonated poly(arylene ether sulfone) copolymer (6F) was synthesized. The protonic conductivity and methanol permeability of the 6F copolymer membranes were strikingly similar to the BPSH copolymers on an ion exchange capacity basis. However, MEAs composed of 6F copolymer showed an appreciable decrease in interfacial resistance compared to BPSH MEAs (45% decrease versus 60% decrease, respectively). The exact mechanism of the improvement in electrochemical contact between the Nafion-based electrode and 6F membrane remains unknown, but it is reasonable to assume that a fluorinated copolymer such as 6F could be more compatible with highly fluorinated Nafion than a non-fluorinated copolymer such as BPSH. To compliment the high frequency resistance measurements, the 6F copolymers proved to perform better in direct methanol fuel cells under standard conditions. From this study, it cannot be determined how much fluorine in the membrane is desirable, but the synthesis strategy used to produce BPSH and 6F copolymers affords precise control of the chemical structure of the copolymer including the fluorine content. Copolymers that may further promote electrochemical contact with Nafion electrodes and increase the lifetime performance of DMFCs remain under investigation in our laboratory.

This study demonstrates that not only are intrinsic membrane properties important, but the compatibility of the membrane and the electrode is a key issue when MEA and DMFC studies are undertaken. The concepts presented here will help guide polymer synthesis efforts and proton exchange membrane and MEA development programs to create membranes that not only have desirable intrinsic properties, but consider the electrochemical bonding between the membrane and the electrode as a key variable. An addition to optimizing the membrane

chemical structure, synergy between the membrane and electrode can also be accomplished by constructing new electrodes from an ionomer that is electrochemically compatible with the membrane. Novel electrode morphologies, processing, or compositions may also help to decrease the interfacial resistances in the MEA.

# CHAPTER 7. RECOMMENDATIONS FOR FUTURE RESEARCH

## 7.1 Influence of Chemical Structure on the State of Water and Transport Properties of Proton Exchange Membranes

The extent of phase separation was introduced as a key concept in the morphology of proton exchange membranes. The extent of phase separation has been studied in poly(urethane urea)s by calculating the interphase thickness from x-ray scattering measurements.<sup>177</sup> It would be anticipated that Nafion systems would have a smaller interphase thickness compared to the wholly aromatic systems. Conversely, sulfonated polyimides would have the greatest interphase thickness because of the very stiff polymer chains. More detailed morphological studies of the copolymers from this work would be a valuable contribution to the overall understanding of transport properties in wholly aromatic systems.

It was hypothesized that various factors such as backbone stiffness, ion conductor acidity and location, and hydrophilic character of the backbone played a role in the extent of phase separation and thus the state of water and transport properties. A systematic series of copolymers incorporating these features could be synthesized using the poly(arylene ether) platform. More fluorine could be incorporated into the backbone of the copolymer or the sulfonic acid could be attached in a side chain configuration to test the effects of these changes in

---

177. O'Sickey, M.J., B.D. Lawrey, G.L. Wilkes, *J. Appl. Polym. Sci.* **2002**, 84, 229-243.

chemical structure without relying on Nafion as the most fluorinated or longest side chain membrane.

The state of water was shown to correlate with the other transport properties (protonic conductivity, methanol permeability, electro-osmotic drag) of proton exchange membranes. The state of water was quantified by measuring the water self-diffusion coefficient in the fully hydrated membranes. As was demonstrated by Kim et al.<sup>178</sup> dynamic scanning calorimetry (DSC) can also be used to measure the fractions of tightly bound, loosely bound, and free water in the membrane. It was asserted in this dissertation that the average water self-diffusion coefficient may be more applicable when studying bulk transport properties of the membranes, but additional experiments could enhance the understanding of how water is absorbed in the copolymers.

## **7.2 Elucidating Morphology From Transport**

Again, more detailed morphological information of the ionic domains would be an area of future research that would extend the results of this dissertation. Scattering studies (neutron and x-ray) have been performed on similar wholly aromatic systems such as sulfonated PEEK and other aromatic hydrocarbon membranes; however, very few conclusions have been drawn from these extensive investigations (even for Nafion). The size scale of the characteristic features, scattering contrast, equipment requirements, and data interpretation complicates scattering studies in these ion-containing systems. The copolymers discussed in this dissertation are well

---

178. Kim Y.S., L. Dong, M. Hickner, T.E. Glass, J.E. McGrath, *Macromolecules* **2003**, 36(17), 2003.

defined in terms of chemical structure and ion content, so careful investigations of these systematic series of copolymers (coupled with knowledge of the transport properties) may reveal more information in scattering experiments.

### **7.3 Effect of Inorganic Additives on the Transport Properties of Organic/Inorganic Nanocomposite Proton Exchange Membranes**

The effect of two different inorganic additives on the state of water was shown for organic/inorganic composites formed from BPSH and either zirconium hydrogen phosphate or phosphotungstic acid. These materials are by no means the only organic/inorganic composite systems of interest for fuel cell applications. Nafion composites with phosphotungstic acid, silica, titania and other inorganic compounds have shown promising results in some studies. Aside from Nafion and the array of inorganic compounds, other copolymers whose chemical structure are optimized for complexation<sup>179</sup> with inorganic compounds may provide an interesting platform for future studies. The transport properties of these composites should be controlled by the state of water just as with the systems explored in this work. Extending the ideas of this work to other systems or studying the state of water by means other than pulsed field gradient NMR could help to elucidate more information on the fundamental processes occurring in organic/inorganic composites and the fundamental mechanisms by which the inorganic additives influence the transport properties of the proton exchange membrane.

---

179. Sumner, M.J., W.L. Harrison, R.M. Weyers, Y.S. Kim, J.E. McGrath, J.S. Rifle, A.D. Brink, "Proton conducting sulfonated poly(arylene ether) copolymers containing aromatic nitriles," *J. Membrane Science* **2003**, submitted.

In addition to the transport properties in organic/inorganic systems, the inorganic component of the composite could serve as a mechanical reinforcing filler. The presence of the inorganic phase could enhance the modulus of the material and also delay the onset of the viscoelastic relaxation of the proton conducting polymer which has been linked to a decrease in protonic conductivity.<sup>180</sup> Operation of proton exchange membrane fuel cells above 120°C is currently a major objective for the industry. Aside from proton conduction problems at this temperature, mechanical properties of the membrane will also be important. Inorganic additives may help to alleviate some of the issues associated with high temperature operation of fuel cells.

#### **7.4 The Importance of Molecular Weight in High Performance Direct Methanol Fuel Cell Proton Exchange Membranes**

The effect of molecular weight on the transport properties of proton exchange membranes was demonstrated for PATS copolymers. It was asserted that the effects of molecular weight are generally true for most proton exchange membranes even of the post-sulfonated variety. A certain next step would be to compare a directly copolymerized sulfonated copolymer such as BPSH with its post-sulfonated analog. Careful characterization of the molecular weight of each type of copolymer could help to further extend the results of this work and strengthen the case that the molecular weight of proton exchange membranes is a key parameter whose role must be understood. However, post sulfonated and directly polymerized copolymers do have slightly different chemical structures even though they may have the same ion exchange capacity. This

---

180. Kim Y.S., L. Dong, M. Hickner, B.S. Pivovar, J.E. McGrath, "Processing Induced Morphological Development in Hydrated Sulfonated Poly(Arylene Ether Sulfone) Copolymer Membranes," *Polymer* **2003**, accepted.

is due to the post-sulfonation reactions placing a sulfonate group on the activated aryl rings of the bisphenol residue whereas the sulfonated group resides (two per sulfonated monomer) on the dihalide residue in directly copolymerized systems. Never-the-less, a detailed comparison of the transport properties and molecular weights of directly polymerized and post-sulfonated copolymers with similar chemical structures would be a significant contribution to the field.

In addition to comparisons of pre and post sulfonated systems, a series of directly polymerized sulfonated copolymers with controlled molecular weights could be prepared by off-setting the stoichiometry of the reactants during the copolymerization reaction. The transport properties of membranes with exact chemical structures could then be compared similar to the PATS work in this dissertation. The synthesis portion of this future work has already been undertaken by Wang et al.,<sup>181</sup> but a more in depth study of the transport and mechanical properties is needed. The same methodology could be applied in a study of post-sulfonated systems. Unsulfonated copolymers with initially different molecular weights could be utilized in post-sulfonation reactions to yield a series of proton exchange membranes with different molecular weights.

## **7.5 Fabrication of High Performance MEAs**

It was demonstrated that a decrease in electrode/membrane interfacial resistance was achieved with a fluorinated copolymer proton exchange membrane when coupled with standard Nafion direct methanol fuel cell electrodes. There are two obvious next steps; further optimization of the proton exchange membrane copolymer chemical structure and substituting Nafion for a

---

181. Wang, F., T. Glass, X. Li, M. Hickner, Y.S. Kim, J.E. McGrath, *Polymer Preprints* **2002**, 43(1), 492.

different ion containing polymer in the electrode. The first method was explored in this work and is currently under further investigation. 6F, with its modest amount of fluorine, showed enhanced electrochemical compatibility with Nafion electrodes. It would be interesting to further explore the variable of fluorine content to ascertain if more or less fluorine or another functional group increased the electrochemical compatibility of the copolymer membrane and the Nafion electrode. Exact control of the amount of fluorine or and precise alteration of the chemical substituents of the copolymer is major advantage of the direct copolymerization scheme highlighted throughout this work. For direct methanol fuel cell applications, the wholly aromatic membranes show promise. Their intrinsic properties indicate that these membranes would produce higher performance fuel cells than Nafion. However, the fabrication of membrane electrode assemblies from these membranes must be further optimized.

Fabricating an electrode from a copolymer other than Nafion, principally the same (or a similar) copolymer as the proton exchange membrane could provide enhanced electrochemical contact between the membrane and the electrode. Preliminary studies have been conducted to this end by incorporating BPSH copolymers in the electrode in concert with BPSH membranes, but the BPSH-based electrodes have thus far not shown very good electrochemical activity. At present, twice the amount of platinum is required in the BPSH electrodes to equal the performance of a Nafion electrode. More work is needed to understand the structure, transport properties, and electrochemical activity of non-Nafion electrodes.

## VITA

Michael Anthony Hickner was born to John and Valerie Hickner on January 27, 1976 in Charleston, South Carolina. He spent his formative years in Escanaba, Michigan and graduated from Michigan Technological University in May, 1999 as a Bachelor of Science in Chemical Engineering. Upon graduation he embarked on the graduate studies described herein to lead to the Ph.D. in Chemical Engineering.